이학박사 학위논문

Development of Biomarkers for Hepatocellular Carcinoma Using Multiple Reaction Monitoring-Mass Spectrometry (MRM-MS) and Bioinformatics

질량분석기 다중반응검지법 및 생물정보학을 이용한 간암 바이오마커 개발에 대한 연구

2015 년 02 월

서울대학교 대학원

의과학과 의과학전공

김 현 수

A thesis of the Degree of Doctor of Philosophy

질량분석기 다중반응검지법 및 생물정보학을 이용한 간암 바이오마커 개발에 대한 연구

Development of Biomarkers for Hepatocellular Carcinoma Using Multiple Reaction Monitoring-Mass Spectrometry (MRM-MS) and Bioinformatics

February 2015

Major in Biomedical Sciences

Department of Biomedical Sciences

Seoul National University

Graduate School

Hyunsoo Kim

ABSTRACT

Development of Biomarkers for Hepatocellular Carcinoma Using Multiple Reaction Monitoring-Mass Spectrometry (MRM-MS) and Bioinformatics

Hyunsoo Kim

Major in Biomedical Sciences

Department of Biomedical Sciences

Seoul National University

Graduate School

Introduction: Hepatocellular carcinoma (HCC) is one of the most common cancers and is associated with a poor survival rate. Serum alpha-fetoprotein (AFP) has long been used as a diagnostic marker for HCC, albeit controversially. Although it remains widely used in clinics, the value of AFP in HCC diagnosis has recently been challenged due to its significant rates of false positive and false negative findings.

Methods: In chapter I, to improve the efficacy of AFP as HCC diagnostic marker, we developed a method of measuring total and glycosylated AFP by

multiple reaction monitoring (MRM)-MS. In chapter II, the discovery of useful biomarkers for HCC, focused solely on the proteome, has been difficult; thus, wide-ranging global data mining of genomic and proteomic databases from previous reports would be valuable in screening biomarker candidates.

Results: In chapter I, we verified the total amount of AFP (nonglycopeptide levels) and the degree of glycosylated AFP (deglycopeptide levels) in 60 normal, 35 LC, and 60 HCC subjects. By MRM-MS analysis, the nonglycopeptide had 56.7% sensitivity, 68.3% specificity, and an AUC of 0.687, comparing the normal and HCC group, whereas the deglycopeptide had 93.3% sensitivity, 68.3% specificity, and an AUC of 0.859. In comparing the stage I HCC subgroup with the LC group, the nonglycopeptide had a sensitivity of 66.7%, specificity of 80.0%, and an AUC of 0.712, whereas the deglycopeptide had a sensitivity of 96.7%, specificity of 80.0%, and an AUC of 0.918.

In chapter II, global data mining was performed using 5 types of HCC data to screen for candidate biomarker proteins (cDNA microarray, copy number variation, somatic mutation, epigenetic, and quantitative proteomics data). Next, we applied MRM to verify HCC candidate biomarkers in individual serum samples from 3 groups: a healthy control group, before HCC treatment group, and after HCC treatment group. After determining the relative quantities of the candidate proteins by MRM, we compared their expression levels between the 3 groups, identifying 4 potential biomarkers (ANLN, FLNB, C4A, and AFP)

Conclusions: In chapter I, these data demonstrate that the discriminatory power of the deglycopeptide AFP is greater than that of the nonglycopeptide AFP comparing normal group with HCC group. We conclude that deglycopeptide can distinguish cancer status between normal subjects and HCC patients better than nonglycopeptide. In chapter II, the combination of 2 markers (ANLN, FLNB) improved the discrimination of the before HCC treatment group from the healthy control group compared with AFP. We conclude that the combination of global data mining and MRM verification enhances the screening of potential HCC biomarkers. This efficacious integrative strategy is applicable to the development of markers for cancer and other diseases.

Keywords: Multiple Reaction Monitoring; Biomarker; Hepatocellular Carcinoma; Alpha-Fetoprotein; Glycosylated AFP; Global Data-Mining; Multi-Marker Panel

Student number: 2009-21882

* This work is published in PLOS ONE Journal. Development of Biomarkers for Screening Hepatocellular Carcinoma Using Global Data Mining and Multiple Reaction Monitoring (H.Kim, K.Kim, S-J.Yu, E-S.Jang, J-Y.Yu, G-H.Cho, J-H.Yoon, and Y.Kim). Published 22 May 2013 / PLOS ONE. 10.1371 / journal.pone.0063468

* This work is published in PLOS ONE Journal. Measurement of glycosylated alpha-fetoprotein improves diagnostic power over the native form in hepatocellular carcinoma (H.Kim, K.Kim, J.Jin, J.Park, S-J.Yu, J-H.Yoon, and Y.Kim). Published 13 Oct 2014 / PLOS ONE. 10.1371 / journal.pone.0110366

CONTENTS

LIST OF TABLES

Chapter I

Chapter II

LIST OF FIGURES

Chapter I

Chapter II

LIST OF ABBREVIATIONS

ACADVL: Very-long-chain-specific Acyl-coA Dehydrogenase

ACN: Acetonitrile

AFP: Alpha-fetoprotein

AKT3: RAC-gamma Serine/Threonine-protein Kinase

ANLN: Actin-binding Protein, Anillin

ANOVA: Analysis of Variance

AUC: Area Under the Curve

BASP1: Brain Acid-Soluble Protein 1

BCA: Bicinhoninic Acid

C4A: Complementary C4-A

CAPN1: Calpain-1 Catalytic Subunit

CDKN2A: Cyclin-dependent Kinase Inhibitor 2A, Isoform 4

CE: Collision Energy

CES1: Carboxylesterase 1

COMT: Catechol O-Methyltransferase

CT: Computed Tomography

CTSB: Cathepsin B

CV: Coefficient Variation

DCP: Des-gamma Carboxyprothrombin

DHX9: ATP-dependent RNA helicase A

DP: Declustering Potential

DTT: Dithiothreitol

ECHS1: Enoyl-coA Hydratase, Mitochondrial

ELISA: Enzyme-Linked ImmunoSorbent Assay

EXT1: Exostosin-1

FA: Formic Acid

FLNB: Filamin-B

FWHM: Full Width at Half Maximum

HBV: Hepatitis B Virus

HCC: Hepatocellular Carcinoma

HPLC: High Performance Liquid Chromatography

IAA: Iodoacetic Acid

INV1: Invertase-1

IRB: Institutional Review Board

LC: Liquid Chromatography

LCA: Lens Culinaris Agglutinin

LOOCV: Leave-One-Out Cross Validation

LR: Logistic Regression

MA: Multivariate Analysis

MARS: Multiple Affinity Removal System

MRM-MS: Multiple Reaction Monitoring-Mass Spectrometry

MTHFD1: C-1-Tetrahydrofolate Synthase, Cytoplasmic

PABPC1: Polyadenylate-binding Protein 1

PIVKA II: Prothrombin Induced by Vitamin K Absence II

PNGase F: Peptide-N-glycosidase F

PTMs: Post-Translational Modifications

PVDF: Polyvinylidene Difluoride

QQQ: Triple Quadrupole

QTRAP: Hybrid Triple Quadrupole/Ion Trap Mass Spectrometer

ROC: Receiver Operating Characteristic

S/N: Signal-to-Noise

SD: Standard Deviation

SIS: Stable Isotope-Labeled Standard

TFA: Trifluoroacetic Acid

TGFB2: Transforming Growth Factor Beta-2

TNM: Tumor-Node-Metastasis

VCP: Transitional Endoplasmic Reticulum ATPase

VIFs: Variance Inflation Factors

VIM: Vimentin

XIC: Extracted Ion Chromatogram

GENERAL INTRODUCTION

Hepatocellular carcinoma (HCC) is the fifth most common cancer worldwide and the third leading cancer-related cause of death [1]. Since many HCCs are asymptomatic before the development of end stage disease, regular surveillance for HCC is mandatory for patients with chronic hepatitis or cirrhosis to detect a tumor at an early stage and to improve patients' outcomes after curative treatment [2]. Currently, most practice guidelines recommend routine surveillance for HCC using ultrasonography and serum tumor markers, such as alpha-fetoprotein (AFP). [3,4,5] However, the use of AFP as a single biomarker for HCC is challenging due to its limited specificity and sensitivity.

Glycosylation is one of the most important and common post-translational modifications (PTMs) of proteins that are secreted into serum. Glycosylation influences many functional aspects of proteins, including their structure and functions [6]. The expression and degree of glycosylation is significantly altered by various diseases, such as cancer, and thus, glycoproteins are associated with abnormal phenomena in patients with cancer [7-9]. To this end, quantitative measurements of glycoproteins might be useful in discovering biomarkers for cancer.

In chapter I, we performed MRM measurements for 2 types of peptides (nonglycopeptide and deglycopeptide) that target a glycoprotein and serum AFP, wherein the amount of nonglycopeptide represents the total glycoprotein concentration and the deglycopeptide represents the glycosylated fraction of the glycoprotein. We compared the total AFP concentration (represented as nonglycopeptide) with the glycosylated AFP fraction

(represented as deglycopeptide) between the normal, LC, and HCC groups. Notably, considering that the nonglycopeptide is measuring total AFP, it would be more advantageous to measure the deglycopeptide or take a combined measurement of nonglycopeptide and deglycopeptide, which could improve the diagnostic power in HCC.

In chapter Ⅱ, 50 of 4658 candidate proteins, obtained from the 5-category data mining (proteomics, cDNA microarray, copy number variation, epigenetics and somatic mutation), were selected, based on frequency. Consequently, 28 of 50 candidates were detected in pooled serum, 19 of which were differentially expressed between the 3 groups. After individual serum MRM analysis using 36 healthy control, 18 before HCC treatment, and 18 after HCC treatment samples, 9 candidates had identical expression patterns by MRM analysis using serum that was pooled from the 3 groups, and 4 proteins were verified by western blot. By logistic regression (LR) analysis, a 2-marker panel (ANLN and FLNB) was constructed, showing enhanced discriminatory power compared with AFP with an AUC of 0.981 (healthy control versus before HCC treatment) Thus, global data mining-based MRM verification, combined with multivariate analysis, is a robust method of developing HCC multimarkers.

CHAPTER I

Measurement of glycosylated alpha-fetoprotein improves diagnostic power over the native form in hepatocellular carcinoma

INTRODUCTION

The carbohydrates on glycosylated protein biomarkers undergo modifications in cancer. For example, the carbohydrate moieties of AFP are altered in cancer, and such changes are considered to be more useful markers of HCC [10]. Studies from the past several decades have demonstrated that total AFP is a collection of heterogeneous glycoproteins that can be fractionated by affinity electrophoresis into 3 glycoforms—AFP-L1, AFP-L2, and AFP-L3—based on their reactivity with the lectin Lens culinaris agglutinin (LCA). AFP-L3 binds strongly to LCA through an α1-6 bond between its additional fucose and the reducing terminus of N-acetylglucosamine, in contrast to AFP-L1 [11-13].

AFP levels are sometimes elevated in patients with chronic hepatitis and cirrhosis who have no evidence of HCC [14]. AFP has a reported sensitivity of 39% to 65% and a specificity of 65% to 94%; approximately one-third of early-stage HCC patients with small tumors (< 3 cm) have normal AFP levels [15,16]. Thus, clinicians are dissatisfied with AFP as a marker due to its high false-positive and false-negative rates [17].

Multiple reaction monitoring (MRM)-based quantification using triple quadrupole mass spectrometry (MS) is especially useful for measuring glycosylated biomarkers. MRM-MS, a multiplexed, targeted proteomic platform, is a rapid and cost-effective approach for measuring protein biomarkers for preclinical verification [18]. Nonglycopeptides (unmodified native peptides) and glycopeptides (glycosylated peptides) of glycoprotein markers are valuable biomarkers for the diagnosis and prediction of diseases,

because their expression levels and degree of glycosylation reflect quantitative differences of disease states, as in cancer.

In this study, we measured total AFP and glycosylated AFP by MRM-MS. Total AFP was represented by common nonglycopeptides among all forms of AFP, and glycosylated AFP comprised the portion of deglycosylated peptides after treatment of glycosylated peptides with PNGase F. Measurement of the deglycopeptide fraction from the glycosylated AFP yielded better AUC values than the nonglycopeptides of total AFP. Consequently, on measuring AFP concentrations in serum from HCC patients versus normal healthy controls and early-stage HCC versus liver cirrhosis by MRM-MS, AFP deglycopeptides had greater power in distinguishing, compared with nonglycopeptides.

Notably, total AFP and glycosylated AFP were measured effectively by MRM-MS in the form of nonglycopeptides and deglycopeptides, respectively, improving our diagnosis of HCC versus normal and early-stage HCC versus LC serum. In addition, MRM-MS is a platform that improves the measurement of total AFP and glycosylated AFP in glycoprotein biomarker assays, which is more advantageous compared with conventional methods, such as antibody-based measurements by lectin affinity electrophoresis and liquid-phase binding assays.

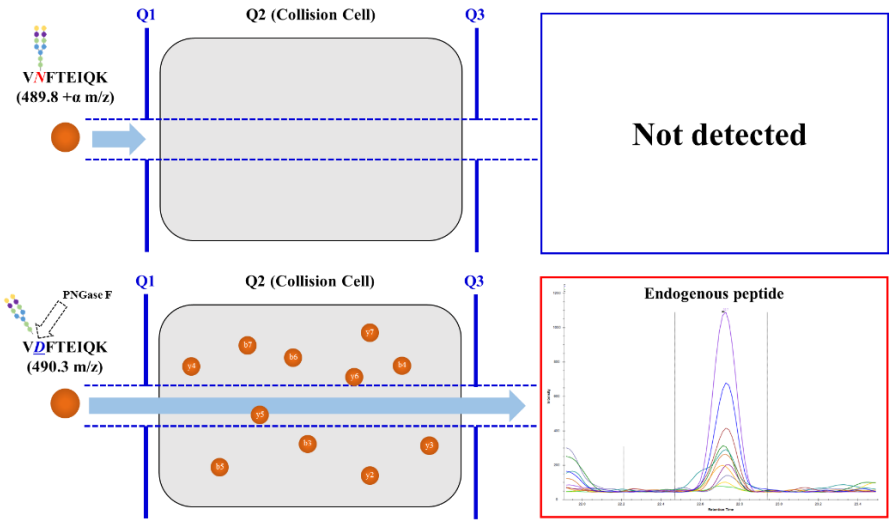

Figure 1-1

Figure 1-1. MRM analysis of glycopeptide (V*N*FTEIQK) was conducted targeting AFP glycosylated samples and deglycopeptide (V*D*FTEIQK) was conducted targeting AFP deglycosylated sample.

MATERIALS AND METHODS

1. Materials

Standard glycoprotein (origin: yeast) was purchased from Sigma-Aldrich (St. Louis, MO). Trypsin was obtained from Promega (Madison, WI). Peptide-N-glycosidase F (PNGase F) was purchased from New England Biolabs (NEB, Beverly, MA). HPLC-grade water and acetonitrile were obtained from Thermo Fisher Scientific (Bremen, Germany). Serum depletion was performed for the 6 most abundant proteins using a multiple affinity removal system (MARS), consisting of an LC column (Agilent, 5185–5984); buffer A for sample loading, washes, and equilibration (Agilent, 5185–5987); and buffer B for elution (Agilent, 5185–5988). Stable isotope-labeled peptides [isotopically labeled (^{13}C and ^{15}N) amino acids] were obtained from JPT (Berlin, Germany).

2. Clinical sample information

The institutional review board (IRB) of Seoul National University Hospital (approval No. H-1103-056-355) approved the study protocol, and written informed consent was obtained from each patient or legally authorized representative. The clinical characteristics of the patients are shown in Table 1-1.

The clinical sample set comprised healthy controls (n = 60), patients with liver cirrhosis (n = 35), and patients with hepatocellular carcinoma (n = 60). The healthy control group (normal group) comprised sixty healthy

volunteers who visited the Healthcare Center of Seoul National University Hospital. All control subjects were confirmed, based on normal liver function test results, including serum alanine and aspartate aminotransferases, and were negative for hepatitis B virus surface antigen and anti-hepatitis C virus. Liver ultrasonography was performed to screen for fatty liver disease, and all healthy controls had normal findings.

The liver cirrhosis group (LC group) included 35 patients with compensated HBV cirrhosis and no HCC. The cirrhosis group had at least 1 year of follow-up from the time that serum was obtained for these studies. Patients were diagnosed with cirrhosis, based on established clinical, laboratory, and imaging criteria with ultrasound examination.

Sixty patients before HCC treatment who were infected with hepatitis B virus (HBV) were also enrolled, from whom serum samples were collected and defined as the HCC group. The diagnosis of HCC was made per the American Association for the Study of Liver Diseases by a hepatologist with more than 20 years of experience [19]. To reduce causal heterogeneity, HCC patients who had other types of chronic liver disease, except chronic hepatitis B, such as chronic hepatitis C and alcoholic hepatitis, were excluded.

HCC stage was classified per the tumor-node-metastasis (TNM) staging system (7^{th} edition, 2010, the American Joint Committee on Cancer staging system). TNM staging of the 55 cases demonstrated stage I in 30 cases, stage II in 15 cases, stage III in 10 cases, and stage IV in 0 cases. Insufficient information was available to assign stage in 5 HCC cases.

All subjects (n = 155) were recruited during the study period from September 2005 to August 2012 and collected by the Liver Research Institute, Seoul National University College of Medicine. Blood samples were centrifuged immediately at 3000 rpm for 10 min at 4℃ to fractionate the serum.

The resulting supernatant was aliquoted (100 μL) and stored at -80℃ until analysis.

Table 1-1. Characteristics of clinical subjects for MRM-MS analysis.

	Normal group	LC group	HCC group
Total patient number	60	35	60
Gender (Male / Female)	41 / 19	23 / 12	42 / 18
Age (Mean, Range)	53 (32-74)	56 (43-78)	58 (38-76)
Etiology of liver disease		HBV, 35 (100%)	HBV, 60 (100%)
AFP value (mean, range)			
< 20 ng/ml	60	35	26
20-400 ng/ml	0	0	18
> 400 ng/ml	0	0	16
Albumin (g/dL)	4.3 ± 0.18	4.2 ± 0.3	3.6 ± 0.5
Bilirubin (mg/dL)	1.3 ± 0.4	1.4 ± 0.7	1.3 ± 0.8
AST (IU/L)	22.5 ± 6.0	32.3 ± 24.3	89.1 ± 142.3
ALT (IU/L)	20.2 ± 8.3	37.6 ± 35.0	97.1 ± 249.9
ALP (IU/L)	41.7 ± 19.2	78.4 ± 20.6	123.5 ± 77.6
HBV DNA levels (IU/mL)[a]			
Not detected		11	1
Detected ($< 10^3$/units)		9	3
Detected ($\geq 10^3$/units)		6	25
Antiviral therapy[b]			
Yes (%)		23 (65.7%)	17 (28.3%)
No (%)		12 (34.3%)	43 (71.7%)
Treatment type			
Surgical resection			1
RFA			3
PEIT			22
TACE			30
TACE & PEIT			4
Tumor size (cm)[c]			
< 2			21
2 ~ 5			16
> 5			3
Tumor stage[d]			
Ⅰ			30
Ⅱ			15
Ⅲ			10
Ⅳ			0
Target lesion response			
CR			38
PR			19
SD			3
PD			0

Albumin, Bilirubin, AST, ALT, ALP, and HBV DNA levels data are presented as mean ± SD

[a] HBV DNA levels were provided for 26 among a total of 35 liver cirrhosis patients, and 29 among the 60 HCC patients

[b] Antiviral therapy was treatment with Entecavir, Tenofovir, Zeffix, Hepsera and Revovir

[c] Tumor size was provided for 40 among a total of 60 HCC patients

[d] According to American Joint Committee on Cancer (AJCC) staging system (7th edition, 2010)

Table 1-1

3. Sample size calculation

We calculate the sample size that was needed for clinical MRM verification with reference to previous studies using AUC (area under the curve) [20]. The sample size was calculated, based on an AUC with a type I error rate α of 0.05 and type II error rate β of 0.10 (90% power). To anticipate similar AUC values as in previous studies, we needed a sample size of 29 each in the normal and HCC groups, each totaling 58, and 24 each in the HCC and recovery groups, totaling 48. A minimum sample size of 29 per group was necessary for the MRM assays to determine a significant difference between groups (Table 1-2).

Table 1-2. Sample size calculation by previous studies using AUC.

Normal group vs HCC group

Area under ROC curve (0.735)		Type I Error - Alpha			
		0.20	0.10	**0.05**	0.01
Type II Error - Beta	0.20	13 + 13	17 + 17	22 + 22	33 + 33
	0.10	18 + 18	23 + 23	**29 + 29**	41 + 41
	0.05	22 + 22	29 + 29	35 + 35	49 + 49
	0.01	33 + 33	41 + 41	48 + 48	64 + 64

HCC group vs Recovery group

Area under ROC curve (0.756)		Type I Error - Alpha			
		0.20	0.10	**0.05**	0.01
Type II Error - Beta	0.20	10 + 10	14 + 14	19 + 19	28 + 28
	0.10	15 + 15	19 + 19	**24 + 24**	34 + 34
	0.05	18 + 18	24 + 24	29 + 29	40 + 40
	0.01	27 + 27	33 + 33	39 + 39	52 + 52

Table 1-2

4. Standard glycoprotein preparation

Standard glycoprotein (INV1) was prepared to 100 μg/μL. Standard glycoprotein samples were denatured with 6 M urea, 100 mM Tris, pH 8.0, and 20 mM dithiothreitol (DTT) at 37℃ for 60 min and alkylated with 50 mM iodoacetamide (IAA) at room temperature in the dark for 30 min. The urea was diluted 15-fold with 100 mM Tris, pH 8.0. One INV1 sample was deglycosylated with 2 μL of PNGase F (500,000 units/mL) at 37°C for 12 h and incubated and digested in a solution of 1:50 trypsin (w/w) at 37℃ for 16 h. The other INV1 sample was incubated in 2 μL 100 mM Tris, pH 8.0 (untreated PNGase F) at 37℃ for 12 h and digested as described above. The 2 INV1 digests were dried on a speed vacuum, diluted in mobile phase A, and spiked with stable isotope-labeled standard (SIS) peptide, as needed.

5. Clinical serum sample preparation

The 6 most abundant proteins in human serum (albumin, transferrin, IgG, IgA, haptoglobin, and α1-antitrypsin) were depleted on an HPLC system (Shimadzu Co., Kyoto, Japan) that was equipped with a multiple affinity removal system LC column (Agilent Technologies, Santa Clara, CA). Crude human serum samples were diluted by a factor of 5 with buffer A and passed through 0.22-μm filters by centrifugation (12,000 g, room temperature, 2–3 min). Diluted crude serum was injected at 0.25 mL/min, and flowthrough fractions were collected and stored at -80℃ (Figure 1-2). Depleted serum samples were concentrated by centrifugal filtration using a 3000-Da molecular weight cutoff (MWCO) (Millipore, Bedford, MA). Concentrated serum protein was quantified by bicinchoninic acid (BCA) assay (Figure 1-3).

Aliquots of serum samples (100 µg) were denatured and digested as described above. Tryptic digestion was stopped with formic acid (FA) at a final concentration of 1% and desalted on OASIS HLB 1-cc (30 mg) extraction cartridges (Waters Corp., Milford, MA). The cartridges were equilibrated sequentially with 3 mL acetonitrile (ACN) and 5 mL water/0.1% FA prior to loading of the tryptic digestions. The cartridges were washed with 3 mL water/0.1% FA and eluted with 1 mL of 60% ACN/0.1% FA. The eluted samples were frozen and lyophilized on a speed vacuum. Before MRM-MS analysis, the samples were reconstituted in mobile phase A to 1 µg/µL.

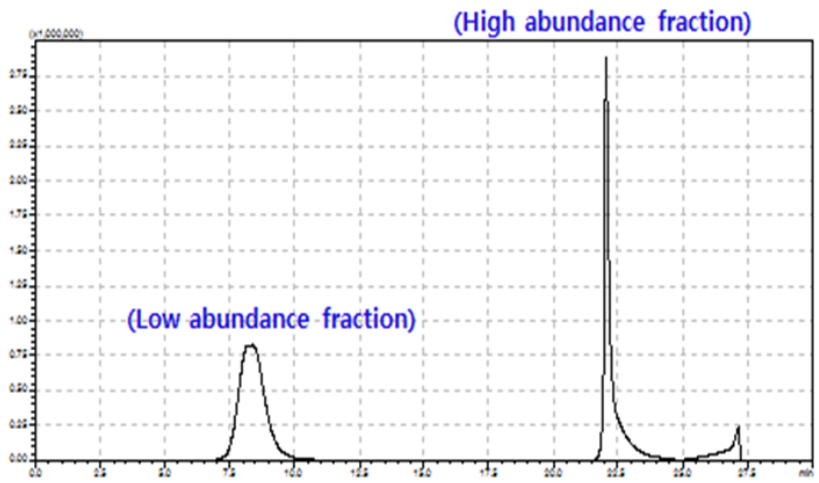

Figure 1-2

Figure 1-2. Chromatogram from a typical MARS HPLC depletion of human serum.

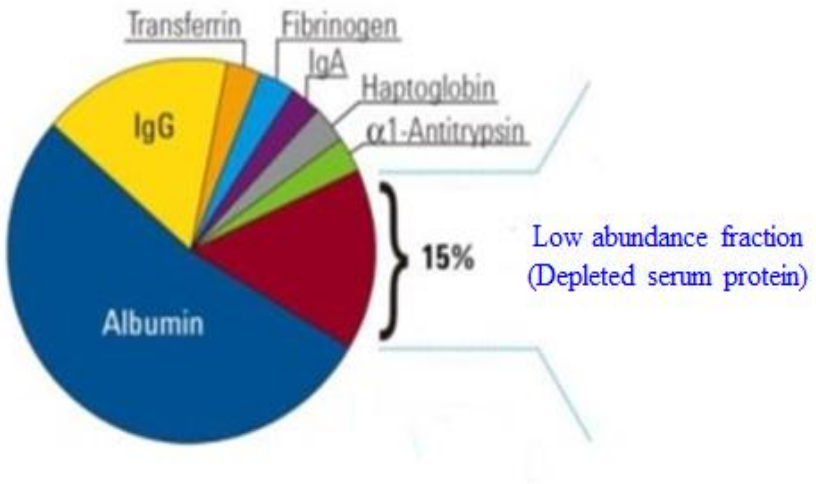

Figure 1-3

Figure 1-3. Percentage of protein remaining in the blood after depletion.

6. MRM-MS transition (Q1/Q3) selection

Skyline software was used to generate a list of all possible b-, y- series fragment ions for 2^+ precursor ion charge states, spanning the m/z range from 300 to 1400. In brief, full-length protein sequences were imported into Skyline in FASTA format and designed into peptides, each with a list of product ions for monitoring by MRM-MS. In selecting transitions through Skyline, the peptide filter condition was as follows: maximum length of peptide of 24, including at least 6 amino acids.

Peptides with repeat arginines (Arg, R) or lysines (Lys, K) were discarded. If methionine (Met, M) was included in the peptide, it was discarded to avoid the risk of modification. If proline (Pro, P) was next to arginine (Arg,

R) or lysine (Lys, K), the peptide was discarded. If a peptide contained histidine (His, H), it was discarded to avoid the risk of charge alterations. Peptides that satisfied these conditions were used as Q1 transitions. Next, we selected a maximum of 10 Q3 transitions from the fragmentation ions that were derived from the Q1 transitions in descending order.

For glycopeptides, theoretical transition values were selected, based on the original FASTA sequences after changing asparagine (Asn, N) in the NxS/T motif into aspartic acid (Asp, D), using Skyline. In addition, to verify that the measured peptides originated from the endogenous peptide that was tested, a stable isotope-labeled standard (SIS) peptide was used. The sequence of the SIS peptide is identical to that of the measured peptide but has ^{13}C and ^{15}N in the C-terminal arginine (Arg, R) and lysine (Lys, K). This result is described in Table 1-3.

Table 1-3. List of peptides and product ions for the standard glycoprotein (INV1).

Peptide type	Peptide sequence	Q1 (m/z)	Q1 ion charge	Q3 (m/z)	Q3 ion charge	Q3 ion type	Retention time (min)	Isotype	Fragmentor (volt)	Collision energy (volt)
Non glycopeptide	IEIYSSDDLK	591.8	2	1069.5	1	y9	23.5	light	380	20.9
				940.5	1	y8	23.5	light	380	20.9
				827.4	1	y7	23.5	light	380	20.9
				664.3	1	y6	23.5	light	380	20.9
				356.2	1	b3	23.5	light	380	20.9
	IEIYSSDDLK	595.8	2	1077.5	1	y9	23.5	heavy	380	20.9
				948.5	1	y8	23.5	heavy	380	20.9
				835.4	1	y7	23.5	heavy	380	20.9
				672.3	1	y6	23.5	heavy	380	20.9
				356.2	1	b3	23.5	heavy	380	20.9
Non glycopeptide	VVDFGK	332.7	2	565.3	1	y5	16.1	light	380	11.6
				466.2	1	y4	16.1	light	380	11.6
				351.2	1	y3	16.1	light	380	11.6
				204.1	1	y2	16.1	light	380	11.6
				199.1	1	b2	16.1	light	380	11.6
	VVDFGK	336.7	2	573.3	1	y5	16.1	heavy	380	11.6
				474.2	1	y4	16.1	heavy	380	11.6
				359.2	1	y3	16.1	heavy	380	11.6
				212.1	1	y2	16.1	heavy	380	11.6
				199.1	1	b2	16.1	heavy	380	11.6
Glycopeptide	NFVLAAA*N*STQFR	659.3	2	1007.5	1	y9	22.4	light	380	23.3
				894.4	1	y8	22.4	light	380	23.3
				823.4	1	y7	22.4	light	380	23.3
				752.4	1	y6	22.4	light	380	23.3
				638.3	1	y5	22.4	light	380	23.3
	NFVLAAA*N*STQFR	664.4	2	1017.5	1	y9	22.4	heavy	380	23.3
				904.5	1	y8	22.4	heavy	380	23.3
				833.4	1	y7	22.4	heavy	380	23.3
				762.4	1	y6	22.4	heavy	380	23.3
				648.3	1	y5	22.4	heavy	380	23.3
Deglycopeptide	NFVLAAA*D*STQFR	659.8	2	1008.5	1	y9	23.2	light	380	23.3
				895.4	1	y8	23.2	light	380	23.3
				824.4	1	y7	23.2	light	380	23.3
				753.4	1	y6	23.2	light	380	23.3
				638.3	1	y5	23.2	light	380	23.3
	NFVLAAA*D*STQFR	664.8	2	1018.5	1	y9	23.2	heavy	380	23.3
				905.4	1	y8	23.2	heavy	380	23.3
				834.4	1	y7	23.2	heavy	380	23.3
				763.4	1	y6	23.2	heavy	380	23.3
				648.3	1	y5	23.2	heavy	380	23.3
Glycopeptide	FAT*N*TTLTK	498.8	2	849.5	1	y8	18.9	light	380	17.6
				778.4	1	y7	18.9	light	380	17.6
				677.4	1	y6	18.9	light	380	17.6
				563.3	1	y5	18.9	light	380	17.6
				462.3	1	y4	18.9	light	380	17.6
	FAT*N*TTLTK	502.8	2	857.5	1	y8	18.9	heavy	380	17.6
				786.4	1	y7	18.9	heavy	380	17.6
				685.4	1	y6	18.9	heavy	380	17.6
				571.4	1	y5	18.9	heavy	380	17.6
				470.3	1	y4	18.9	heavy	380	17.6
Deglycopeptide	FAT*D*TTLTK	499.3	2	850.5	1	y8	18.9	light	380	17.6
				779.4	1	y7	18.9	light	380	17.6
				678.4	1	y6	18.9	light	380	17.6
				563.3	1	y5	18.9	light	380	17.6
				462.3	1	y4	18.9	light	380	17.6
	FAT*D*TTLTK	503.3	2	858.5	1	y8	18.9	heavy	380	17.6
				787.4	1	y7	18.9	heavy	380	17.6
				686.4	1	y6	18.9	heavy	380	17.6
				571.4	1	y5	18.9	heavy	380	17.6
				470.3	1	y4	18.9	heavy	380	17.6

Table 1-3

7. Quantification by multiple reaction monitoring.

An Agilent 1260 Infinity HPLC system was used to inject 5 μL of digestion samples directly into a reversed phase analytical column (150 mm × 0.5 mm i.d., Agilent Zorbax SB-C18, 3.5-μm particle size) that was maintained at 40℃. Mobile phase A consisted of water/0.1% FA, and mobile phase B comprised ACN/0.1% FA. The peptides were separated and eluted at 20 μL/min on a linear gradient of mobile phase B from 3% to 40% B in 45 min. The gradient was ramped to 70% B for 5 min and 3% B for 10 min to equilibrate the column for the next run. The total LC run time was 60 min.

The MRM-MS data were analyzed using ESI on an Agilent 6490 triple quadrupole (QQQ) mass spectrometer (Agilent Technologies, Santa Clara, CA) that was equipped with an iFunnel Technology source and controlled by MassHunter Workstation software (Agilent, B.06.00). The MRM-MS analysis was conducted in the positive ion mode with the ion spray capillary voltage and nozzle voltage set to 2500 and 2000 V, respectively. The drying gas temperature was set to 250℃ at 15 L/min, and the sheath gas temperature was 350℃ at 12 L/min. The nebulizer was set to 30 psi, the fragmentor voltage was 380 V, and the cell accelerator voltage was 5 V. For the MRM-MS acquisition, delta EMV was set to 200 V. Quadrupoles 1 and 3 were maintained at unit (0.7 FWHM, full width at half maximum) resolution.

8. Collision energy optimization

The initial collision energy (CE) linear equation was derived from our optimized experiments, prior to the Skyline CE optimization step, using 600 stable isotope-labeled standard (SIS) peptides that were measured (data not

shown). In the CE optimization module in Skyline, "Step count" was set to 5 on either side of the equation-predicted value, and "Step size" was set to 2V. The b and y ions for 2^+ precursor ion charge states were used, and in total, 11 collision energy voltage values were considered for each fragment ion. The maximum number of concurrent measurements was set to 132. The data were acquired and imported into Skyline for peak area integration, which was reviewed manually and finalized by a single investigator.

9. Study design for blocking and randomization

Blocking and randomization can prevent the negative impacts of nonbiologic effects on molecular biomarker discovery [21]. In our experiments, nonbiologic effects could have been introduced during the sample preparation (order of MARS depletion and order of tryptic digestion) and MRM-MS analysis (order of injection). Three step where the experimenter's subjectivity could have led to bias of sample groups was negated by blocked randomization method.

We applied the blocked randomization design when assigning the sample group to remove confounding nonbiologic effects. There were equal numbers of cases (HCC group) and controls (normal group) in every block, with random block size. We then assigned each group of order to a random permutation of the samples in the corresponding group (Table 1-4). Blocked randomization was performed using Excel (2013, Microsoft) and Random Allocation (version 1.00, University of Medical Sciences).

Table 1-4. Study design for the blocking and randomization.

Sample ID	Number Annotation	Step 01 MARS depletion	Step 02 Sample preparation	Step 03 MRM-MS analysis	Group Annotation	Statistic analysis Normal group : 0 HCC group : 1
Normal_01	060	026	086	106	HCC	1
Normal_02	104	116	033	020	HCC	1
Normal_03	003	023	007	105	Normal	0
Normal_04	098	019	078	070	HCC	1
Normal_05	051	010	030	053	Normal	0
Normal_06	040	089	035	013	Normal	0
Normal_07	042	022	001	104	Normal	0
Normal_08	038	062	023	073	HCC	1
Normal_09	049	096	107	095	HCC	1
Normal_10	015	117	038	117	HCC	1
Normal_11	119	074	075	090	HCC	1
Normal_12	085	118	076	066	Normal	0
Normal_13	027	014	013	019	Normal	0
Normal_14	113	041	063	040	Normal	0
Normal_15	031	107	065	059	HCC	1
Normal_16	039	001	067	041	Normal	0
Normal_17	046	016	101	091	HCC	1
Normal_18	026	102	049	014	HCC	1
Normal_19	084	028	094	115	HCC	1
Normal_20	102	047	016	037	Normal	0
Normal_21	065	040	085	045	HCC	1
Normal_22	055	095	068	049	Normal	0
Normal_23	029	114	040	118	Normal	0
Normal_24	076	058	090	023	HCC	1
Normal_25	054	005	025	032	HCC	1
Normal_26	033	105	099	015	Normal	0
Normal_27	089	***	047	085	Normal	0
Normal_28	048	059	055	113	Normal	0
Normal_29	019	098	***	030	Normal	0
Normal_30	107	013	118	039	Normal	0
Normal_31	050	091	036	064	HCC	1
Normal_32	101	071	045	088	HCC	1
Normal_33	010	069	037	***		
Normal_34	043	115	010	120	HCC	1
Normal_35	001	054	080	026	Normal	0
Normal_36	041	075	022	084	Normal	0
Normal_37	008	021	026	077	HCC	1
Normal_38	018	099	114	119	Normal	0
Normal_39	078	119	109	079	HCC	1
Normal_40	044	032	034	035	HCC	1
Normal_41	030	033	021	102	Normal	0
Normal_42	072	109	041	096	HCC	1
Normal_43	066	093	079	065	Normal	0
Normal_44	118	110	060	097	HCC	1
Normal_45	105	042	050	057	HCC	1
Normal_46	110	004	024	029	Normal	0
Normal_47	017	029	097	076	Normal	0
Normal_48	024	043	071	075	HCC	1
Normal_49	058	048	084	021	HCC	1
Normal_50	108	066	028	022	Normal	0
Normal_51	111	085	014	068	HCC	1
Normal_52	013	060	044	017	Normal	0
Normal_53	036	063	006	048	Normal	0
Normal_54	092	006	116	083	HCC	1
Normal_55	022	009	043	018	Normal	0
Normal_56	009	025	004	107	Normal	0
Normal_57	080	024	073	002	HCC	1
Normal_58	087	045	102	103	HCC	1
Normal_59	053	008	061	050	Normal	0
Normal_60	037	052	***	***		

Table 1-4 (continue)

HCC_01	069	108	100	061	HCC	1
HCC_02	077	***	012	101	Normal	0
HCC_03	083	094	039	114	HCC	1
HCC_04	064	046	113	098	Normal	0
HCC_05	002	113	103	043	Normal	0
HCC_06	020	120	105	094	HCC	1
HCC_07	103	017	106	008	Normal	0
HCC_08	061	111	019	086	HCC	1
HCC_09	067	038	093	044	Normal	0
HCC_10	114	106	054	072	Normal	0
HCC_11	071	034	008	025	HCC	1
HCC_12	007	027	074	087	Normal	0
HCC_13	086	051	083	078	Normal	0
HCC_14	057	061	031	016	HCC	1
HCC_15	025	100	087	081	HCC	1
HCC_16	088	101	003	024	Normal	0
HCC_17	081	035	046	006	HCC	1
HCC_18	079	057	032	056	HCC	1
HCC_19	056	112	064	082	HCC	1
HCC_20	116	044	059	058	Normal	0
HCC_21	082	092	117	071	HCC	1
HCC_22	068	037	017	051	Normal	0
HCC_23	023	080	057	110	Normal	0
HCC_24	005	007	053	004	HCC	1
HCC_25	062	002	***	005	HCC	1
HCC_26	096	011	062	116	HCC	1
HCC_27	117	097	048	062	HCC	1
HCC_28	074	072	027	036	Normal	0
HCC_29	014	018	002	028	HCC	1
HCC_30	016	030	081	003	Normal	0
HCC_31	028	064	072	033	Normal	0
HCC_32	047	083	052	031	Normal	0
HCC_33	059	090	015	***		
HCC_34	075	104	098	060	Normal	0
HCC_35	091	012	020	093	HCC	1
HCC_36	115	003	077	074	HCC	1
HCC_37	021	049	082	069	HCC	1
HCC_38	099	067	066	099	HCC	1
HCC_39	032	***	120	055	Normal	0
HCC_40	109	081	069	111	Normal	0
HCC_41	093	015	042	012	HCC	1
HCC_42	004	020	005	009	Normal	0
HCC_43	063	031	011	089	Normal	0
HCC_44	006	039	091	046	Normal	0
HCC_45	045	084	051	063	HCC	1
HCC_46	052	065	112	108	Normal	0
HCC_47	094	055	111	092	Normal	0
HCC_48	034	070	070	052	HCC	1
HCC_49	120	076	018	109	HCC	1
HCC_50	106	050	092	034	HCC	1
HCC_51	100	073	009	100	HCC	1
HCC_52	035	078	110	054	Normal	0
HCC_53	112	077	104	067	HCC	1
HCC_54	011	103	095	001	Normal	0
HCC_55	097	086	119	042	Normal	0
HCC_56	090	088	***	080	Normal	0
HCC_57	070	079	088	027	Normal	0
HCC_58	012	056	058	007	HCC	1
HCC_59	073	082	089	038	Normal	0
HCC_60	095	068	029	010	Normal	0
		036	115	011	HCC	1
		087	056	047	HCC	1
		053	096	112	HCC	1
			108	i		

*** Blocked

Table 1-4

10. Statistical analysis of MRM-MS data

To analyze the MRM-MS data, raw MRM-MS data files were processed in Skyline. To increase the accuracy of the peak area integration, we manually confirmed and corrected the wrong automatic assignments for each targeted peak area. In our peak integration step, we used the Savitzky-Golay smoothing algorithm. Differences were analyzed by *T*-test between the normal versus HCC group and the LC versus stage I HCC subgroup. To evaluate the discriminatory power of the serum biomarkers between groups, we analyzed the receiver operator characteristic (ROC) curves and generated interactive plots. ROC curves were compared using DeLong's method [22]. All statistical analyses were performed using MedCalc (Mariakerke, Belgium, version 12.2.1).

RESULTS

1. Overall scheme

We performed a combined measurement in a single run of the total AFP concentration and glycosylated AFP fraction after PNGase F treatment. There are 3 glycosylated forms of AFP—AFP-L1, L2, and L3—based on its reactivity to Lens culinaris agglutinin (LCA) by affinity electrophoresis (Figure 1-4A). The concentration of total AFP and the N-linked glycosylated AFP fraction (AFP-L1, L2 and L3) that can be cleaved by PNGase F (Figure 1-4B) could be measured by MRM-MS in the same MRM run.

To develop an MRM-MS method for measuring glycoprotein concentration, such as AFP, we measured a standard glycoprotein of INV1 to determine whether MRM-MS was suitable for measuring glycoprotein concentrations and applied MRM-MS to measure AFP concentrations (Figure 1-5). The total AFP concentration was measured, based on nonglycopeptides, whereas the glycosyated AFP fraction was represented by the corresponding deglycopeptide that was generated by PNGase F treatment. Consequently, the discriminatory power was examined for total AFP and glycosylated AFP in serum samples from normal healthy controls versus HCC patients and liver cirrhosis versus early-stage HCC patients.

(A)

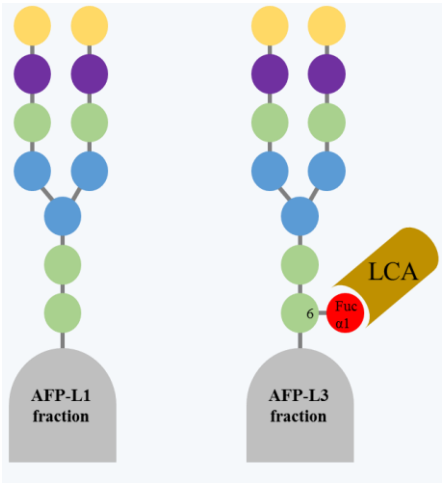

Figure 1-4A

(B)

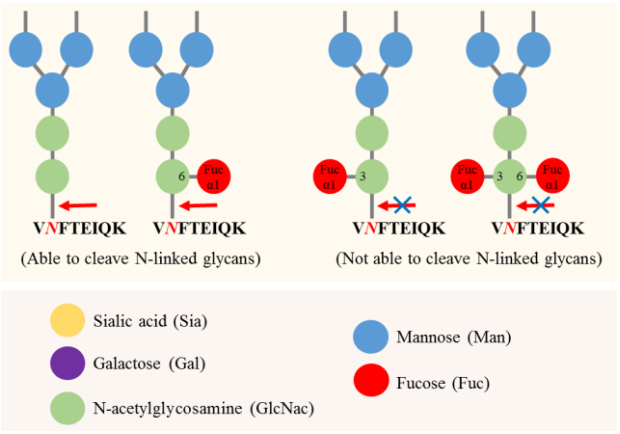

Figure 1-4B

Figure 1-4. Three glycosylated AFP forms (L1, L2, and L3) and cleavage pattern of peptide-N-glycosidase F (PNGase F).

(A) Total AFP can be separated into 3 subspecies—AFP-L1, L2, and L3—based on its reactivity to Lens culinaris agglutinin (LCA) on affinity electrophoresis. AFP-L1 does not react with LCA. AFP-L3 is the LCA-bound fraction of AFP. **(B)** PNGase F is an amidase that cleaves between the GlcNAc and asparagine residues (Asn, N) of high-mannose, hybrid, and complex oligosaccharides from N-linked glycoproteins. Conversely, PNGase F is unable to cleave N-linked glycans from glycoproteins when the GlcNAc residue is linked to an α1-3 fucose residue.

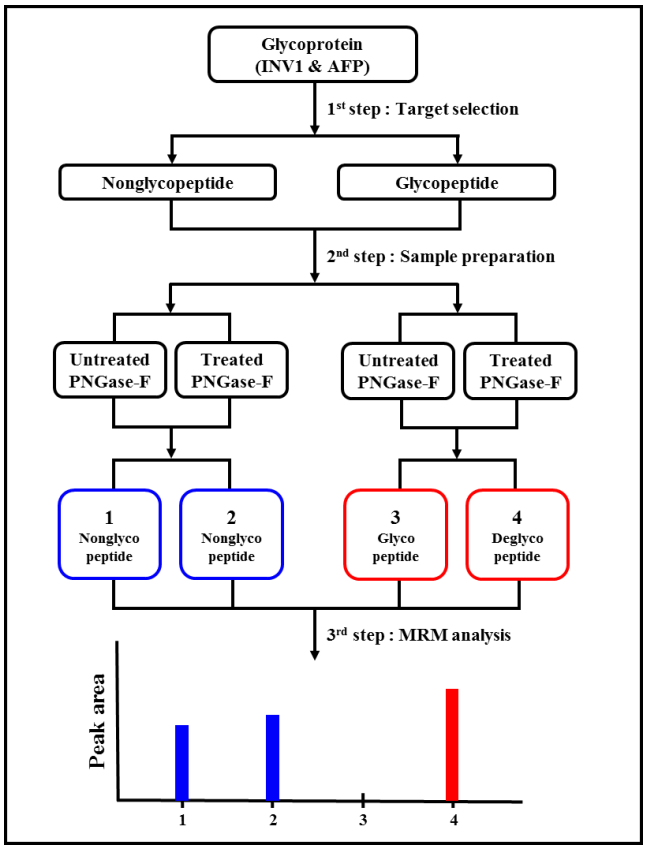

Figure 1-5

Figure 1-5. Development of MRM-MS method for measuring glycoproteins.

To develop the MRM-MS method for measuring nonglycopeptides, glycopeptides, and deglycopeptides, we determined whether our MRM-MS approach was suitable for measuring glycoproteins using a standard glycoprotein, such as yeast invertase 1 (INV1), and applied the MRM-MS method to measure the alpha-fetoprotein (AFP) in human serum samples.

2. Establishment of MRM-MS measurement using standard glycoprotein

We first determine whether MRM-MS is suitable for measuring glycoproteins using standard glycoproteins, such as yeast INV1. Four peptides were examined in developing and assessing the MRM-MS method (Figure 1-6 and Table 1-5): 2 peptides (IEIYSSDDLK and VVDFGK) were nonglycopeptides, and 2 were glycopeptides (NPVLAA*N*STQFR and FAT*N*TTLTK).

In examining their ability to be detected, all nonglycopeptides and deglycopeptides (SIS standard: Asn to Asp) coeluted with the corresponding SIS heavy peptides, whereas glycopeptides did not coelute with its SIS heavy peptide form (SIS standard: Asn with no glycan). Because the SIS heavy peptides were synthesized only using Asn with no glycan, the SIS heavy peptide that represents the glycopeptide comprises only amino acid residues; thus, the existence of a glycopeptide is measured alternatively in the form as in the MRM-MS (eg, glycosylated Asn is measured as Asn or Asp). We measured the 4 peptides using the corresponding SIS heavy peptides, as detailed in Figure 1-7A ~ Figure 1-7H. Because we could not use glycosylated SIS heavy peptides for the 2 glycopeptides, we measured the SIS heavy peptides NPVLAA*D*STQFR and FAT*D*TTLTK indirectly as substitutes for the glycopeptides NPVLAA*N*STQFR and FAT*N*TTLTK (Figure 1-7E & Figure 1-7G).

Two nonglycopeptides (IEIYSSDDLK; Figure 1-7A & 1-7B, and VVDFGK; Figure 1-7C & Figure 1-7D) were detected in the PNGase F-untreated (Figure 1-7A, Figure 1-7C) and PNGase F-treated (Figure 1-7B, Figure 1-7D) samples; the 2 nonglycopeptides had slightly greater intensity with PNGase F treatment (Figure 1-8). It is possible that PNGase F removes

the glycan of a peptide, which may effect the absence of steric hindrance due to the glycan, allowing trypsin approach to a target peptide more easily. Consequently this accessibility might increase digestion and affect the peak intensity of MS/MS spectra [23].

The 2 glycopeptides (NPVLAA*N*STQFR and FAT*N*TTLTK) were detected only with PNGage F treatment as peaks of the corresponding deglycopeptides (NPVLAA*D*STQFR; Figure 1-7E, and FAT*D*TTLTK; Figure 1-7G). In the PNGase F-untreated, no extracted ion chromatogram (XIC) was detected for the endogenous glycopeptide forms, whereas SIS heavy peptides were detected with unglycosylated Asn (NPVLAA*N*STQFR; Figure 1-7E, and FAT*N*TTLTK; Figure 1-7G). In the MRM-MS analysis, glycopeptides could not be detected, because they were measured, based on the original sequence—ie, NPVLAA*N*STQFR and FAT*N*TTLTK, respectively. Conversely, the corresponding deglycosylated sequences for PNGage F-treated glycopeptides—NPVLAA*D*STQFR and FAT*D*TTLTK—were detected as MRM peaks for the glycosylated peptides of NPVLAA*N*STQFR and FAT*N*TTLTK, respectively.

To develop the quantitative method, we evaluated the linearity of nonglycopeptides, glycopeptides, and deglycopeptides that originated from INV1 by analyzing the standard curves of serial dilutions for known concentrations of SIS heavy peptides. To generate calibration curves for the 3 types of peptides, SIS heavy peptides were serially diluted (0, 4, 13, 40, 120, and 370 fmol), with the light peptides as internal standards. Digested light yeast peptide (370 nmol) was added to each diluted sample. Each experiment was repeated in triplicate to generate coefficients of variation (%CV) and calibration curve values (R^2).

The calibration curves demonstrated linearity over more than 2 orders of magnitude for the concentration ranges and strong linear correlation (R^2 > 0.99) in all 3 peptide forms (Figure 1-9A ~ Figure 1-9D). By MRM-MS analysis using the standard peptides, we developed the MRM-MS method for measuring glycoprotein concentrations. Notably, the PNGase F-untreated endogenous light glycopeptides (NPVLAA*N*STQFR and FAT*N*TTLTK, filled downward arrows) did not generate peaks from MRM, as shown in Figure 1-9C & 1-9D.

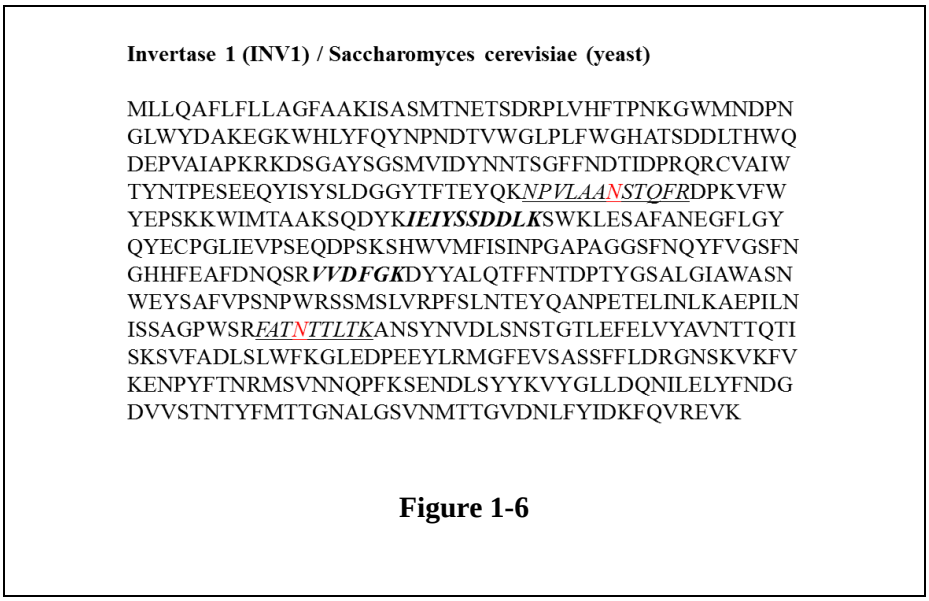

Figure 1-6

Figure 1-6. Full sequence of standard glycoprotein invertase 1 (INV1, yeast).

Glycopeptide is in italics and underlined; N-glycosylation sites are labeled red. Nonglycopeptide is in italics and bold.

Table 1-5. List of peptides and product ions for the standard glycoprotein (INV1).

Peptide type	Peptide sequence	Q1 (m/z)	Q1 ion charge	Q3 (m/z)	Q3 ion charge	Q3 ion type	Retention time (min)	Isotype	Fragmentor (volt)	Collision energy (volt)
Non glycopeptide	IEIYSSDDLK	591.8	2	1069.5	1	y9	23.5	light	380	20.9
				940.5	1	y8	23.5	light	380	20.9
				827.4	1	y7	23.5	light	380	20.9
				664.3	1	y6	23.5	light	380	20.9
				356.2	1	b3	23.5	light	380	20.9
	IEIYSSDDLK	595.8	2	1077.5	1	y9	23.5	heavy	380	20.9
				948.5	1	y8	23.5	heavy	380	20.9
				835.4	1	y7	23.5	heavy	380	20.9
				672.3	1	y6	23.5	heavy	380	20.9
				356.2	1	b3	23.5	heavy	380	20.9
Non glycopeptide	VVDFGK	332.7	2	565.3	1	y5	16.1	light	380	11.6
				466.2	1	y4	16.1	light	380	11.6
				351.2	1	y3	16.1	light	380	11.6
				204.1	1	y2	16.1	light	380	11.6
				199.1	1	b2	16.1	light	380	11.6
	VVDFGK	336.7	2	573.3	1	y5	16.1	heavy	380	11.6
				474.2	1	y4	16.1	heavy	380	11.6
				359.2	1	y3	16.1	heavy	380	11.6
				212.1	1	y2	16.1	heavy	380	11.6
				199.1	1	b2	16.1	heavy	380	11.6
Glycopeptide	NPVLAA*N*STQFR	659.3	2	1007.5	1	y9	22.4	light	380	23.3
				894.4	1	y8	22.4	light	380	23.3
				823.4	1	y7	22.4	light	380	23.3
				752.4	1	y6	22.4	light	380	23.3
				638.3	1	y5	22.4	light	380	23.3
	NPVLAA*N*STQFR	664.4	2	1017.5	1	y9	22.4	heavy	380	23.3
				904.5	1	y8	22.4	heavy	380	23.3
				833.4	1	y7	22.4	heavy	380	23.3
				762.4	1	y6	22.4	heavy	380	23.3
				648.3	1	y5	22.4	heavy	380	23.3
Deglycopeptide	NPVLAA*D*STQFR	659.8	2	1008.5	1	y9	23.2	light	380	23.3
				895.4	1	y8	23.2	light	380	23.3
				824.4	1	y7	23.2	light	380	23.3
				753.4	1	y6	23.2	light	380	23.3
				638.3	1	y5	23.2	light	380	23.3
	NPVLAA*D*STQFR	664.8	2	1018.5	1	y9	23.2	heavy	380	23.3
				905.4	1	y8	23.2	heavy	380	23.3
				834.4	1	y7	23.2	heavy	380	23.3
				763.4	1	y6	23.2	heavy	380	23.3
				648.3	1	y5	23.2	heavy	380	23.3
Glycopeptide	FAT*N*TTLTK	498.8	2	849.5	1	y8	18.9	light	380	17.6
				778.4	1	y7	18.9	light	380	17.6
				677.4	1	y6	18.9	light	380	17.6
				563.3	1	y5	18.9	light	380	17.6
				462.3	1	y4	18.9	light	380	17.6
	FAT*N*TTLTK	502.8	2	857.5	1	y8	18.9	heavy	380	17.6
				786.4	1	y7	18.9	heavy	380	17.6
				685.4	1	y6	18.9	heavy	380	17.6
				571.4	1	y5	18.9	heavy	380	17.6
				470.3	1	y4	18.9	heavy	380	17.6
Deglycopeptide	FAT*D*TTLTK	499.3	2	850.5	1	y8	18.9	light	380	17.6
				779.4	1	y7	18.9	light	380	17.6
				678.4	1	y6	18.9	light	380	17.6
				563.3	1	y5	18.9	light	380	17.6
				462.3	1	y4	18.9	light	380	17.6
	FAT*D*TTLTK	503.3	2	858.5	1	y8	18.9	heavy	380	17.6
				787.4	1	y7	18.9	heavy	380	17.6
				686.4	1	y6	18.9	heavy	380	17.6
				571.4	1	y5	18.9	heavy	380	17.6
				470.3	1	y4	18.9	heavy	380	17.6

Table 1-5

(A)

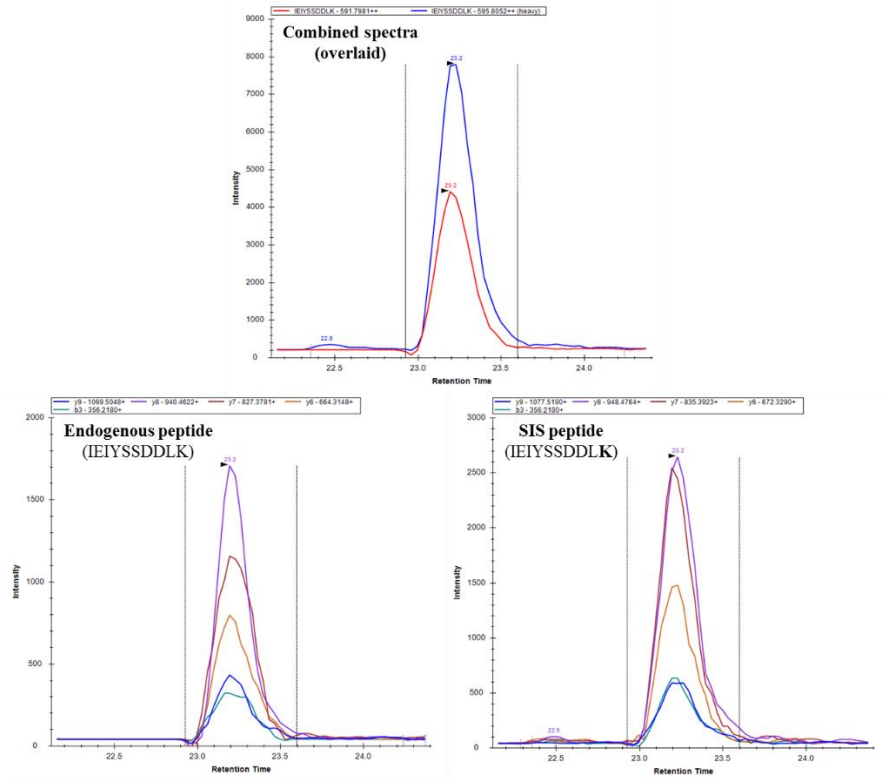
Combined spectra
(overlaid)
Intensity
Retention Time
Endogenous peptide
(IEIYSSDDLK)
SIS peptide
(IEIYSSDDLK)

Figure 1-7A

(B)

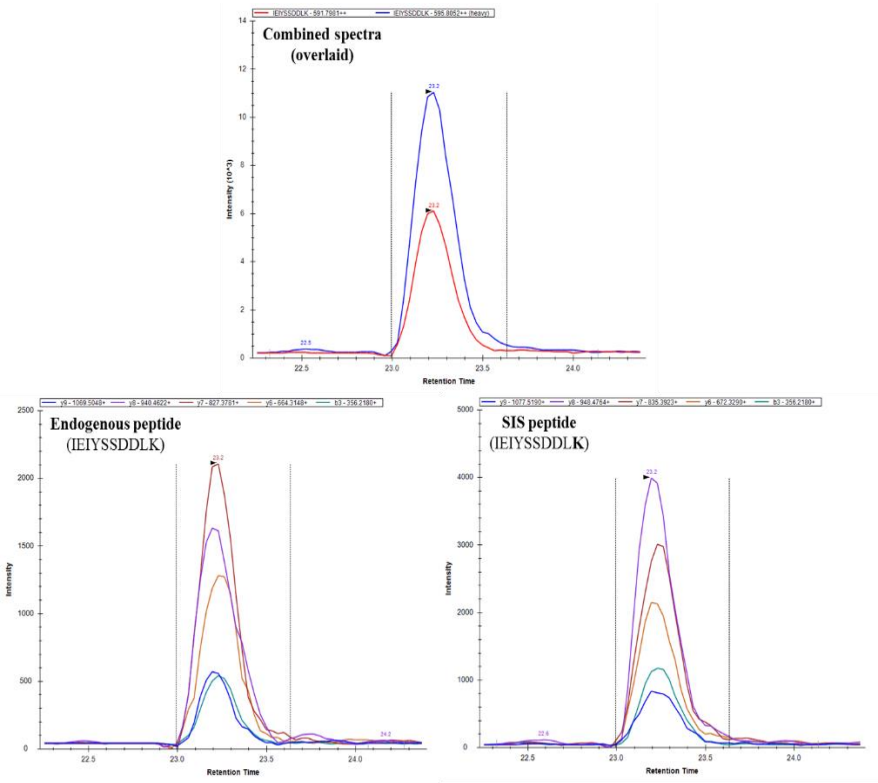
Combined spectra
(overlaid)
Intensity (1E+3)
Retention Time
Endogenous peptide
(IEIYSSDDLK)
Intensity
Retention Time
SIS peptide
(IEIYSSDDLK)
Intensity
Retention Time

Figure 1-7B

(C)

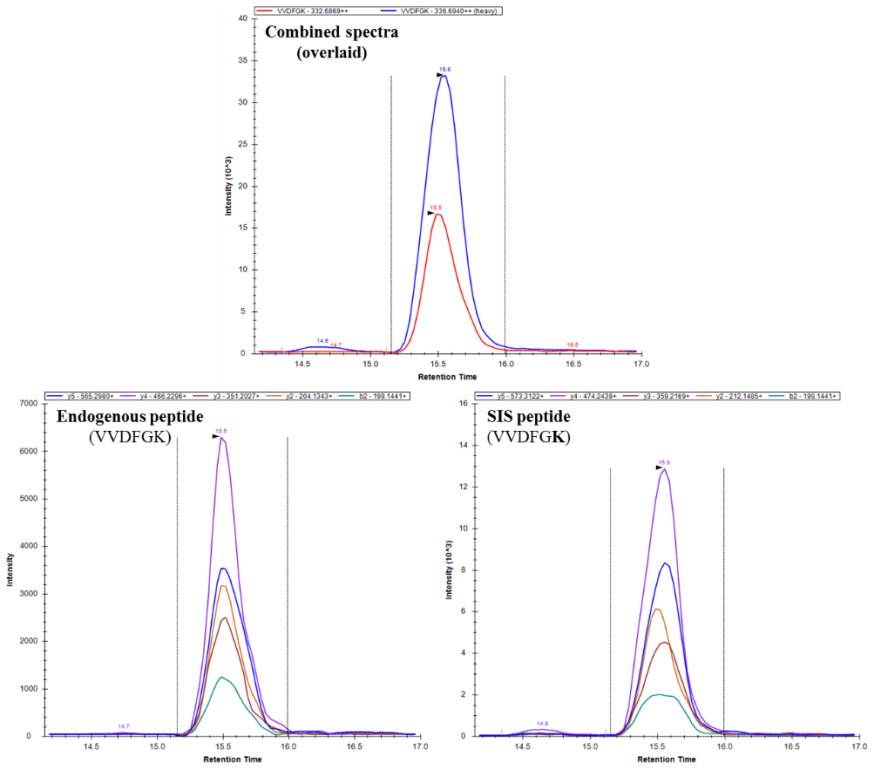
Combined spectra
(overlaid)
Intensity (10^3)
Retention Time
Endogenous peptide
(VVDFGK)
Intensity
Retention Time
SIS peptide
(VVDFGK)
Intensity (10^3)
Retention Time

Figure 1-7C

(D)

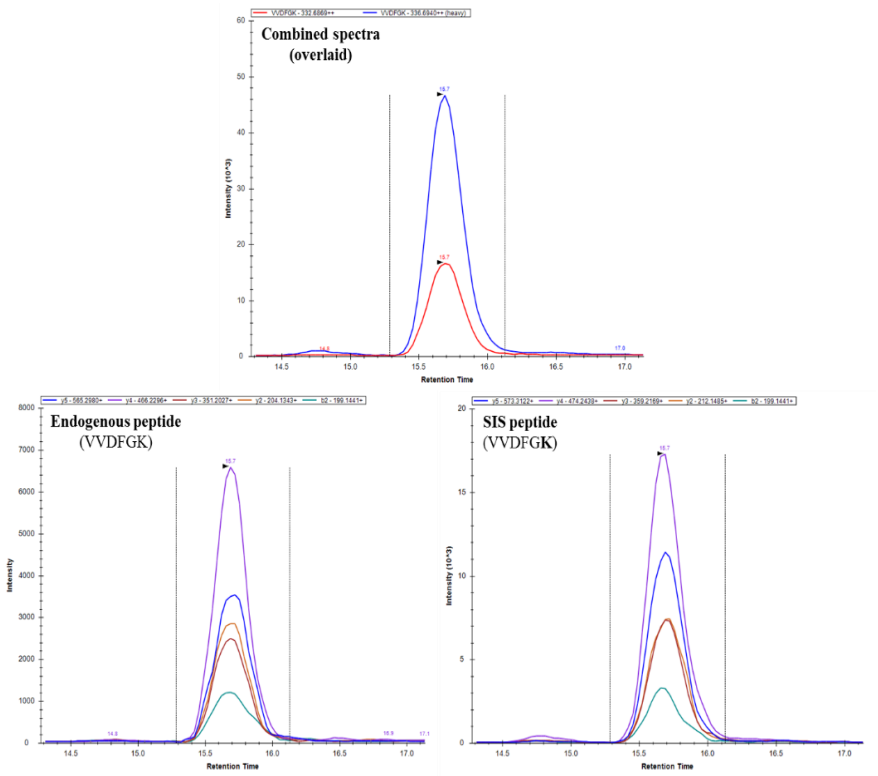
Combined spectra
(overlaid)
Intensity (10^3)
Retention Time
Endogenous peptide
(VVDFGK)
Intensity
Retention Time
SIS peptide
(VVDFGK)
Intensity (10^3)
Retention Time

Figure 1-7D

(E)

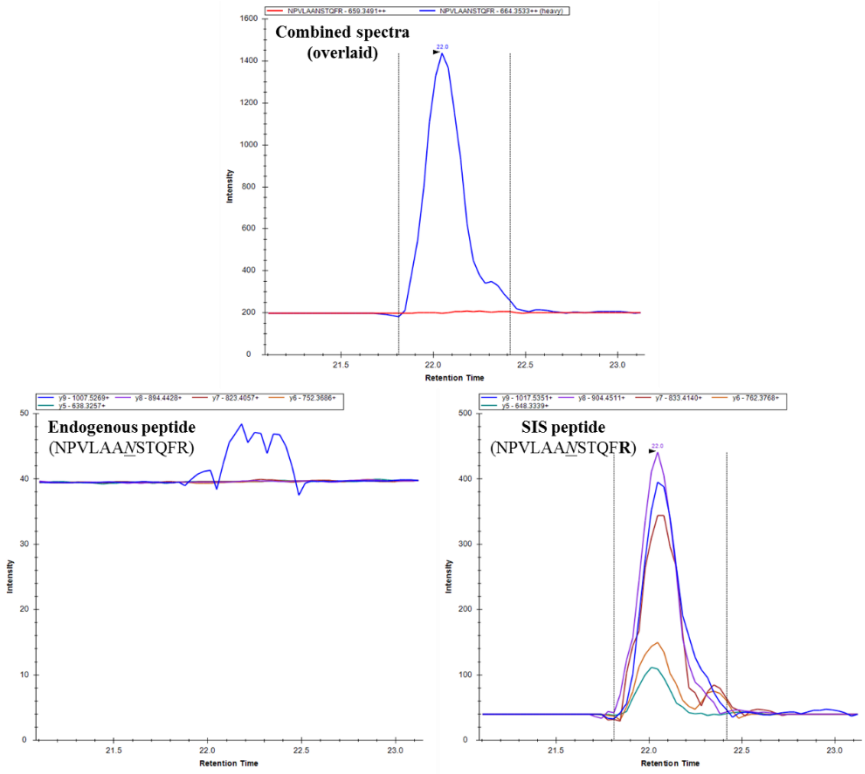
Combined spectra
(overlaid)
Intensity
Retention Time
Endogenous peptide
(NPVLAANSTQFR)
SIS peptide
(NPVLAANSTQFR)

Figure 1-7E

(F)

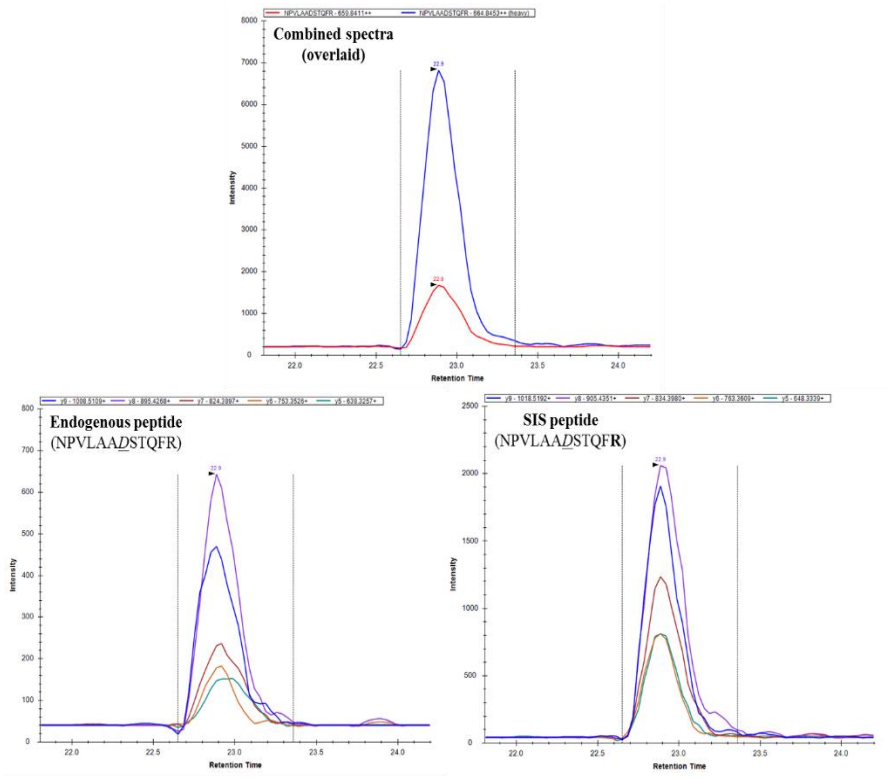
Combined spectra
(overlaid)
Intensity
Retention Time
Endogenous peptide
(NPVLAADSTQFR)
SIS peptide
(NPVLAADSTQFR)

Figure 1-7F

(G)

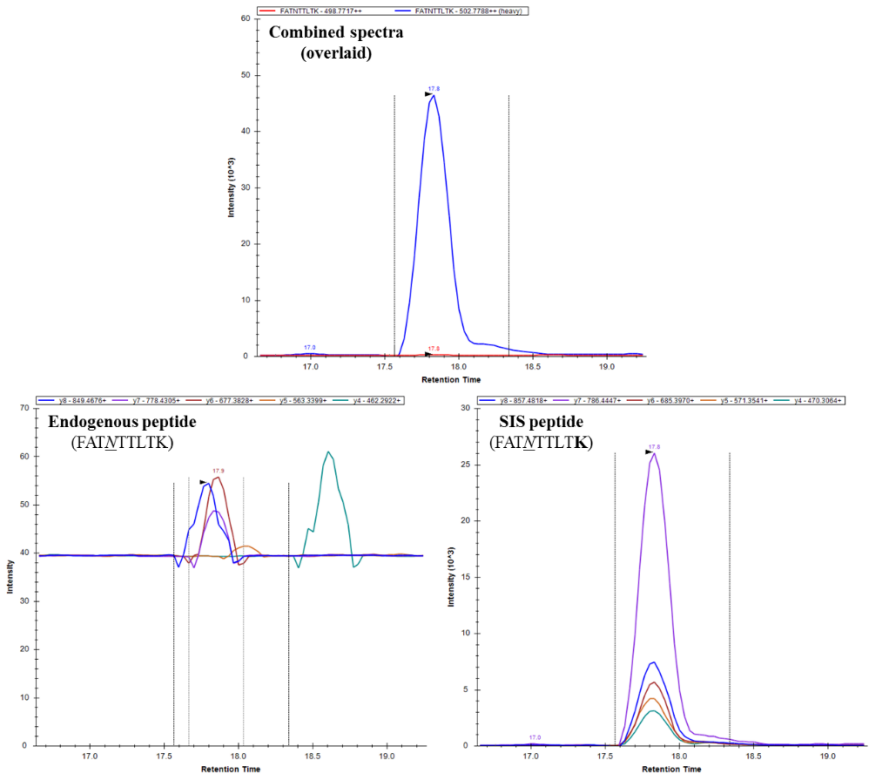
Combined spectra
(overlaid)
Intensity (10^3)
Retention Time
Endogenous peptide
(FATNTTLTK)
Intensity
Retention Time
SIS peptide
(FATNTTLTK)
Intensity (10^3)
Retention Time

Figure 1-7G

(H)

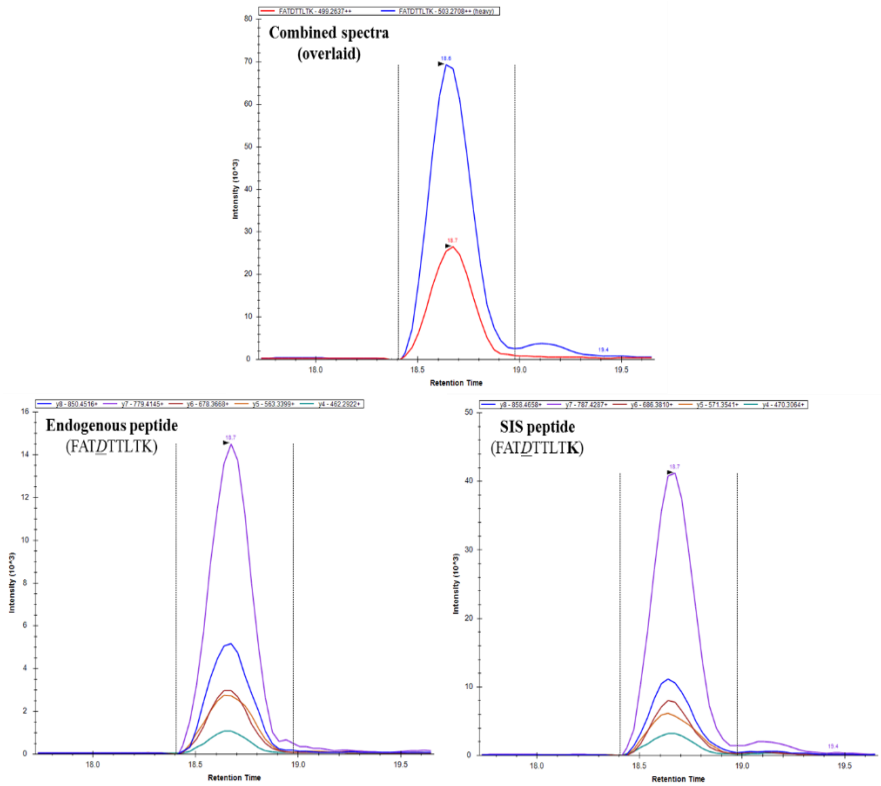

Figure 1-7H

Figure 1-7. Confirmation of detectability for nonglycopeptides, glycopeptides, and deglycopeptides.

(A-D) Two nonglycopeptides were treated with PNGase F or not, wherein the endogenous light peptides and corresponding SIS heavy peptides coeluted at the same retention time and the transitions were well overlaid. **(E, G)** For the glycopeptide, the endogenous light peptides did not coelute with their corresponding SIS heavy peptides. **(F, H)** For the deglycopeptide, the

endogenous light peptides coeluted with their corresponding SIS heavy peptides. In the MRM-MS analysis, all nonglycopeptides and deglycopeptides were detected as endogenous light and SIS heavy peptides that coeluted, whereas glycopeptides were detected only in their SIS heavy peptide form.

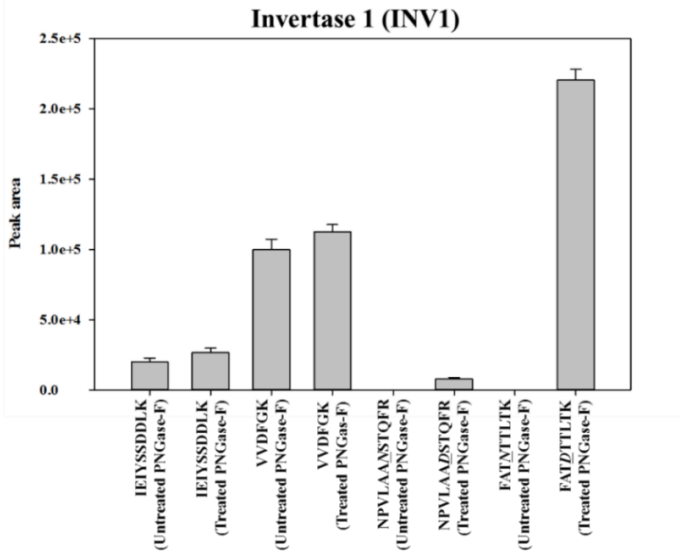

Figure 1-8

Figure 1-8. Peak intensities of MRM analysis for target peptides.

Two nonglycopeptides (IEIYSSDDLK, VVDFGK), 2 glycopeptides (NPVLAA*N*STQFR, FAT*N*TTLTK), and 2 deglycopeptides (NPVLAA*D*STQFR, FAT*D*TTLTK) of the standard glycoprotein (INV1) are shown.

(A)

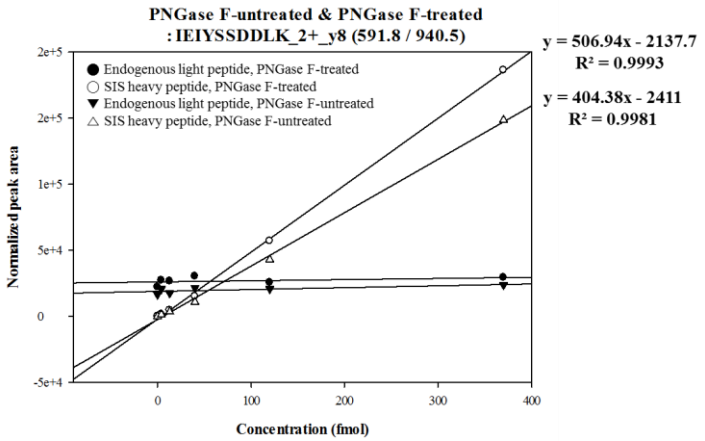

Figure 1-9A

(B)

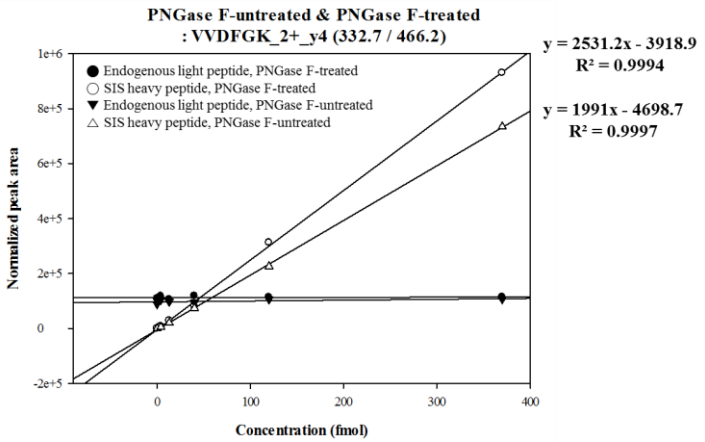

Figure 1-9B

(C)

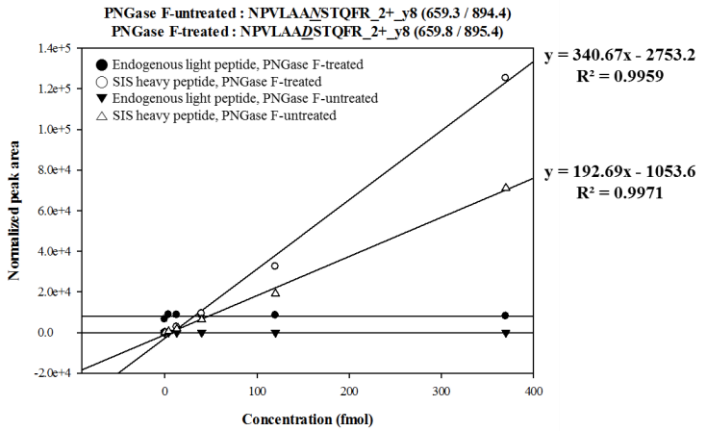

Figure 1-9C

(D)

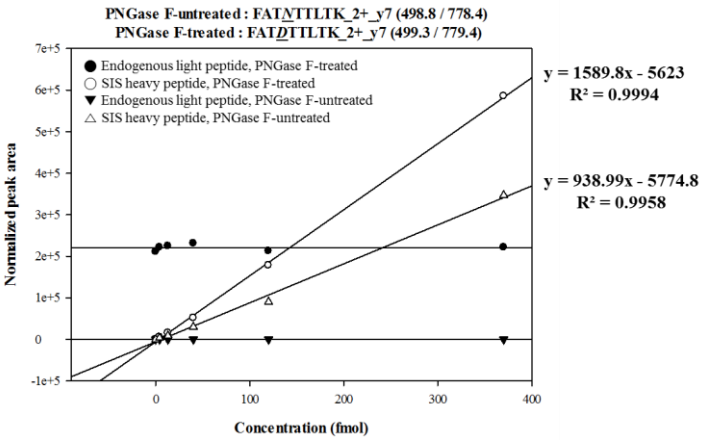

Figure 1-9D

Figure 1-9. Linear response curves for target peptides.

A, B) Two nonglycopeptides (IEIYSSDDLK, VVDFGK) of the standard glycoprotein (INV1) are shown. **C, D)** Two glycopeptides (NPVLAA*N*STQFR, FAT*N*TTLTK), and 2 deglycopeptides (NPVLAA*D*STQFR, FAT*D*TTLTK) of the standard glycoprotein (INV1) are shown.

3. Preliminary MRM-MS using pooled serum samples

Prior to MRM-MS of AFP using individual samples, we first selected predictable transitions using Skyline, in which the N-linked glycopeptide included the NxS/T motif, whereas the nonglycopeptide did not. 3 AFP peptides that were used in the MRM-MS; the sequences of the nonglycopeptide, glycopeptide, and deglycopeptide of AFP were GYQELLEK, V*N*FTEIQK, and V*D*FTEIQK, respectively. For MRM-MS of the 3 AFP peptides, we determined their detectability in the preliminary MRM-MS run (Table 1-6 and Figure 1-10).

Nonglycopeptides (GYQELLEK) and deglycopeptide (V*D*FTEIQK) of AFP coeluted with the endogenous light and SIS heavy peptides at the same retention time. In brief, the nonglycopeptide (GYQELLEK) was coeluted in the PNGase F-untreated (Figure 1-11A) and PNGase F-treated (Figure 1-11B) conditions. However, the glycopeptide was not detected (Figure 1-11C) when the PNGase F-untreated glycosylated peptide was analyzed by the glycopeptide form with the no-glycan form (V*N*FTEIQK). The PNGage F-treated glycosylated peptide coeluted (Figure 1-11D) with the deglycopeptide form (V*D*FTEIQK).

Serum AFP concentrations rise in HCC patients versus normal subjects [24-27]; thus, we examined this difference between the normal healthy

and HCC group using MRM-MS measurements. 20 normal samples and 20 HCC samples were pooled separately and analyzed by MRM-MS using the nonglycopeptide (GYQELLEK). The MS/MS intensity for the nonglycopeptide increased in the normal versus HCC group (Figure 1-12).

With regard to measuring glycopeptide concentrations, because the glycosylated glycopeptide form (V*N*FTEIQK) could not be detected directly using MRM-MS, we analyzed the deglycopeptide form (V*D*FTEIQK), which was generated by treating V*N*FTEIQK with PNGase F. The normalized peak area for the nonglycopeptide and deglycopeptide increased in HCC patients versus the normal group (Figure 1-12). Particularly, the peak area ratio of HCC to the normal group was 6.5 and 66.5 for the nonglycopeptide and deglycopeptide, respectively, indicating that total AFP concentration is a useful index for liver cancer diagnostics and that measuring the fraction of glycosylated AFP that has been treated by PNGase F is a more important element in HCC diagnosis.

Alpha-fetoprotein (AFP) / Homo sapiens (human)

MKWVESIFLIFLLNFTESRTLHRNEYGIASILDSYQCTAEISLADLA
TIFFAQFVQEATYKEVSKMVKDALTAIEKPTGDEQSSGCLENQLP
AFLEELCHEKEILEKYGHSDCCSQSEEGRHNCFLAHKKPTPASIPL
FQVPEPVTSCEAYEEDRETFMNKFIYEIARRHPFLYAPTILLWAAR
YDKIIPSCCKAENAVECFQTKAATVTKELRESSLLNQHACAVMKN
FGTRTFQAITVTKLSQKFTK*IVNFTEIQK*LVLDVAHVHEHCCRGDV
LDCLQDGEKIMSYICSQQDTLSNKITECCKLTTLERGQCIIHAEND
EKPEGLSPNLNRFLGDRDFNQFSSGEKNIFLASFVHEYSRRHPQL
AVSVILRVAK***GYQELLEK***CFQTENPLECQDKGEEELQKYIQESQA
LAKRSCGLFQKLGEYYLQNAFLVAYTKKAPQLTSSELMAITRKM
AATAATCCQLSEDKLLACGEGAADIIIGHLCIRHEMTPVNPGVGQ
CCTSSYANRRPCFSSLVVDETYVPPAFSDDKFIFHKDLCQAQGVA
LQTMKQEFLINLVKQKPQITEEQLEAVIADFSGLLEKCCQGQEQE
VCFAEEGQKLISKTRAALGV

Figure 1-10

Figure 1-10. Full sequence of alpha-fetoprotein (AFP, human).

Glycopeptide is in italics and underlined; N-glycosylation sites are labeled red.

Nonglycopeptide is in italics and bold.

Table 1-6. AFP peptides and their parameters for MRM-MS.

Peptide type	Peptide sequence	Q1 (m/z)	Q1 ion charge	Q3 (m/z)	Q1 ion charge	Q3 ion type	Retention time (min)	Isotype	Fragmentor (volt)	Initial CE (volt)	Optimized CE (volt)
Nonglycopeptide	GYQELLEK	490.3	2	759.4	1	y6	23.6	light	380	17.3	11.3
				631.4	1	y5	23.6	light	380	17.3	13.3
				502.3	1	y4	23.6	light	380	17.3	15.3
				389.2	1	y3	23.6	light	380	17.3	17.3
				276.2	1	y2	23.6	light	380	17.3	21.3
				221.1	1	b2	23.6	light	380	17.3	11.3
				349.2	1	b3	23.6	light	380	17.3	9.3
				591.3	1	b5	23.6	light	380	17.3	11.3
				704.4	1	b6	23.6	light	380	17.3	7.3
				833.4	1	b7	23.6	light	380	17.3	9.3
	GYQELLE**K**	494.3	2	767.4	1	y6	23.6	heavy	380	17.3	11.3
				639.4	1	y5	23.6	heavy	380	17.3	13.3
				510.3	1	y4	23.6	heavy	380	17.3	15.3
				397.3	1	y3	23.6	heavy	380	17.3	17.3
				284.2	1	y2	23.6	heavy	380	17.3	21.3
				221.1	1	b2	23.6	heavy	380	17.3	11.3
				349.2	1	b3	23.6	heavy	380	17.3	9.3
				591.3	1	b5	23.6	heavy	380	17.3	11.3
				704.4	1	b6	23.6	heavy	380	17.3	7.3
				833.4	1	b7	23.6	heavy	380	17.3	9.3
Glycopeptide[a]	V*N*FTEIQK	489.8	2	879.5	1	y7	22.0	light	380	17.3	13.3
				765.4	1	y6	22.0	light	380	17.3	13.3
				618.3	1	y5	22.0	light	380	17.3	15.3
				517.3	1	y4	22.0	light	380	17.3	11.3
				388.3	1	y3	22.0	light	380	17.3	21.3
				275.2	1	y2	22.0	light	380	17.3	21.3
				361.2	1	b3	22.0	light	380	17.3	9.3
				462.2	1	b4	22.0	light	380	17.3	9.3
				591.3	1	b5	22.0	light	380	17.3	11.3
				704.4	1	b6	22.0	light	380	17.3	9.3
				832.4	1	b7	22.0	light	380	17.3	7.3
	V*N*FTEIQ**K**	493.8	2	887.5	1	y7	22.0	heavy	380	17.3	13.3
				773.4	1	y6	22.0	heavy	380	17.3	13.3
				626.4	1	y5	22.0	heavy	380	17.3	15.3
				525.3	1	y4	22.0	heavy	380	17.3	11.3
				396.3	1	y3	22.0	heavy	380	17.3	21.3
				283.2	1	y2	22.0	heavy	380	17.3	21.3
				361.2	1	b3	22.0	heavy	380	17.3	9.3
				462.2	1	b4	22.0	heavy	380	17.3	9.3
				591.3	1	b5	22.0	heavy	380	17.3	11.3
				704.4	1	b6	22.0	heavy	380	17.3	9.3
				832.4	1	b7	22.0	heavy	380	17.3	7.3
Deglycopeptide	V*D*FTEIQK	490.3	2	880.4	1	y7	22.7	light	380	17.3	13.3
				765.4	1	y6	22.7	light	380	17.3	13.3
				618.3	1	y5	22.7	light	380	17.3	15.3
				517.3	1	y4	22.7	light	380	17.3	11.3
				388.3	1	y3	22.7	light	380	17.3	21.3
				275.2	1	y2	22.7	light	380	17.3	21.3
				362.2	1	b3	22.7	light	380	17.3	9.3
				463.2	1	b4	22.7	light	380	17.3	9.3
				592.3	1	b5	22.7	light	380	17.3	11.3
				705.3	1	b6	22.7	light	380	17.3	9.3
				833.4	1	b7	22.7	light	380	17.3	7.3
	V*D*FTEIQ**K**	494.3	2	888.5	1	y7	22.7	heavy	380	17.3	13.3
				773.4	1	y6	22.7	heavy	380	17.3	13.3
				626.4	1	y5	22.7	heavy	380	17.3	15.3
				525.3	1	y4	22.7	heavy	380	17.3	11.3
				396.3	1	y3	22.7	heavy	380	17.3	21.3
				283.2	1	y2	22.7	heavy	380	17.3	21.3
				362.2	1	b3	22.7	heavy	380	17.3	9.3
				463.2	1	b4	22.7	heavy	380	17.3	9.3
				592.3	1	b5	22.7	heavy	380	17.3	11.3
				705.3	1	b6	22.7	heavy	380	17.3	9.3
				833.4	1	b7	22.7	heavy	380	17.3	7.3

[a] The molecular mass of glycopeptide is estimated based on Asn with no glycan moiety.

Table 1-6

(A)

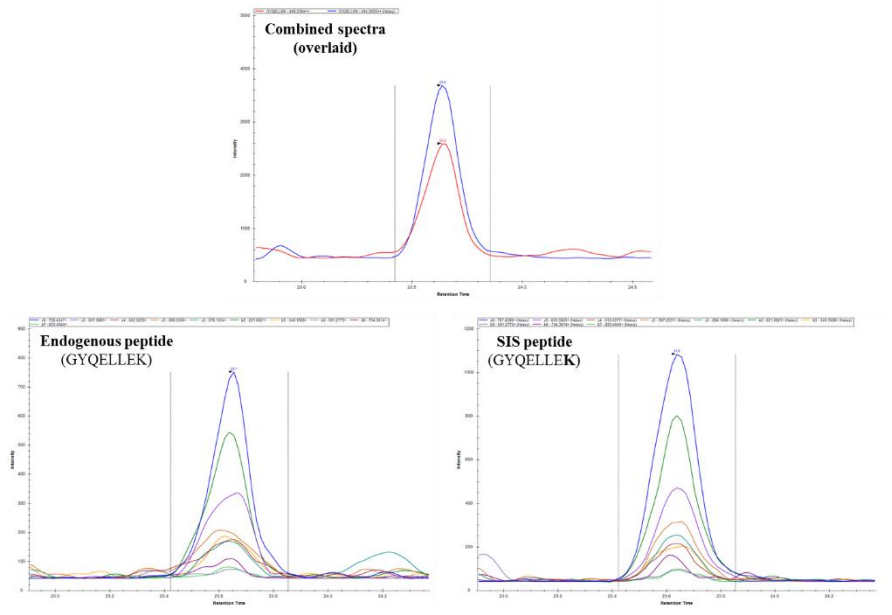

Figure 1-11A

(B)

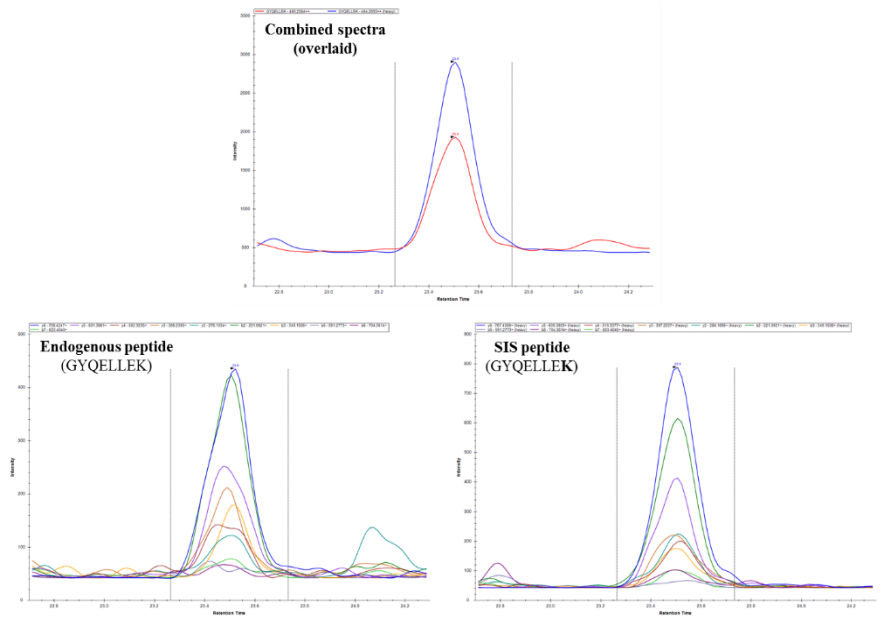

Figure 1-11B

(C)

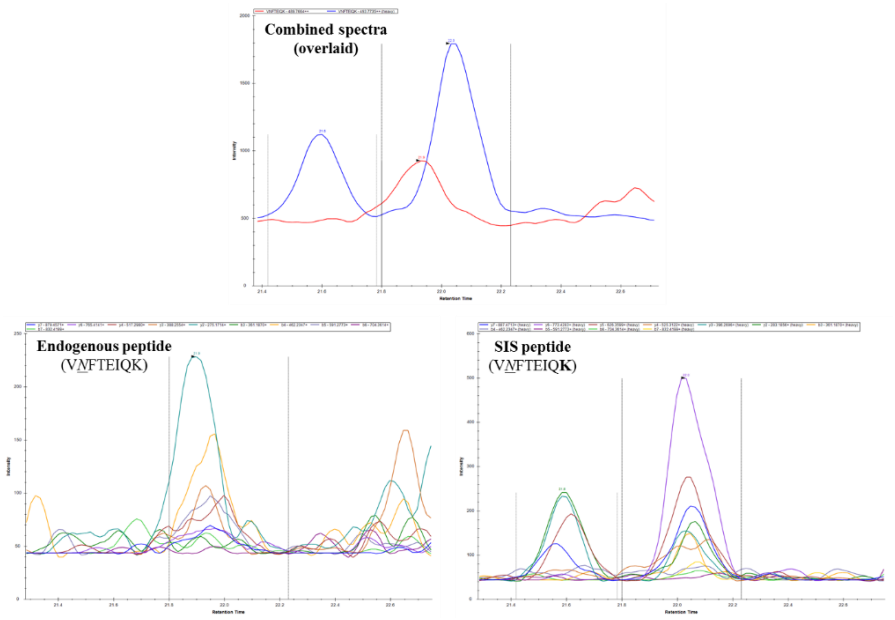

Figure 1-11C

(D)

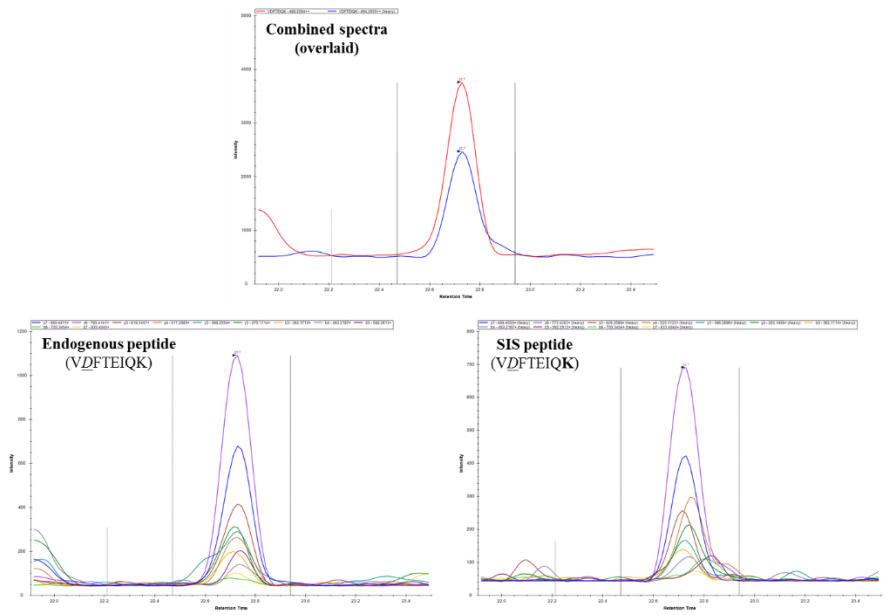

Figure 1-11D

Figure 1-11. Confirmation of detectability for nonglycopeptide, glycopeptide, and deglycopeptide.

(A, B) The nonglycopeptide was treated with PNGase F or not, wherein the endogenous light peptides and corresponding SIS heavy peptides coeluted at the same retention time and the transitions were well overlaid. **(C)** The glycopeptide was untreated with PNGase F, and endogenous light peptide that did not coelute with the SIS heavy peptide. **(D)** The deglycopeptide was treated with PNGase F, and the endogenous light peptide coeluted with the SIS heavy peptide. The nonglycopeptide and deglycopeptide were detected as coeluted endogenous light and SIS heavy peptides, whereas the glycopeptide was

detected only in its SIS heavy peptide form, because the glycopeptide with a glycan could not be identified in this MRM-MS.

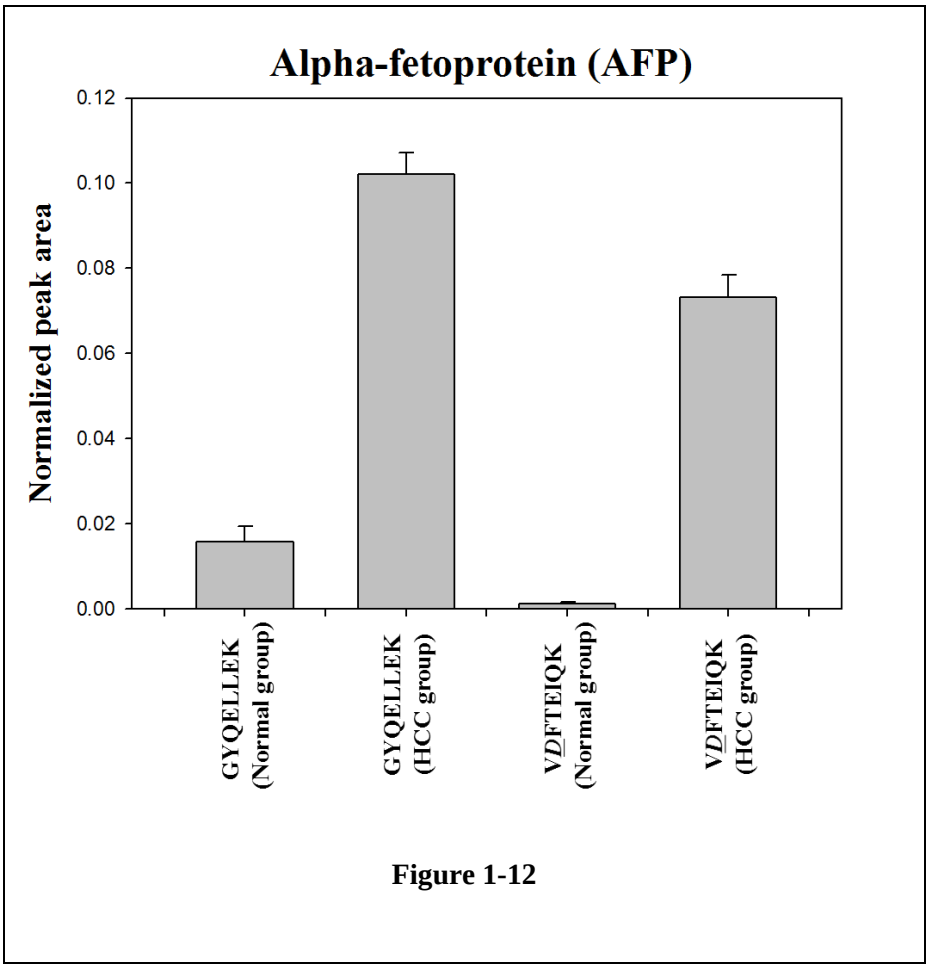

Figure 1-12

Figure 1-12. Preliminary MRM-MS analysis using pooled serum samples. Normal samples (n = 20) and HCC samples (n = 20) were pooled separately and analyzed by MRM-MS using the nonglycopeptide (GYQELLEK) and deglycopeptide (V*D*FTEIQK).

4. Linearity of calibration curve for SIS AFP peptide

In the quantitative MRM-MS analysis, we determined the linearity of the nonglycopeptide (GYQELLEK) and deglycopeptide (V*D*FTEIQK) with regard to AFP, which was performed by generating a standard curve for the nonglycopeptide and deglycopeptide, composed of serial dilutions for known concentrations of SIS heavy peptides. SIS heavy peptides were serially diluted (9 concentrations: 0.0, 0.8, 1.6, 3.1, 6.3, 12.5, 25.0, 50.0, and 100.0 fmol) with the endogenous light peptide as an internal standard (pooled serum: 5 μg), added to each serially diluted sample. Each experiment was repeated in triplicate to generate coefficients of variation (%CV) and calibration curve values (R^2). The calibration curves were linear over more than 2 orders of magnitude in concentration, wherein the nonglycopeptide (GYQELLEK) and deglycopeptide (V*D*FTEIQ) showed strong linearity ($R^2 > 0.99$) (Figure 1-13).

(A)

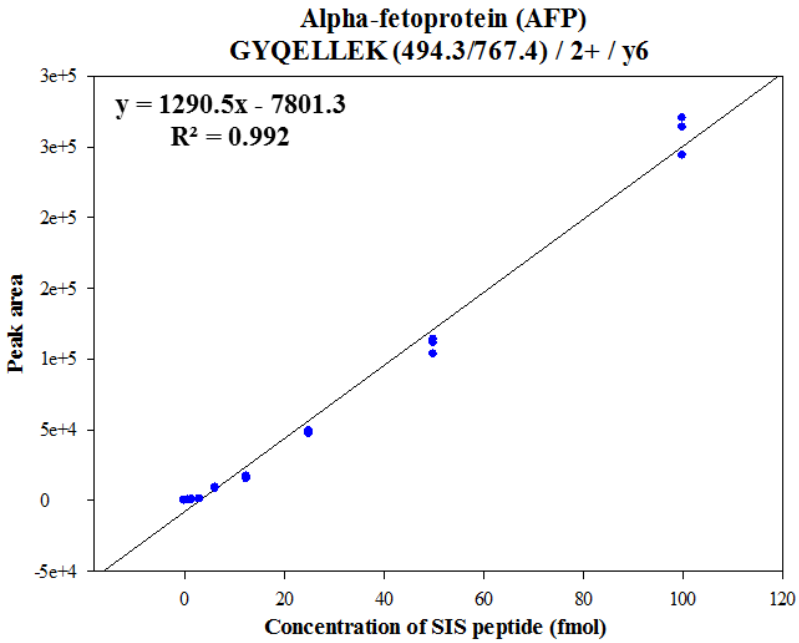

Figure 1-13A

(B)

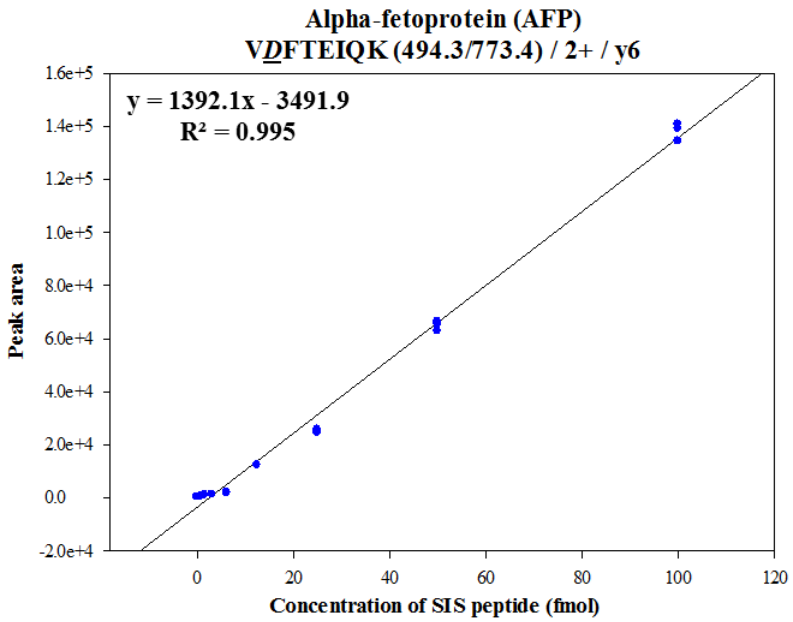

Figure 1-13B

Figure 1-13. Generation of calibration curve for nonglycopeptide (GYQELLEK) and deglycopeptide (V*D*FTEIQK) of AFP.

(A) To generate a calibration curve for the nonglycopeptide and **(B)** deglycopeptide, SIS heavy peptides were serially diluted (9 concentration points: 0.0, 0.8, 1.6, 3.1, 6.3, 12.5, 25.0, 50.0, and 100.0 fmol) with the endogenous light peptide as an internal standard (pooled serum: 5 µg), added to each serially diluted sample. Each experiment was performed in triplicate to generate coefficients of variation (%CV) and calibration curve values (R^2).

5. MRM-MS measurements of AFP peptides using individual serum samples

To measure the nonglycopeptide (GYQELLEK) and deglycopeptide (V*D*FTEIQK) of AFP using MRM-MS in individual normal and HCC serum samples, we determined the optimal spiking concentrations for SIS heavy peptides that minimized the measurement errors for the peak area ratio between endogenous light peptide and SIS heavy peptide. By MRM analysis using pooled samples, which comprised endogenous light (pooled serum: 5 µg) and serially diluted SIS heavy peptides (0–200 fmol), we determined the optimal range of SIS heavy peptide for spiking (peak area ratio of light peptide to heavy peptide = 1). The concentrations of SIS heavy peptides for the nonglycopeptide (GYQELLEK) and deglycopeptide (V*D*FTEIQK) that were used to spike were 10.3 and 7.3 fmol, respectively.

Individual serum samples were analyzed using the MRM-MS measurements with the spiked SIS heavy peptide mixture of nonglycopeptide (GYQELLEK) and deglycopeptide (V*D*FTEIQK) as the internal standard. Based on the MRM measurements using 155 individual serum samples, we measured the concentrations of the nonglycopeptide (GYQELLEK) and deglycopeptide (V*D*FTEIQK) of AFP in the normal (n = 60), LC group (n = 35) and HCC group (n = 60). The MRM measurements were imported into Skyline, and the peak areas of each transition were calculated, after normalization by the peak area of the spiked SIS heavy peptide. Next, the relative quantities of each transition were compared between the nonglycopeptide (GYQELLEK) and deglycopeptide (V*D*FTEIQK) in the normal versus HCC group and the LC versus stage I HCC subgroup (Figure 1-14).

To determine the efficacy of serum biomarkers in distinguishing HCC versus normal controls and the stage I HCC subgroup versus LC group, we drew receiver operator characteristic (ROC) curves and interactive plots, and the MRM-MS data on the nonglycopeptide (GYQELLEK) and deglycopeptide (V*D*FTEIQK) from both groups were analyzed (Figure 1-15).

HCC group was compared to normal control group, the nonglycopeptide had a sensitivity of 56.7%, specificity of 68.3%, AUC of 0.687 [cutoff value: ≥ 0.02 (light/heavy ratio)] whereas the deglycopeptide had sensitivity of 93.3%, specificity of 68.3%, AUC of 0.859 [cutoff value: ≥ 0.02 (light/heavy ratio)] (Figure 1-15A). In comparing the stage I HCC subgroup with the LC group, the nonglycopeptide had a sensitivity of 66.7%, specificity of 80.0%, and AUC of 0.712 [cutoff value: ≥ 0.02 (light/heavy ratio)], whereas the deglycopeptide had a sensitivity of 96.7%, specificity of 80.0%, and AUC of 0.918 [cutoff value: ≥ 0.02 (light/heavy ratio)] (Figure 1-15B). Thus, the discriminatory power of the deglycopeptide was greater versus the nonglycopeptide.

Pairwise differences in AUC values between nonglycopeptide and deglycopeptide estimations were analyzed by DeLong test [22]—the difference in AUC values was significant (normal vs HCC: *P*-value = 0.0010; LC vs stage I HCC: *P*-value = 0.0042) (Table 1-7).

Notably, considering that the nonglycopeptide (GYQELLEK) is measuring total AFP, it would be more advantageous to measure the deglycopeptide (V*D*FTEIQK) or take a combined measurement of nonglycopeptide (GYQELLEK) and deglycopeptide (V*D*FTEIQK), which could improve the diagnostic power in HCC.

(A)

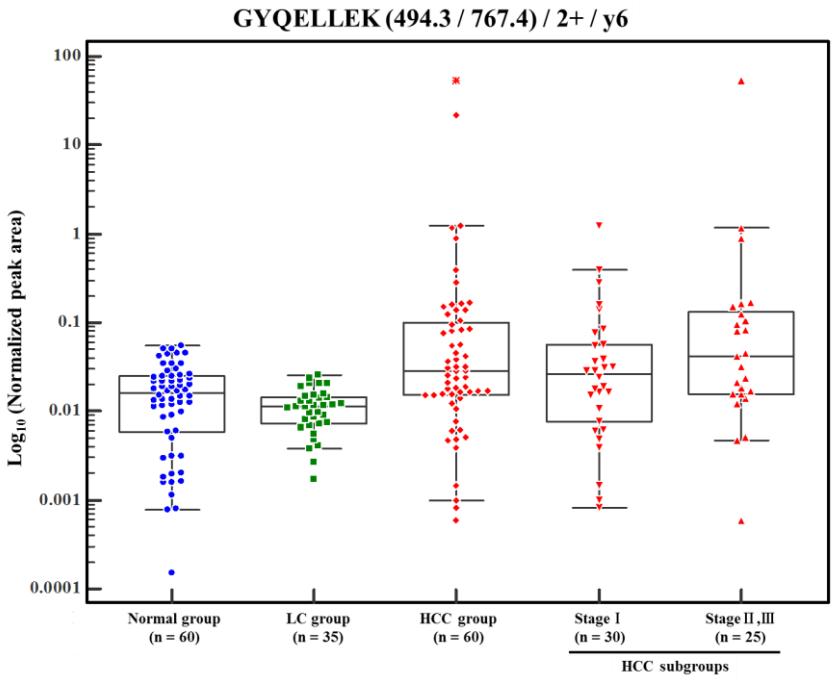

Figure 1-14A

(B)

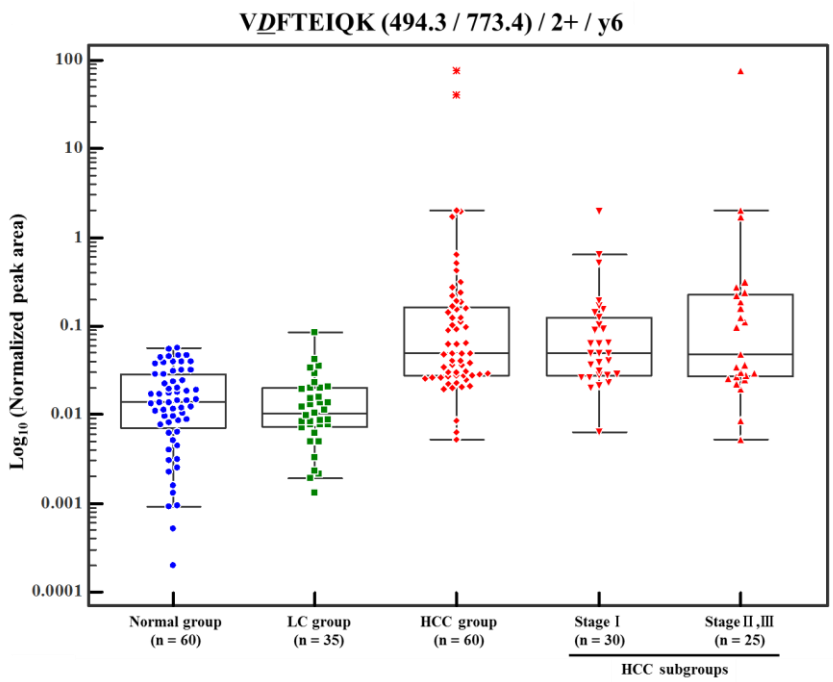

Figure 1-14B

Figure 1-14. Box plots of the nonglycopeptide and deglycopeptide levels measured by MRM in 60 Normal, 35 LC and 60 HCC cases.

(A) Box plots comparing nonglycopeptide and **(B)** deglycopeptide in the following patient groups: normal (n = 60), cirrhosis (n = 35), Total HCC (n = 60), stage I (early HCC; n = 30) and stage II and III (late HCC; n = 25). Patients of TNM stage II and III were combined because of the low number of samples. The ends of the boxes define the 25th and 75th percentiles. A line inside the box represents the mean, and error bars define the 10th and 90th percentiles. Points beyond the 10th and 90th percentiles are also displayed. For definitions of the HCC subgroups, see text. Both the normal and

cirrhosis groups are significantly different from the total HCC group and HCC subgroup (stage I and stage II, III) at *P*-value ≤ 0.05. The serum values of nonglycopeptide and deglycopeptide were significantly increased in HCC compared with those in normal and cirrhosis group (*P*-value $\leq$ 0.05). However, there was no significant difference between normal subjects versus cirrhosis and stage I HCC versus stage II and III HCC (*P*-value > 0.05).

(A)

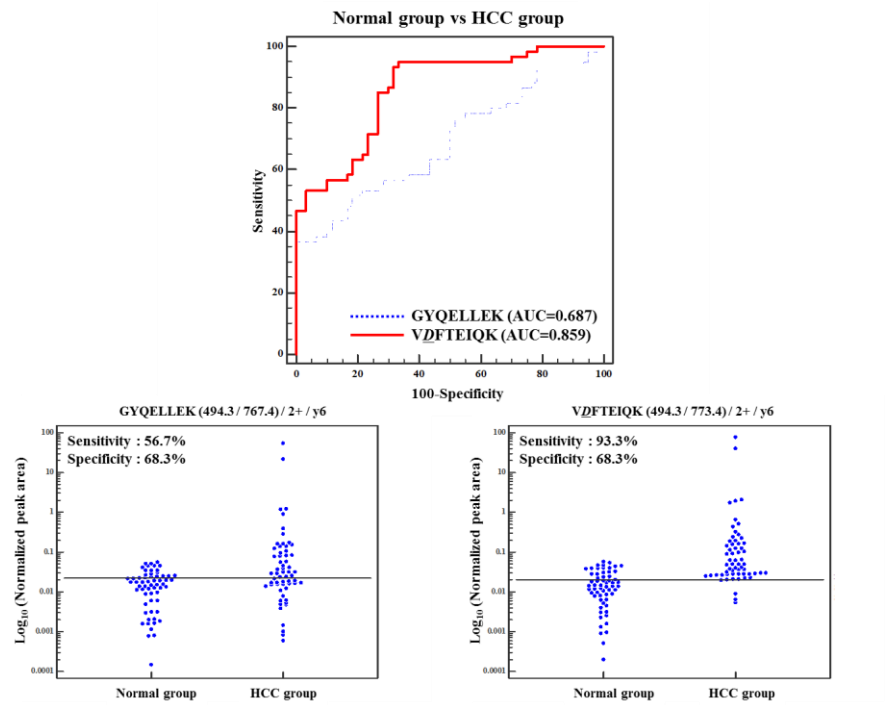

Figure 1-15A

(B)

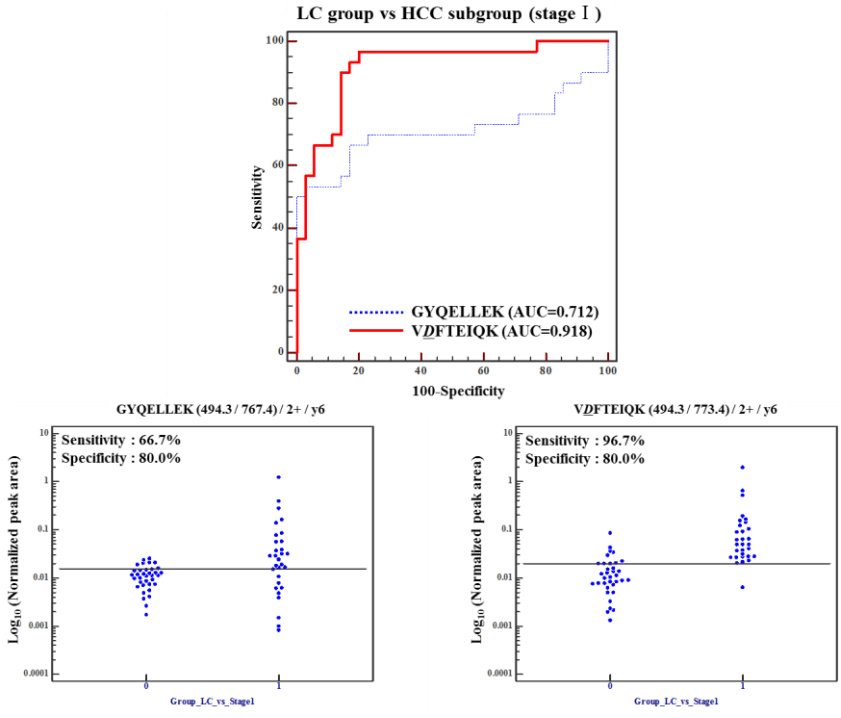

Figure 1-15B

Figure 1-15. Receiver operating characteristic (ROC) curves and interactive plots for the nonglycopeptide (GYQELLEK) and deglycopeptide (V*D*FTEIQK) of AFP, respectively.

(A) The normalized peak areas of transitions were compared between normal and HCC group. In the interactive plots, sensitivity was calculated based on a specificity of 68.3%, which was calculated per an AFP cutoff value of 20 ng/mL (56.7% sensitivity), representing significant prognostic impact for HCC. **(B)** LC was compared to Stage I HCC subgroup, in the

interactive plots, sensitivity was calculated based on a specificity of 80.0% which was calculated with optimal deglycopeptide level.

Table 1-7. Comparing the areas under two receiver operating characteristic curves.

(A)

Normal group vs HCC group

	AUC	SE [a]	95% CI [b]
Nonglycopeptide	0.687	0.0489	0.597 to 0.769
Deglycopeptide	0.859	0.0332	0.784 to 0.916

[a] DeLong et al., 1988

[b] Binomial exact

Pairwise comparison of ROC curves	
Difference between areas	0.171
Standard Error[c]	0.0523
95% Confidence Interval	0.0689 to 0.274
z statistic	3.278
Significance level	***P* = 0.0010**

[c] DeLong et al., 1988

Table 1-7A

(B)

LC group vs HCC subgroup (stage Ⅰ)

	AUC	SE [a]	95% CI [b]
Nonglycopeptide	0.712	0.0738	0.587 to 0.818
Deglycopeptide	0.918	0.0360	0.823 to 0.972

[a] DeLong et al., 1988

[b] Binomial exact

Pairwise comparison of ROC curves	
Difference between areas	0.206
Standard Error[c]	0.0718
95% Confidence Interval	0.0649 to 0.347
z statistic	2.863
Significance level	***P* = 0.0042**

[c] DeLong et al., 1988

Table 1-7B

DISCUSSION

Most protein biomarkers are based on the premise that native proteins are differentially expressed in normal versus disease states. Recent studies have also demonstrated that protein biomarkers can discriminate such states according to the degree of glycosylation of native proteins [28-33].

To quantitatively analyze the total AFP and glycosylated AFP, respectively, we established an MRM-MS method for measuring the nonglycopeptide and deglycopeptide that corresponded to the glycosylated glycopeptide in serum samples. In developing this method, we first assessed whether the MRM-MS approach was suitable for measuring glycoprotein levels. We observed that MRM-MS measured the nonglycopeptide and deglycopeptide as alternatives to total AFP concentration and the glycosylated AFP fraction that was cleaved by PNGase F, respectively. Then, we performed MRM measurements for the endogenous light peptides and the SIS heavy peptides that coeluted with them as internal standards.

The nonglycopeptide was detected in the PNGase F-untreated and PNGase F-treated conditions, whereas the glycosylated glycopeptide was seen only after PNGase F treatment in the deglycopeptide form, because the original amino acid sequence with glycan could not be detected by MRM-MS. Specifically, although the PNGase F-treated deglycosylated state could be measured based on the deglycopeptide sequence (Asn changed to Asp), no glycopeptide could be detected by MRM in the glycosylated state (PNGase F-untreated). Thus, this sequence-based approach to the MRM measurements is useful in measuring the glycoprotein concentrations.

AFP is a significant marker for the clinical diagnosis and evaluation of suspected HCC patients. As a diagnostic tool for HCC, AFP level is determined by immunoenzymatic chemiluminescence; the cutoff of serum AFP levels for significant prognostic impact for HCC is 20 ng/mL (AFP-negative: < 20 ng/mL and AFP-positive: ≥ 20 ng/mL) [27].

However, some reports have demonstrated that AFP level (cutoff value: ≥ 20 ng/mL) is a poor diagnostic tool in HCC, with a sensitivity of 54%. For example, 46%, 36%, and 18% of 1158 HCC patients had normal (< 20 ng/mL), elevated (20–400 ng/mL), and diagnostic AFP levels (> 400 ng/mL), respectively [34,35]. We noted the similar trend in AFP level in our HCC patients—as shown in Table 1-1, 43%, 30%, and 27% of 60 HCC patients had normal (< 20 ng/mL), elevated (20–400 ng/mL), and diagnostic levels of AFP (> 400 ng/mL), respectively (yielding a sensitivity of 56.7%). This result suggests that solely using total AFP level is not an effective method for distinguishing HCC from healthy subjects.

There are other biomarkers besides AFP that can be used to screen for HCC, such as DCP (Des-gamma carboxyprothrombin), also known as prothrombin induced by vitamin K absence II (PIVKA II). DCP is an abnormal product of liver carboxylation during thrombogen formation. The serum level of DCP in patients with HCC is significantly higher than in healthy adults and patients with nonmalignant hepatopathy (chronic hepatitis and cirrhosis) [36,37].

DCP can be used as a prognostic indicator for patients with small HCC tumors. High serum levels of DCP are also associated with a greater risk of HCC recurrence and worse overall survival in patients with an HCC tumor under 3 cm [38,39]. DCP can be used to evaluate the prognosis of patients with

small HCC tumors but remains insufficient in the primary screening of HCC patients [40].

Recently, AFP-L3 (%) has been used as an additional indicator of total AFP in the diagnosis of HCC, demonstrating superior performance compared with measuring total AFP alone [41-46]. Similarly, we developed a MRM-based measurement approach using a deglycopeptide of AFP as an alternative to the glycosylated AFP fraction (AFP-L1, L2 and L3). By MRM-MS, the nonglycopeptide had a sensitivity of 56.7%, specificity of 68.3%, and AUC of 0.687 in distinguishing normal and HCC subjects versus 93.3%, 68.3%, and 0.859, respectively with the deglycopeptide. Also, the nonglycopeptide had a sensitivity of 66.7%, specificity of 80.0%, and AUC of 0.712 in distinguishing LC and the stage I HCC subgroup versus 96.7%, 80.0%, and 0.918, respectively, with the deglycopeptide. Thus, the discriminatory power of the deglycopeptide was better than that of the nonglycopeptide (Figure 1-15). To compare the nonglycopeptide and deglycopeptide of AFP accurately, we fixed their specificity in calculating the sensitivity.

In total, 30 HCC patients were primarily TNM stage I—ie, the early stage of HCC—suggesting that these findings can be applied to clinical settings in discriminating early-stage HCC from LC. Thus, deglycopeptide levels can differentiate small tumors from cirrhotic liver, which is significant, because other markers can not distinguish between early-stage HCC and LC. Our data indicate that upregulated deglycopeptide levels in early-stage HCC patients function in tumorigenesis and can be used as a marker for the early detection of a cirrhotic liver that progresses to HCC.

Our MRM-MS-based method has benefits in verifying glycoprotein biomarkers in human samples, because it does not require any complex or

irreproducible glycoprotein enrichment steps. Further, determining the amount and extent of glycosylation in glycoproteins is difficult through conventional methods. Specifically, the differences in expression and degree of glycosylation of AFP have not been compared using antibody-based assays, such as western blot and ELISA (enzyme-linked immunosorbent assay).

Ultimately, 2 types of peptide markers—a nonglycopeptide and deglycopeptide—were used to distinguish HCC from normal controls and early-stage HCC from the LC group. Further verification of their value in larger samples should facilitate the development of better biomarkers for HCC.

CHAPTER II

Development of Biomarkers for Screening Hepatocellular Carcinoma Using Global Data Mining and Multiple Reaction Monitoring

INTRODUCTION

Tumor biomarkers are defined as substances that reflect current cancer status or predict its future characteristics. Biomarkers are potentially useful for screening cancers and determining their prognosis, predicting therapeutic efficacy [47]. The most commonly used serum marker of HCC is AFP, which has a reported sensitivity of 39% to 65% and specificity of 65% to 94%; approximately one-third of early-stage HCC patients with small tumors (< 3 cm) have normal levels of AFP [48]. Thus, clinicians are dissatisfied with AFP as a marker due to its high false-positive and false-negative rates [49]. Consequently, there is an urgent clinical need to identify new biomarkers that classify HCC more accurately.

To obtain HCC biomarker candidates, we initially screened a published database on HCC using 5 types of datasets, comprising proteomics, cDNA microarray, copy number variation, somatic mutation, and epigenetic data. This method easily encompassed all biological heterogeneities of liver cancer. The candidates that resulted from global data mining were subject to high-throughput verification using individual HCC serum samples by multiple reaction monitoring (MRM) [50]. In MRM verification, specific peptides of candidates are selected to represent the protein from which they are quantitated against a spiked internal standard (a synthetic stable isotope-labeled peptide), yielding a measure of its concentration [51].

Three clinically well-characterized serum samples—from the healthy control, before HCC treatment, and after HCC treatment groups—were used to quantify the candidate biomarkers, of which we identified significant candidates for differentiation between the before the former and latter groups.

Two MRM-verified biomarkers were distinguished between the 3 groups. Further, in combination, this 2-marker panel distinguished the groups better than the individual markers.

In this study, MRM verification was combined with global data mining to verify the biomarker candidates that were screened from an initial global data mining step in identifying and developing valuable HCC biomarkers. The MRM verification resulted in 9 potential markers with an area under the curve (AUC) that exceeded 0.700, wherein 2 of the 9 verified markers were combined to construct a 2-marker panel by multivariate analysis. The 2-marker panel had an improved AUC compared with AFP (0.981 versus 0.756, respectively). This approach enabled us to verify HCC biomarkers—especially a promising multimarker panel that can be used to improve HCC detection alone or in combination with AFP levels.

MATERIALS AND METHODS

1. Ethics statement and clinical sample information

The institutional review board of Seoul National University Hospital (approval No. H-1103-056-355) approved the study protocol, and written informed consent was obtained from each patient or legally authorized representative. The clinical characteristics of the study patients are shown in Table 2-1.

Healthy control group samples were obtained from 36 healthy volunteers who visited the Healthcare Center of Seoul National University Hospital. All subjects in healthy control group were confirmed with normal liver function test results, including serum alanine and aspartate aminotransferases, and with negative results for hepatitis B virus surface antigen and anti-hepatitis C virus antibody. Liver ultrasonography was performed to screen fatty liver disease, and all healthy controls had normal findings. Eighteen patients before HCC treatment who were infected with hepatitis B virus (HBV) and underwent successful locoregional therapy were also enrolled, from whom serum samples were collected and classified as the before and after HCC treatment groups, respectively.

The diagnosis of HCC was based on the recommendation of the American Association for the Study of Liver Diseases by a hepatologist with more than 20 years of experience [52]. All HCC patients were after treatment with locoregional modality including transarterial chemoembolization and percutaneous ethanol injection therapy. The treatment response was evaluated with serum AFP and enhanced liver computed tomography (CT) at 3 months after the first treatment, and no enrolled patient showed any evidence of tumor

recurrence. In each HCC patient, serum samples were obtained twice: before the first locoregional therapy (before HCC treatment group), and at 3 months after the treatment (after HCC treatment group) (Table 2-2). To reduce causal heterogeneity, HCC patients who had other types of chronic liver disease, except chronic hepatitis B, such as chronic hepatitis C and alcoholic hepatitis, were excluded.

All serum samples were collected by the Liver Research Institute, Seoul National University College of Medicine. The blood samples were centrifuged immediately at 3000 rpm for 10 min at 4℃ to fractionate the serum. The resulting supernatant was aliquoted (50 μL) and stored at -80℃ until analysis.

Table 2-1. Clinical characteristics of patient groups used in MRM analysis and Western blot analysis.

	MRM analysis		Western blot analysis	
	Untreated HCC group and corresponding treated HCC Group	Healthy control group	Untreated HCC group and corresponding treated HCC Group	Healthy control group
Total patient number	**18 in each group**	**36**	**13 in each group**	**13**
Gender (Male / Female)	**13 / 5**	**18 / 18**	**10 / 3**	**8 / 5**
Age (Mean, Range)	**60.6 (47-81)**	**58.7 (50-69)**	**62.4 (48-79)**	**56.2 (52-67)**
Etiology of liver disease	**HBV, 18 (100%)**		**HBV, 13 (100%)**	
Locoregional modality				
TACE	**7**		**4**	
PEIT	**11**		**9**	
AFP value (Mean, Range)	**1079.4 (14.1-6900)**		**245.2 (16-730)**	
< 20 ng/ml	**2**		**1**	
20-200 ng/ml	**4**		**6**	
200-1000 ng/ml	**7**		**6**	
> 1000 ng/ml	**5**		**0**	
PIVKA value (Mean, Range)[a]	**916 (5-10720)**		**117.6 (28-612)**	
< 20 ng/ml	**4**		**0**	
20-100 ng/ml	**6**		**7**	
100-1000 ng/ml	**3**		**6**	
> 1000 ng/ml	**3**		**0**	
Tumor stage[b]				
I	**12**		**9**	
II	**4**		**2**	
III	**2**		**2**	
IV	**0**		**0**	

Abbreviations
AFP : Alpha-Fetoprotein
PIVKA : Protein induced by vitamin K absence or antagonist
TACE : Transcatheter arterial chemoembolization
PEIT : Percutaneous ethanol injection therapy
[a] : PIVKA values were provided for 16(M11/F5) among a total of 18 untreated HCC group
[b] : According to American Joint Committee on Cancer (AJCC) staging system (7th edition, 2010)

Table 2-1

Table 2-2. AFP level information on liver cancer patients after the treatment.

Treatment response			
Posttreatment AFP (Mean, Range)		8184 (2.6-144000)	
Decreased AFP		Number of persons	Means
		16	88.9
Target lesion response*	CR	6	33.3
	PR	6	33.3
	SD	0	0
	PD	6	33.3

Table 2-2

2. Preparation of serum tryptic digestions

Serum protein was quantified by bicinchoninic acid (BCA) assay. Two hundred-microgram aliquots of the serum samples were denatured with 6 M urea, 50 mM Tris, pH 8.0, and 30 mM dithiothreitol (DTT) at 37℃ for 60 min and alkylated with 50 mM iodoacetamide (IAA) at room temperature in the dark for 30 min. The urea was diluted 15-fold with 50 mM Tris, pH 8.0 prior to overnight digestion at 37℃ with trypsin (Promega, sequencing-grade modified) using a 1:50 (w/w) enzyme-to-serum concentration ratio.

Tryptic digestion was stopped with formic acid at a final concentration of 1% and desalted on Sep-pak tC18 cartridges (Waters Corp., Milford, MA). The Sep-pak tC18 cartridges were equilibrated sequentially with 1 mL methanol and 5 mL water that contained 0.1% trifluoroacetic acid (TFA) prior to loading of the tryptic digestion. The cartridges were washed with 3 mL 0.1% trifluoroacetic acid (TFA) and eluted with 1 mL of 60% ACN, 0.1% TFA. The eluted samples were frozen and lyophilized on a speed vacuum. Prior to MRM analysis, the samples were reconstituted in 0.1% formic acid to 2 μg/μL.

3. Experimental MRM design using Skyline

For each target protein, we selected peptides and fragment ions for MRM using Skyline (http://proteome.gs.washington.edu/software/skyline), an open-source software application for developing MRM methods and analyzing MRM data [53]. In brief, the full-length protein sequences were imported into Skyline in FASTA format and designed into peptides, each with a list of product ions for monitoring by MRM. In selecting transitions through Skyline, the peptide filter condition was as follows: maximum length of peptide of 20, including at least 8 amino acids. Peptides with repeat arginines (Arg, R) or lysines (Lys, K) were discarded. If methionine (Met, M) was included in the

peptide, it was discarded to avoid the risk of modification. If proline (Pro) lay next to arginine (Arg, R) or lysine (Lys, K), the peptide was discarded. If a peptide contained histidine (His, H), it was discarded to avoid the risk of charge alteration. Peptides that satisfied these conditions were used as Q1 transitions. Next, we selected a maximum of 5 Q3 transitions from the fragmentation ions that were derived from the Q1 transitions in descending order.

4. Quantification by multiple reaction monitoring

MRM was performed on a nano LC system, which was connected to a hybrid triple quadrupole/ion trap mass spectrometer (4000 QTRAP, AB SCIEX, Foster City, CA) that was equipped with a nanoelectrospray interface. The 4000 QTRAP was operated in positive ion MRM mode, in which Q1 and Q3 were set to transmit different precursor/product ion pairs.

The LC buffer system was as follows: mobile phase A, 2% acetonitrile/0.1% formic acid and mobile phase B, 98% acetonitrile/0.1% formic acid. The peptides were separated and eluted at a flow rate of 300 nL/min on a linear gradient of mobile phase B from 2% to 40% B in 43 min. The gradient was ramped up to 70% B for 5 min and 2% B for 10 min to equilibrate the column for the next run. The total LC run time was 60 min. The analytical column was 75 μm, 15 cm, packed with Magic C18AQ resin (5 μm, 100 Å, Michrom Bioresources).

Typical instrument settings were as follows: ion spray (IS) voltage of 2.3 kV, an interface heater temperature of 200℃, a GS1 (nebulizer gas) setting of 12, and curtain gas set to 15. MS parameters for declustering potential (DP) and collision energy (CE) were determined by linear regression of previously optimized values in Skyline. MRM experiments were performed with a scan time of 50 ms and scan width of 0.002 m/z, using a unit resolution of 0.7 Da

(FWHM) for Q1 and Q3. In the MRM runs, scan time was maintained at 50 ms for each transition, and the pause between transition scans was set to 3 ms [54].

5. Statistical analysis for verification of biomarker candidates

Raw data files from the MRM analysis were processed using Skyline. Because the peak intensity is sometimes low due to low abundance in a normal versus cancer sample and vice versa, the peak area integration was confirmed manually to correct the wrong automatic assignments for each targeted peptide. The default peak integration and Savitzky-Golay smoothing algorithm were applied. Peptides with at least 3-fold signal-to-noise ratios were considered detectable.

Two approaches were used to assess HCC candidate proteins. First, we distinguished a disease group (before HCC treatment) from a nondisease group (healthy controls and after HCC treatment). Comparisons between the before HCC treatment (n=18) versus healthy control groups (n=36) and the before HCC treatment (n=18) versus after HCC treatment groups (n=18) were made using analysis of variance (ANOVA). Based on ANOVA, we selected target peptides that had a significance level below 0.05 in mean intensity level between groups.

Second, to evaluate the efficacy of serum biomarkers in distinguishing the disease from nondisease group, we analyzed receiver operator characteristic (ROC) curves and scatter plots. We performed all statistical analyses and generated all scatter plots and ROC curves with MedCalc (MedCalc, Mariakerke, Belgium, version 12.2.1).

6. Western blot analysis

The clinical samples in the Western blot experiment comprised 13 individual samples from the healthy control, before HCC treatment, and after HCC treatment groups (Table 2-1). Serum sample concentrations were determined by BCA protein assay. Equal amounts of protein (30 μg) were mixed with SDS loading buffer (62 mM Tris-HCl, pH 6.8, 10% glycerol, 2% SDS, 2% ß-mercaptoethanol, and bromophenol blue), boiled for 10 min, and separated by SDS-PAGE on a 12% acrylamide gel. After separation, serum samples were transferred to polyvinylidene difluoride (PVDF) membranes (Bio-Rad, Cat. #162-0177), which were blocked with 5% BSA (w/v) in TBS-T (25 mM Tris, pH 7.5, 150 mM NaCl, and 0.05% (w/v) Tween-20) for 2 hr at room temperature.

Membranes were incubated overnight at 4℃ with individual primary antibodies (diluted 1:100 to 1:1000). Membranes were washed 5 times with TBS-T and incubated for 2 hr with the appropriate secondary peroxidase-conjugated antibody (1:5000, Santa Cruz Biotechnology, USA). The membranes were then washed 5 times with TBS-T, and target protein bands were visualized using the Chemiluminescent Substrate Kit (GenDEPOT, W3651-012). Western blot band intensities were quantified using Multi Gauge. (Fujifilm, ScienceLab 2005, version 3.0). Pooled serum was used as a loading control (13 healthy control, 13 untreated HCC, and 13 treated HCC group samples) and in each Western blot gel. All blots were normalized to the band intensity of the pooled serum. Band intensities were analyzed by *T*-test to

identify meaningful differences between sample groups.

7. Statistical analysis to construct multimarker panel

In this study, we compared the nondisease with the disease group using multimarker panel proteins. Logistic regression (LR) analysis was performed to generate the multimarker panel, consisting of several individual markers that differentiated cancerous from noncancerous subjects. The discriminatory power was examined in 3 situations: healthy control versus before HCC treatment groups, before HCC treatment versus after HCC treatment groups, and healthy control plus after HCC treatment versus before HCC treatment groups. LR and ROC curves were constructed using MedCalc, and the analysis was performed.

ROC curves were used to evaluate the efficacy of the multimarker panel—in this case, a 2-marker panel. AUC values for individual markers and the 2-marker panel were calculated to examine the discriminatory power of various combinations of HCC candidate markers. Multicollinearity of the panel was checked using IBM SPSS Statistics (version 20, commuter license).

Leave-one-out cross validation (LOOCV) was performed to avoid overfitting that might be caused by the small number of samples, even if LOOCV is a suboptimal substitution of independent validation; thus, the same sample set was used to generate the training and test data. A single observation was selected from the dataset as the test variable, and the remaining samples were used as the training set to construct an LR model. LOOCV was performed in the open-source Weka program computing environment (version 3.6.0, Knighton Rd, Hamilton 3240 New Zealand).

RESULTS

1. Candidate biomarker selection from global data mining

The overall scheme for this study is shown in Figure 2-1. Our first task was to obtain a list of biomarker candidate proteins. We believed that if we could acquire candidate proteins from established resources, the number of candidate screening experiments could be reduced. To screen candidates, we performed global data mining with regard to liver cancer in several disciplines: proteomics, cDNA microarray, copy number variation, epigenetics, and somatic mutation data.

The second task was to prioritize marker candidates from the resulting list (Figure 2-2). The term "frequency" was used for each target protein. Frequency was defined as the total number of occurrences in 5 biological fields. As a result of data mining of these 5 areas, 4658 liver cancer-related proteins were selected and filtered by prioritizing candidate proteins. The top 50 high-frequency proteins were chosen and examined with regard to whether they were secreted into plasma, and final candidates were selected by confirmation with the Plasma Proteome Database (http://www.plasmaproteomedatabase.org). All 4658 proteins from the global data mining are listed in Figure 2-2. Then, sequence files of the 50 selected candidates were prepared in FASTA format and harvested using the Uniprot website (http://*www.uniprot.org*). The 50 FASTA files were input into Skyline to generate theoretical transitions for the MRM analysis. The list of potential biomarkers was filtered per the verification steps, as summarized in the summary list file (Table 2-3).

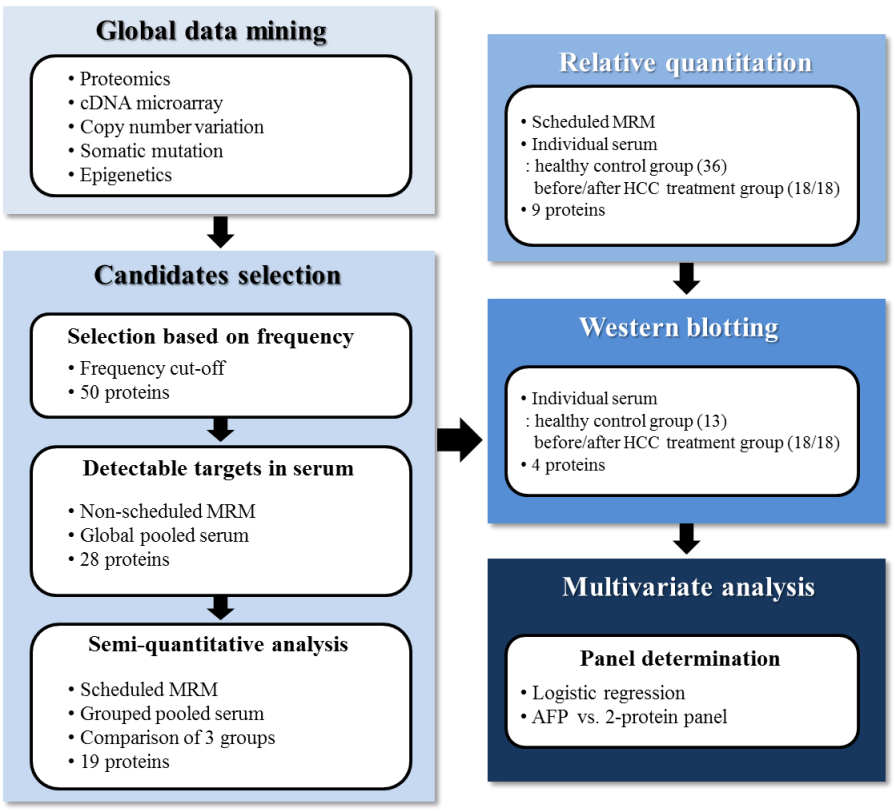

Figure 2-1

Figure 2-1. Workflow of HCC biomarker discovery.

First, we selected candidate HCC biomarkers, based on global data mining using preexisting databases. In the first and second screening steps, preliminary MRM analysis of the target peptides/transitions was conducted using pooled serum samples to examine whether the transitions were detectable in serum samples. In the first verification step, MRM analysis of individual serum samples was performed using the predetermined retention time. In the second verification step, the data were analyzed and verified by Western blot. In the

multivariate analysis, logistic regression (LR) analysis was performed to construct a multimarker panel of potential markers that could differentiate cancerous from noncancerous subjects.

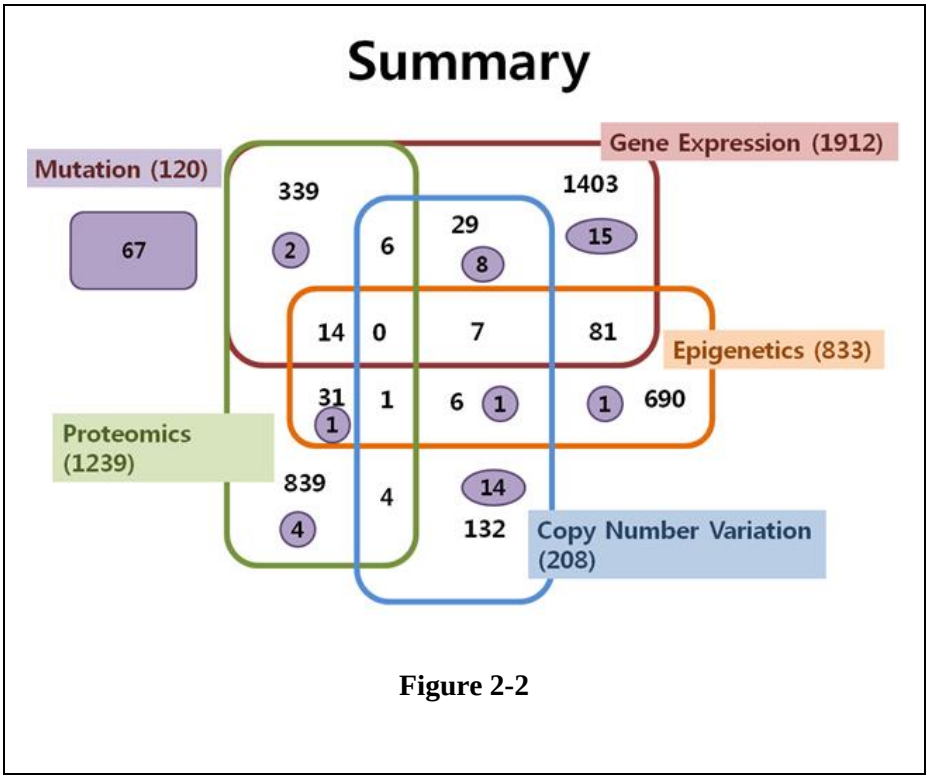

Figure 2-2

Figure 2-2. Lists of candidate proteins obtained from global data mining. Global data mining covers proteomics, cDNA microarray, copy number variation, and somatic mutation.

Detailed information of previous publications including journal name, volume, page, publication year, citation indices and title were shown.

Table 2-3. The list of potential biomarkers was filtered step by step per the verification steps.

Serial No.	Gene symbol	Protein name	1st Screening Step (28 Proteins)	2nd Screening Step (19 Proteins)	3rd Screening Step (9 Proteins)
1	ABCD3	ATP-binding cassette sub-family D member 3	O	X	X
2	ACADVL	Very long-chain specific acyl-CoA dehydrogenase, mitochondrial	O	O	O
3	AFM	Afamin	O	X	X
4	AFP	Alpha-fetoprotein	O	O	O
5	ALB	Serum albumin	O	O	X
6	ALDH4A1	Delta-1-pyrroline-5-carboxylate dehydrogenase, mitochondrial	O	X	X
7	ANLN	Actin-binding protein anillin	O	O	O
8	APOA2	Apolipoprotein A-II	O	O	X
9	ARHGDIB	Rho GDP-dissociation inhibitor 2	X	X	X
10	BASP1	Brain acid soluble protein 1	O	O	O
11	C3	Complement C3	O	O	X
12	C4A	Complement C4-A	O	O	O
13	C9	Complement component C9	O	X	X
14	CALD1	Caldesmon	X	X	X
15	CAPN1	Calpain-1 catalytic subunit	O	O	O
16	CD44	CD44 antigen	X	X	X
17	CFH	Complement factor H	X	X	X
18	CLCC1	Chloride channel CLIC-like protein 1	X	X	X
19	COL18A1	Collagen alpha-1(XVIII) chain	X	X	X
20	COL1A2	Collagen alpha-2(I) chain	X	X	X
21	CTSB	Cathepsin B	X	X	X
22	CYP2E1	Cytochrome P450 2E1	X	X	X
23	DDX1	ATP-dependent RNA helicase DDX1	O	O	X
24	DHCR7	7-dehydrocholesterol reductase	X	X	X
25	DHRS7	Dehydrogenase/reductase SDR family member 7	X	X	X
26	DLD	Dihydrolipoyl dehydrogenase, mitochondrial	X	X	X
27	FBP1	Fructose-1,6-bisphosphatase 1	O	X	X
28	FLNB	Filamin-B	O	O	O
29	FYB	FYN-binding protein	O	X	X
30	HSPA1B	Heat shock 70 kDa protein 1A/1B	X	X	X
31	HSPD1	60 kDa heat shock protein, mitochondrial	O	O	X
32	ITGB1	Integrin beta-1	X	X	X
33	LPCAT1	Lysophosphatidylcholine acyltransferase 1	X	X	X
34	MMP9	Matrix metalloproteinase-9	O	X	X
35	MTHFD1	C-1-tetrahydrofolate synthase, cytoplasmic	O	O	O
36	MYO10	Unconventional myosin-X	X	X	X
37	NID1	Nidogen-1	X	X	X
38	OAT	Ornithine aminotransferase, mitochondrial	X	X	X
39	PABPC1	Polyadenylate-binding protein 1	O	O	O
40	PGK1	Phosphoglycerate kinase 1	O	O	X
41	PHGDH	D-3-phosphoglycerate dehydrogenase	X	X	X
42	PLG	Plasminogen	O	X	X
43	PRKCSH	PRKCSH protein	O	O	X
44	PTPN1	Tyrosine-protein phosphatase non-receptor type 1	O	O	X
45	SERPING1	Plasma protease C1 inhibitor	X	X	X
46	SLC7A2	Low affinity cationic amino acid transporter 2	O	O	X
47	SQSTM1	Sequestosome-1	X	X	X
48	TAGLN	Transgelin	O	O	X
49	TUBA4A	Tubulin alpha-4A chain	O	X	X
50	VTN	Vitronectin	X	X	X

Table 2-3

2. Data mining of proteomic research

Ten research papers, all published after 2004, were selected with impact factors above 4.0 [55-64]. Two ICAT labeling, 4 ITRAQ labeling, and 4 SILAC labeling reports were used for our proteomic data mining. The maximum frequency of the target proteins in the 10 journals was 5. Based on the frequency, the most commonly reported genes were vimentin (VIM), catechol O-methyltransferase (COMT), enoyl-CoA hydratase, mitochondrial (ECHS1), and transitional endoplasmic reticulum ATPase (VCP), which were reported 5 times (Figure 2-3).

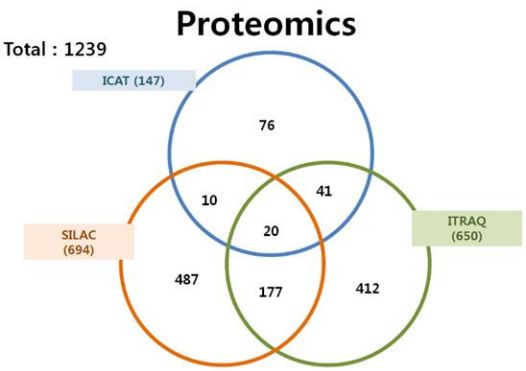

Figure 2-3

Figure 2-3. Lists of candidate proteins obtained from proteomic research. Each number such as 0 and 1 in the cell represents hit count of candidate protein. Detailed information of previous publications including journal name, volume, page, publication year, citation indices and title were shown.

3. Data mining of cDNA microarray research

cDNA microarray research papers that examined gene expression using liver cancer and control tissues were examined. Nine such reports were selected (all published after 2003), with impact factors above 6.7 [65-73]. The total number of screened proteins was 3241, and the most cited gene was liver carboxylesterase 1 (CES1), which was reported in 6 papers (Figure 2-4).

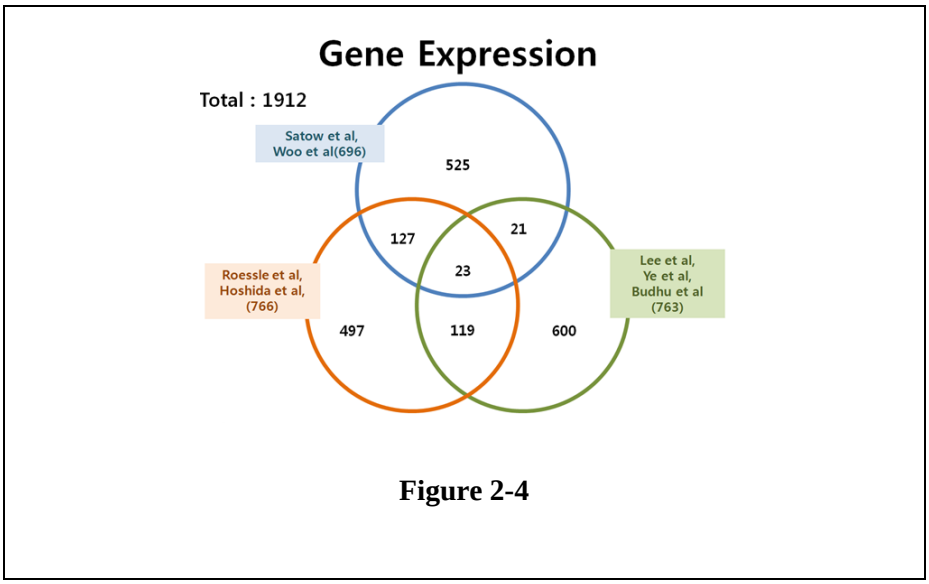

Figure 2-4

Figure 2-4. Lists of candidate proteins obtained from cDNA microarray research.

Each number such as 0 and 1 in the cell represents hit count of candidate protein. Detailed information of previous publications including journal name, volume, page, publication year, citation indices and title were shown.

4. Data mining of copy number variation research

Earlier publications on copy number variation (CNV) by amplification or mutation of liver cancer [74-76] were investigated, yielding 3 papers after 2004 with impact factors above 4.4. OncoDB (http://oncodb.hcc.ibms.sinica.edu.tw/index.htm) was also used to report copy number variation. In the 3 papers and OncoDB, CNVs in exostosin-1 (EXT1), transforming growth factor beta-2 (TGFB2), RAC-gamma serine/threonine-protein kinase (AKT3), and cathepsin B (CTSB) were reported twice. (Figure 2-5)

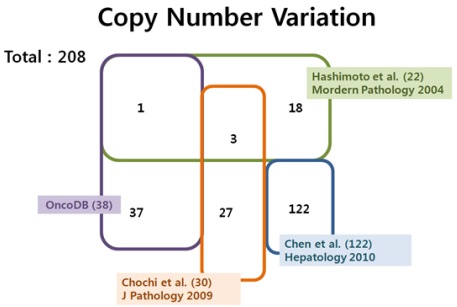

Figure 2-5

Figure 2-5. Lists of candidate proteins obtained from copy number variation research.

Each number such as 0 and 1 in the cell represents hit count of candidate protein. Detailed information of previous publications including journal name, volume, page, publication year, citation indices and title were shown.

5. Data mining of epigenetic research

On surveying epigenetic research papers, we selected 3 studies from after 2005 with impact factors above 4.3 [69,77,78], all of which reported cyclin-dependent kinase inhibitor 2A, isoform 4 (CDKN2A). (Figure 2-6)

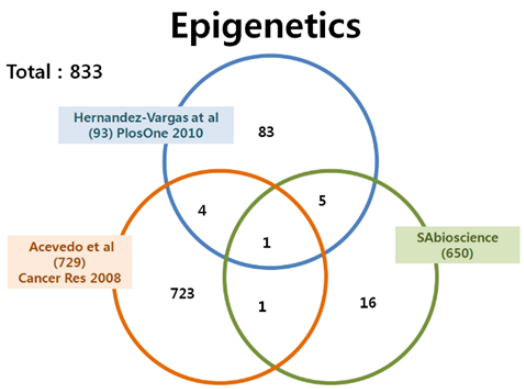

Figure 2-6

Figure 2-6. Lists of candidate proteins obtained from epigenetic research. Each number such as 0 and 1 in the cell represents hit count of candidate protein. Detailed information of previous publications including journal name, volume, page, publication year, citation indices and title were shown.

6. Data mining of somatic mutation research

Three databases on somatic mutations were searched: the OncoDB (http://oncodb.hcc.ibms.sinica.edu.tw/index.htm), Japan Liver Cancer (NCC, Riken), and International Cancer Genome Consortium (http://www.icgc.org/icgc/cgp/66/420/824) databases. Using HCC as the query term, 102 proteins (54, 25, and 23 proteins in NCC, Riken, and Onco.DB.HCC, respectively) were screened for somatic mutation data. (Figure 2-7)

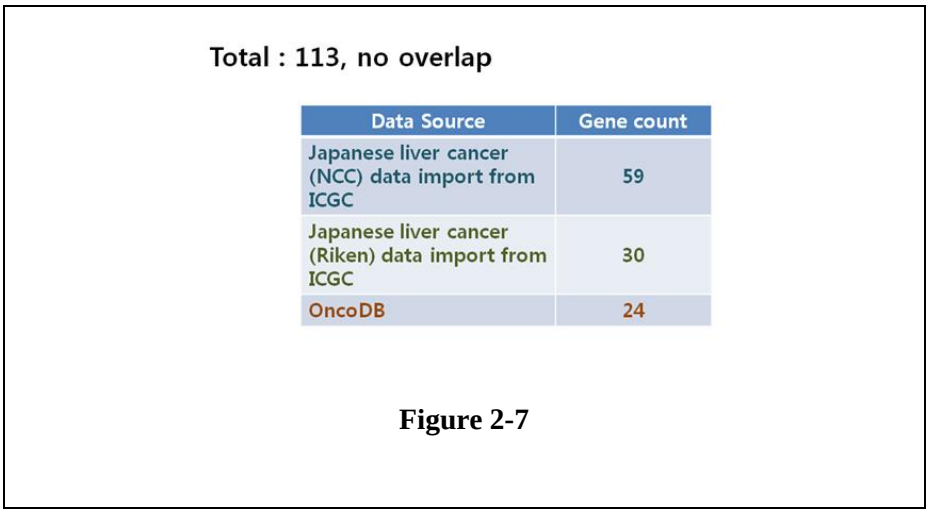

Figure 2-7

Figure 2-7. Lists of candidate proteins obtained from somatic mutation research.

Each number such as 0 and 1 in the cell represents hit count of candidate protein. Detailed information of previous publications including journal name, volume, page, publication year, citation indices and title were shown.

7. Examine the linearity of the internal standard peptide

The peak area of the internal standard peptide in each sample was used to normalize that of each target peptide in each MRM run. Thus, to assess the quantitative linearity of MRM, a response curve of the standard peptide (sequence of ELDALDANDELTPLG*R*, ATP-dependent RNA helicase A (DHX9)) in the presence of matrix peptides was generated. The internal standard peptide was diluted serially to 1, 5, 10, 50, 100, 250, and 500 fmol in 200 μg of serum peptide mixture, which is similar to the MRM conditions for target peptides. Further, to verify the endogenous signal of the target peptide, a blank sample that lacked the internal standard peptide was run. Each MRM analysis was performed three times repeatedly (Figure 2-8).

The CV% of the experiment was below 20%, and the correlation coefficient was 0.9984. The response curve of the standard peptide with the serum peptide mixture as matrix indicated that the quantitative linearity of serum MRM at the given concentrations was sufficiently valid to obtain relative quantities of target peptides.

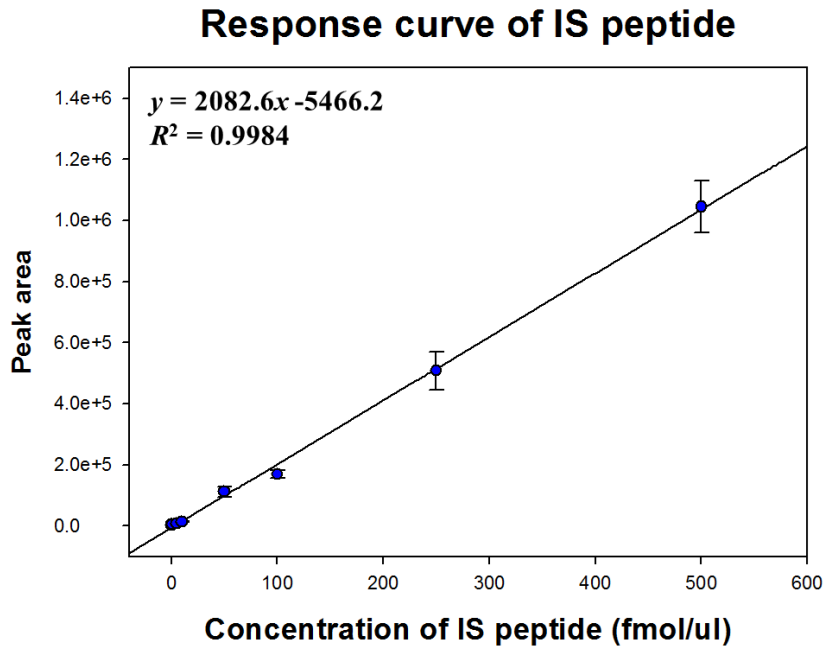

Figure 2-8

Figure 2-8. Response curve using ATP-dependent RNA helicase A (DHX9) peptide.

MRM runs were performed using an internal standard peptide (ELDALDANDELTPLGR) of ATP-dependent RNA helicase A (DHX9) at a Q1/Q3 transition of 876.4/1095.57 m/z, with which the standard curve was drawn. Triplicate MRM analyses were performed at 8 concentrations of the peptide (0, 1, 5, 10, 50, 100, 250, 500 fmol). The curve showed a linearity of R^2=0.9984.

8. Detectability of target candidates in pooled serum

Before conducting individual MRM analyses using the 72 serum samples, a preliminary MRM analysis was performed on the target peptides/transitions using pooled serum of all patients to obtain transition information, such as the detectability in serum and the suitability of the transition. The FASTA files of the 50 proteins yielded 498 peptides and 2174 transitions on applying the hierarchy data in Skyline software. After obtaining the resulting MRM data, the final transition was selected using the following criteria: at least 2 peptides were selected per protein, and at least 3 transitions per peptide were chosen as detectable transitions that had a signal-to-noise (S/N) ratio above 3. Ultimately, 28 of 50 candidates met the criteria in the first screening step (Table 2-3).

9. Selecting the transitions with technical reproducibility for MRM analysis

The reproducibility of MRM analyses is critical in making quantitative measurements [79]. In this study, the technical reproducibility of MRM analysis was examined using pooled serum. Serum from the 3 groups (36 healthy control, 18 before and after HCC treatment each) was pooled with the same weight according to each group; 333 transitions for 111 peptides, corresponding to the 28 candidate proteins from the detectability experiment (the first screening step, Table 2-3), were used to determine the technical reproducibility in MRM analysis. Five repetitive scheduled MRM runs for the pooled serum peptide mixture were performed using the retention time from the detectability experiment, with a window size of 120 seconds.

The data from the 5 MRM runs were imported into Skyline, and after normalization of the peak area using the internal standard peptides, the averaged relative quantities of each transition were compared. Peptides that showed a confident difference in quantity (fold-change > 1.5) and low variance (CV < 30%) between nondisease and disease groups were chosen as the final quantifiable transitions. Consequently, 30 peptides, comprising 90 transitions that corresponded to 19 proteins, were selected (second screening step, Table 2-3). The average relative quantities and standard deviations from the 5 repeat MRM analyses of the 30 peptides, and the final transition list is shown in Table 2-4.

Table 2-4. List of peptides and fragment ions for the analyzed proteins.

Gene symbol	Protein Name	Peptide Sequence	Precursor (m/z)	Charge	Product (m/z)	Retention Time (min)	Product ion Type	Light / Heavy	Declustering Potential (V)	Collision Energy (V)
ACADVL	Very long-chain specific acyl-CoA dehydrogenase, mitochondrial	ASNTAEVFFDGVR	706.84	2	1039.52	38.91	y9	Light	82.6	36
			706.84	2	968.48	38.91	y8	Light	82.6	36
			706.84	2	740.37	38.91	y6	Light	82.6	36
AFP	Alpha-fetoprotein	GYQELLEK	490.26	2	922.49	36.82	y7	Light	66.9	23.7
			490.26	2	759.42	36.82	y6	Light	66.9	23.7
			490.26	2	502.32	36.82	y4	Light	66.9	23.7
ALB	Serum albumin	DLGEENFK	476.22	2	723.33	9.59	y6	Light	65.8	22.9
			476.22	2	666.31	9.59	y5	Light	65.8	22.9
			476.22	2	537.27	9.59	y4	Light	65.8	22.9
		VPQVSTPTLVEVSR	756.43	2	1088.59	20.47	y10	Light	86.3	38.9
			756.43	2	1001.56	20.47	y9	Light	86.3	38.9
			756.43	2	900.51	20.47	y8	Light	86.3	38.9
ANLN	Actin-binding protein anillin	TQSLPVTEK	501.78	2	901.50	7.69	y8	Light	67.7	24.3
			501.78	2	773.44	7.69	y7	Light	67.7	24.3
			501.78	2	686.41	7.69	y6	Light	67.7	24.3
APOA2	Apolipoprotein A-II	EQLTPLIK	471.29	2	694.47	14.95	y6	Light	65.5	22.6
			471.29	2	571.38	14.95	y5	Light	65.5	22.6
			471.29	2	470.33	14.95	y4	Light	65.5	22.6
BASP1	Brain acid soluble protein 1	AEGAATEEEGTPK	645.30	2	890.41	26.63	y8	Light	78.2	32.5
			645.30	2	789.36	26.63	y7	Light	78.2	32.5
			645.30	2	660.32	26.63	y6	Light	78.2	32.5
		TEAPAAPAAQEIK	642.83	2	815.43	21.39	y8	Light	78	32.4
			642.83	2	744.39	21.39	y7	Light	78	32.4
			642.83	2	647.34	21.39	y6	Light	78	32.4
C3	Complement C3	QELSEAEQATR	631.30	2	891.42	26.42	y8	Light	77.1	31.7
			631.30	2	804.38	26.42	y7	Light	77.1	31.7
			631.30	2	675.34	26.42	y6	Light	77.1	31.7
		SGSDEVQVGQQR	645.31	2	1058.52	7.78	y9	Light	78.2	32.5
			645.31	2	814.45	7.78	y7	Light	78.2	32.5
			645.31	2	715.38	7.78	y6	Light	78.2	32.5
		SSLSVPYVIVPLK	701.42	2	928.59	23.03	y8	Light	82.3	35.7
			701.42	2	831.53	23.03	y7	Light	82.3	35.7
			701.42	2	357.25	23.03	y3	Light	82.3	35.7
C4A	Complement C4-A	DSSTWLTAFVLK	684.36	2	1078.63	44.15	y9	Light	81	34.7
			684.36	2	977.58	44.15	y8	Light	81	34.7
			684.36	2	791.50	44.15	y7	Light	81	34.7
		VGDTLNLNLR	557.81	2	843.50	20.05	y7	Light	71.8	27.5
			557.81	2	742.46	20.05	y6	Light	71.8	27.5
			557.81	2	629.37	20.05	y5	Light	71.8	27.5
CAPN1	Calpain-1 catalytic subunit	YLGQDYEQLR	642.81	2	1008.47	21.53	y8	Light	78	32.4
			642.81	2	951.45	21.53	y7	Light	78	32.4
			642.81	2	823.39	21.53	y6	Light	78	32.4
DDX1	ATP-dependent RNA helicase DDX1	DGFVALSK	418.73	2	721.42	10.81	y7	Light	61.6	19.6
			418.73	2	664.40	10.81	y6	Light	61.6	19.6
			418.73	2	517.33	10.81	y5	Light	61.6	19.6
		ELAEQTLNNIK	636.94	2	1030.55	29.98	y9	Light	77.5	32
			636.94	2	830.47	29.98	y7	Light	77.5	32
			636.94	2	702.41	29.98	y6	Light	77.5	32
FLNB	Filamin-B	APLNVQFNSPLPGDAVK	883.98	2	1371.73	31.09	y13	Light	95.6	46.1
			883.98	2	1272.66	31.09	y12	Light	95.6	46.1
			883.98	2	586.32	31.09	y6	Light	95.6	46.1
		TGEEVGFVVDAK	625.82	2	834.47	20.86	y8	Light	76.7	31.4
			625.82	2	735.40	20.86	y7	Light	76.7	31.4
			625.82	2	678.38	20.86	y6	Light	76.7	31.4
		EAGAGGLSIAVEGPSK	721.88	2	1000.57	24.99	y10	Light	83.7	36.9
			721.88	2	887.48	24.99	y9	Light	83.7	36.9
			721.88	2	331.20	24.99	y3	Light	83.7	36.9
HSPD1	60 kDa heat shock protein, mitochondrial	VGLQVVAVK	456.80	2	756.50	30.53	y7	Light	64.4	21.8
			456.80	2	643.41	30.53	y6	Light	64.4	21.8
			456.80	2	515.36	30.53	y5	Light	64.4	21.8
		VGEVIVTK	422.76	2	745.45	25.43	y7	Light	61.9	19.8
			422.76	2	688.42	25.43	y6	Light	61.9	19.8
			422.76	2	460.31	25.43	y4	Light	61.9	19.8
MTHFD1	C-1-tetrahydrofolate synthase, cytoplasmic	TDTESELDLISR	689.84	2	932.50	40.06	y8	Light	81.4	35.1
			689.84	2	845.47	40.06	y7	Light	81.4	35.1
			689.84	2	716.43	40.06	y6	Light	81.4	35.1
		AAQAPSSFQLLYDLK	826.44	2	1126.61	45.63	y9	Light	91.4	42.8
			826.44	2	1039.58	45.63	y8	Light	91.4	42.8
			826.44	2	892.51	45.63	y7	Light	91.4	42.8
		GVPTGFILPIR	585.36	2	758.49	27.89	y6	Light	73.8	29.1
			585.36	2	611.42	27.89	y5	Light	73.8	29.1
			585.36	2	385.26	27.89	y3	Light	73.8	29.1
PABPC1	Polyadenylate-binding protein 1	EFSPFGTITSAK	642.83	2	921.50	21.61	y9	Light	78	32.4
			642.83	2	824.45	21.61	y8	Light	78	32.4
			642.83	2	677.38	21.61	y7	Light	78	32.4
PGK1	Phosphoglycerate kinase 1	YSLEPVAVELK	624.35	2	997.59	48.55	y9	Light	76.6	31.3
			624.35	2	755.47	48.55	y7	Light	76.6	31.3
			624.35	2	658.41	48.55	y6	Light	76.6	31.3
PRKCSH	PRKCSH protein	LIELQAGK	436.27	2	758.44	13.71	y7	Light	62.9	20.6
			436.27	2	645.36	13.71	y6	Light	62.9	20.6
			436.27	2	516.31	13.71	y5	Light	62.9	20.6
PTPN1	Tyrosine-protein phosphatase non-receptor type 1	GEPSLPEK	428.72	2	573.32	11.68	y5	Light	62.4	20.2
			428.72	2	486.29	11.68	y4	Light	62.4	20.2
			428.72	2	373.21	11.68	y3	Light	62.4	20.2
SLC7A2	Low affinity cationic amino acid transporter 2	AWSGTFDELLSK	677.34	2	1009.52	21.38	y9	Light	80.5	34.3
			677.34	2	952.50	21.38	y8	Light	80.5	34.3
			677.34	2	704.38	21.38	y6	Light	80.5	34.3
TAGLN	Transgelin	EFTESQLQEGK	648.31	2	918.45	11.95	y8	Light	78.4	32.7
			648.31	2	789.41	11.95	y7	Light	78.4	32.7
			648.31	2	702.38	11.95	y6	Light	78.4	32.7
DHX9	ATP-dependent RNA helicase A	ELDALDANDELTPLGR	876.44	2	1210.59	27.26	y11	Heavy	94.6	45.4
			876.44	2	1095.57	27.26	y10	Heavy	94.6	45.4
			876.44	2	452.29	27.26	y4	Heavy	94.6	45.4

Table 2-4

10. MRM analysis using individual serum samples

Individual MRM analysis was performed using the 90 transitions, corresponding to 19 proteins; thus, MRM analysis per run was conducted once for every sample. The peak areas of each transition were extracted using Skyline and normalized using the peak area of the spiked standard peptide.

Nine proteins had identical expression patterns in the analysis of the pooled and individual samples (Figure 2-9). Specifically, very-long-chain-specific acyl-coA dehydrogenase (ACADVL), actin-binding protein, anillin (ANLN), c-1-tetrahydrofolate synthase, cytoplasmic (MTHFD1), alpha-fetoprotein (AFP), and filamin-B (FLNB) increased in the healthy control versus before HCC treatment group and declined in the before HCC treatment versus after HCC treatment group. Brain acid-soluble protein 1 (BASP1), calpain-1 catalytic subunit (CAPN1), complementary C4-A (C4A), and polyadenylate-binding protein 1 (PABPC1) fell in the healthy control versus the before HCC treatment group and in the before HCC treatment versus after HCC treatment group.

In the statistical analysis, these 9 proteins were differentially expressed between the nondisease and disease groups, with *P*-values < 0.05. The ROCs and interactive plots of the 9 candidates are shown in Figure 2-10. The AUC values of the 9 target proteins ranged from 0.586 to 0.951 (Table 2-5). The AUC values of 6 proteins exceeded 0.8—those of ANLN, BASP1, CAPN1 and PABPC1 were 0.920, 0.951, 0.946 and 0.949, respectively, in the healthy control versus before HCC treatment group, reflecting excellent specificity and sensitivity.

(A)

Very long-chain specific acyl-CoA dehydrogenase, mitochondria (ACADVL)

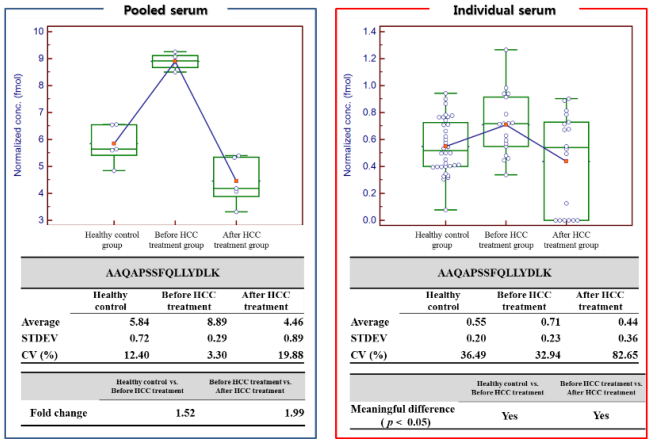

AAQAPSSFQLLYDLK	Healthy control	Before HCC treatment	After HCC treatment
Average	5.84	8.89	4.46
STDEV	0.72	0.29	0.89
CV (%)	12.40	3.30	19.88

	Healthy control vs. Before HCC treatment	Before HCC treatment vs. After HCC treatment
Fold change	1.52	1.99

AAQAPSSFQLLYDLK	Healthy control	Before HCC treatment	After HCC treatment
Average	0.55	0.71	0.44
STDEV	0.20	0.23	0.36
CV (%)	36.49	32.94	82.65

	Healthy control vs. Before HCC treatment	Before HCC treatment vs. After HCC treatment
Meaningful difference ($p < 0.05$)	Yes	Yes

Figure 2-9A

(B)

Actin binding protein, anillin (ANLN)

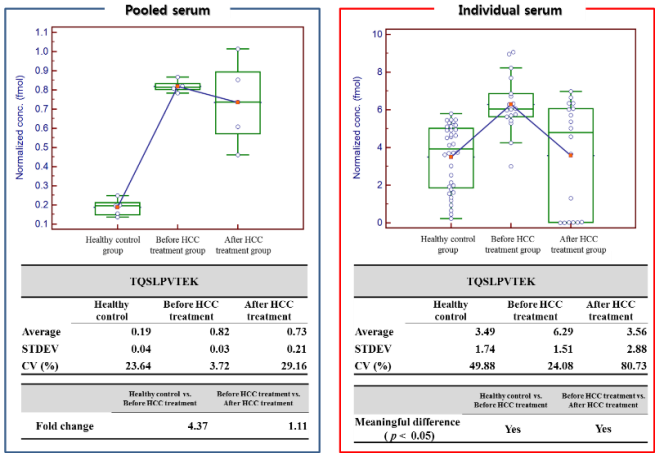

TQSLPVTEK	Healthy control	Before HCC treatment	After HCC treatment
Average	0.19	0.82	0.73
STDEV	0.04	0.03	0.21
CV (%)	23.64	3.72	29.16

	Healthy control vs. Before HCC treatment	Before HCC treatment vs. After HCC treatment
Fold change	4.37	1.11

TQSLPVTEK	Healthy control	Before HCC treatment	After HCC treatment
Average	3.49	6.29	3.56
STDEV	1.74	1.51	2.88
CV (%)	49.88	24.08	80.73

	Healthy control vs. Before HCC treatment	Before HCC treatment vs. After HCC treatment
Meaningful difference ($p < 0.05$)	Yes	Yes

Figure 2-9B

(C)

Brain acid soluble protein 1 (BASP1)

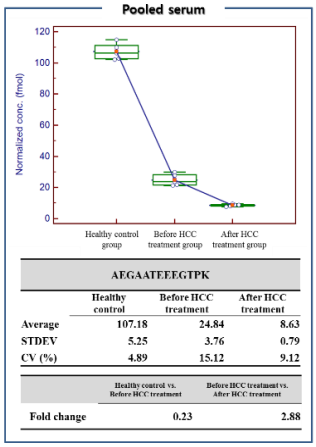

AEGAATEEEGTPK	Healthy control	Before HCC treatment	After HCC treatment
Average	107.18	24.84	8.63
STDEV	5.25	3.76	0.79
CV (%)	4.89	15.12	9.12

	Healthy control vs. Before HCC treatment	Before HCC treatment vs. After HCC treatment
Fold change	0.23	2.88

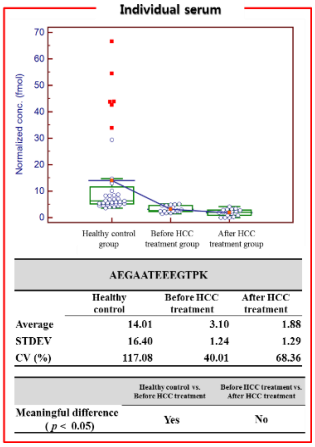

AEGAATEEEGTPK	Healthy control	Before HCC treatment	After HCC treatment
Average	14.01	3.10	1.88
STDEV	16.40	1.24	1.29
CV (%)	117.08	40.01	68.36

	Healthy control vs. Before HCC treatment	Before HCC treatment vs. After HCC treatment
Meaningful difference ($p < 0.05$)	Yes	No

Figure 2-9C

(D)

C-1-tetrahydrofolate synthase, cytoplasmic (MTHFD1)

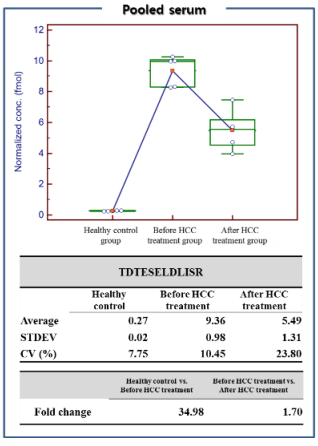

TDTESELDLISR	Healthy control	Before HCC treatment	After HCC treatment
Average	0.27	9.36	5.49
STDEV	0.02	0.98	1.31
CV (%)	7.75	10.45	23.80

	Healthy control vs. Before HCC treatment	Before HCC treatment vs. After HCC treatment
Fold change	34.98	1.70

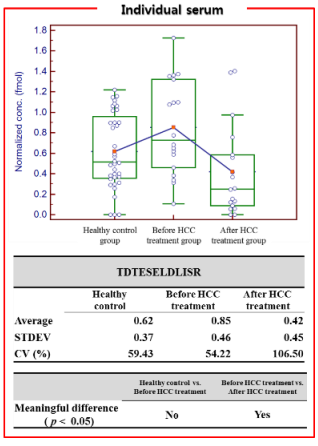

TDTESELDLISR	Healthy control	Before HCC treatment	After HCC treatment
Average	0.62	0.85	0.42
STDEV	0.37	0.46	0.45
CV (%)	59.43	54.22	106.50

	Healthy control vs. Before HCC treatment	Before HCC treatment vs. After HCC treatment
Meaningful difference ($p < 0.05$)	No	Yes

Figure 2-9D

(E)

Calpain-1 catalytic subunit (CAPN1)

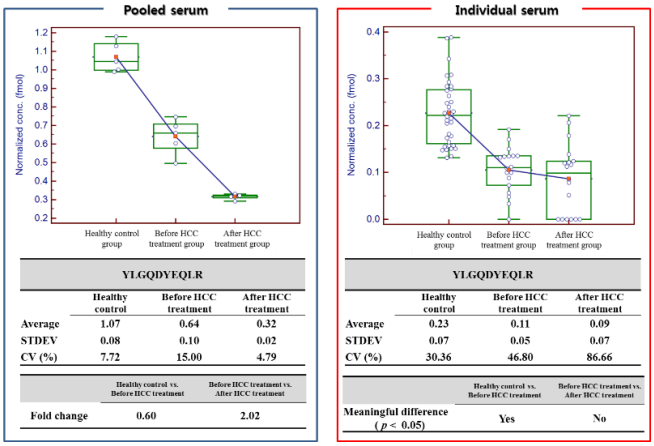

YLGQDYEQLR	Healthy control	Before HCC treatment	After HCC treatment
Average	1.07	0.64	0.32
STDEV	0.08	0.10	0.02
CV (%)	7.72	15.00	4.79

	Healthy control vs. Before HCC treatment	Before HCC treatment vs. After HCC treatment
Fold change	0.60	2.02

YLGQDYEQLR	Healthy control	Before HCC treatment	After HCC treatment
Average	0.23	0.11	0.09
STDEV	0.07	0.05	0.07
CV (%)	30.36	46.80	86.66

	Healthy control vs. Before HCC treatment	Before HCC treatment vs. After HCC treatment
Meaningful difference ($p < 0.05$)	Yes	No

Figure 2-9E

(F)

Complementary C4-A (C4A)

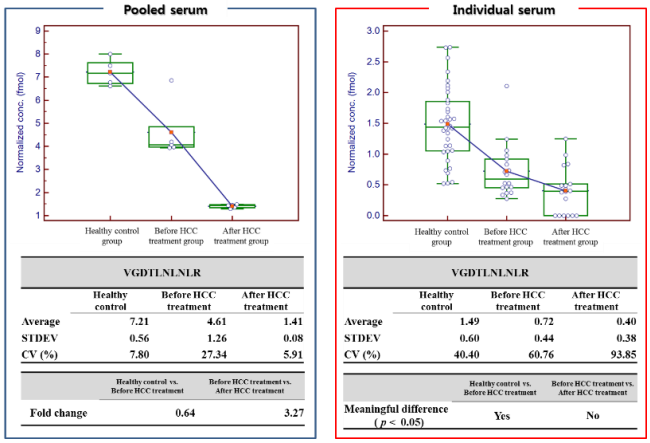

VGDTLNLNLR	Healthy control	Before HCC treatment	After HCC treatment
Average	7.21	4.61	1.41
STDEV	0.56	1.26	0.08
CV (%)	7.80	27.34	5.91

	Healthy control vs. Before HCC treatment	Before HCC treatment vs. After HCC treatment
Fold change	0.64	3.27

VGDTLNLNLR	Healthy control	Before HCC treatment	After HCC treatment
Average	1.49	0.72	0.40
STDEV	0.60	0.44	0.38
CV (%)	40.40	60.76	93.85

	Healthy control vs. Before HCC treatment	Before HCC treatment vs. After HCC treatment
Meaningful difference ($p < 0.05$)	Yes	No

Figure 2-9F

(G)

Alpha-fetoprotein (AFP)

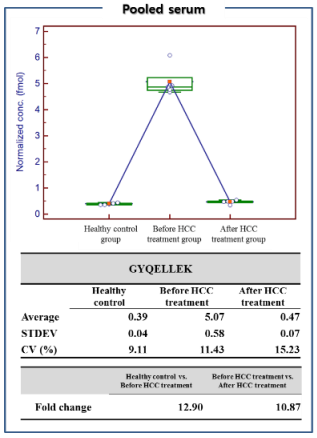

GYQELLEK	Healthy control	Before HCC treatment	After HCC treatment
Average	0.39	5.07	0.47
STDEV	0.04	0.58	0.07
CV (%)	9.11	11.43	15.23

	Healthy control vs. Before HCC treatment	Before HCC treatment vs. After HCC treatment
Fold change	12.90	10.87

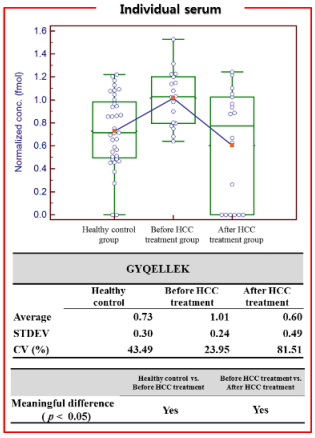

GYQELLEK	Healthy control	Before HCC treatment	After HCC treatment
Average	0.73	1.01	0.60
STDEV	0.30	0.24	0.49
CV (%)	43.49	23.95	81.51

	Healthy control vs. Before HCC treatment	Before HCC treatment vs. After HCC treatment
Meaningful difference ($p < 0.05$)	Yes	Yes

Figure 2-9G

(H)

Filamin-B (FLNB)

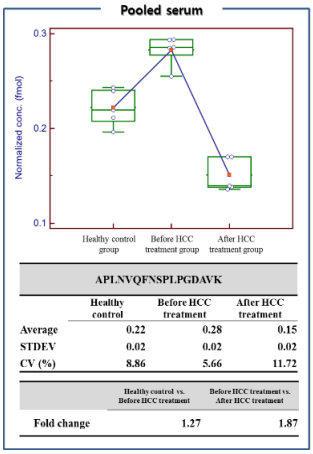

APLNVQFNSPLPGDAVK	Healthy control	Before HCC treatment	After HCC treatment
Average	0.22	0.28	0.15
STDEV	0.02	0.02	0.02
CV (%)	8.86	5.66	11.72

	Healthy control vs. Before HCC treatment	Before HCC treatment vs. After HCC treatment
Fold change	1.27	1.87

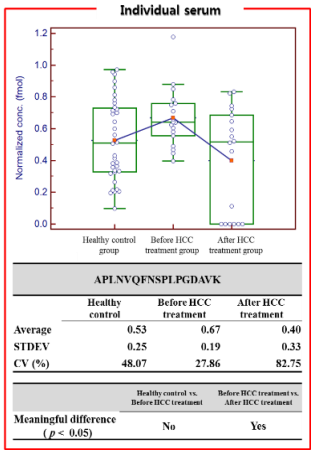

APLNVQFNSPLPGDAVK	Healthy control	Before HCC treatment	After HCC treatment
Average	0.53	0.67	0.40
STDEV	0.25	0.19	0.33
CV (%)	48.07	27.86	82.75

	Healthy control vs. Before HCC treatment	Before HCC treatment vs. After HCC treatment
Meaningful difference ($p < 0.05$)	No	Yes

Figure 2-9H

(I)

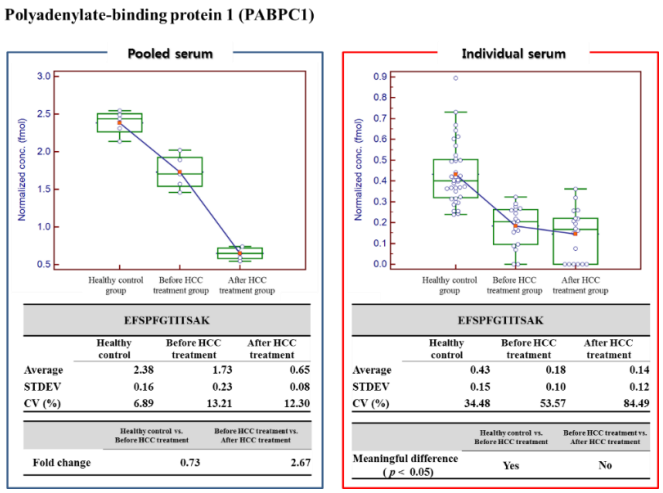

Figure 2-9I

Figure 2-9. As a result of the MRM analysis, a list of the 9 proteins where the expression profile of pooling specimen and individual specimen match with each other.

Scatter plots of MRM quantitation data using pooling serum and individual serum from healthy control group, before HCC treatment group, and after HCC treatment group. Left panel represents pooled serum from healthy control group, before HCC treatment group, and after HCC treatment group. Error bars represent the standard deviations from 5 technical replicates. Horizontal bars indicate the average serum level of the protein; *P*-values were calculated by ANOVA. Right panels indicate individual samples. See also Table S4 and Figure S2.

(A)

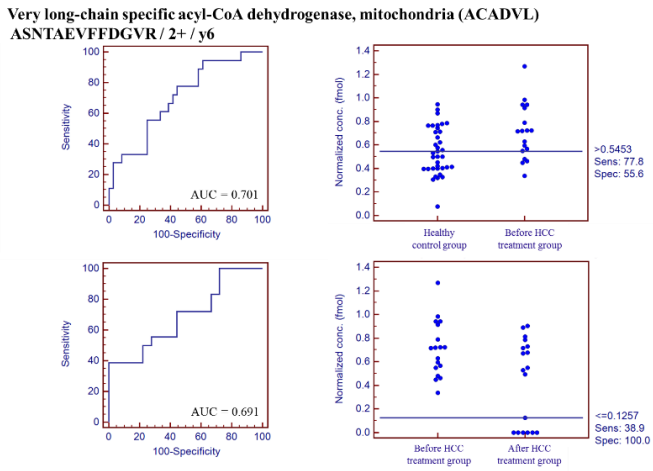

Figure 2-10A

(B)

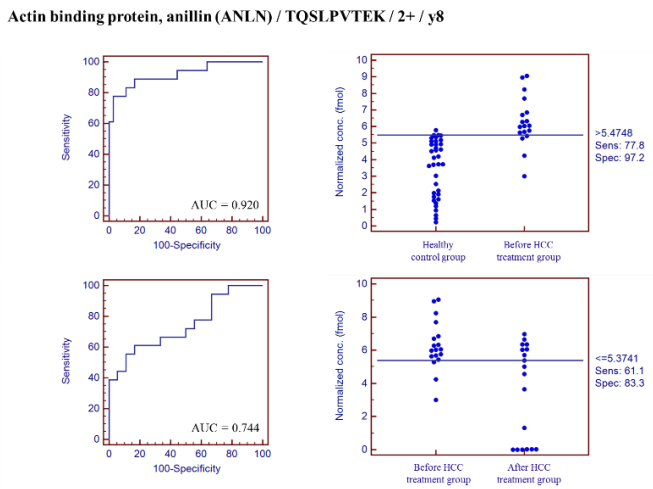

Figure 2-10B

(C)

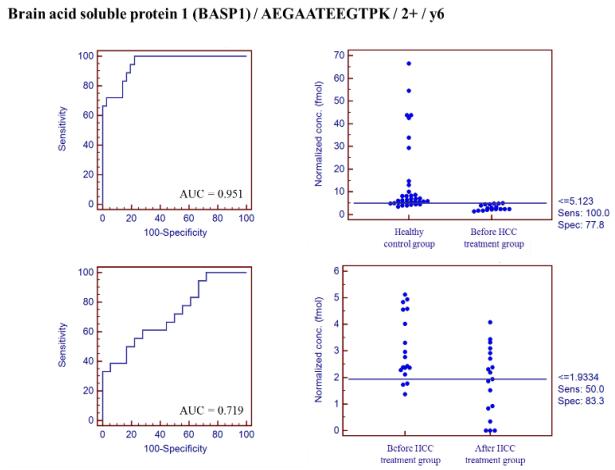

Figure 2-10C

(D)

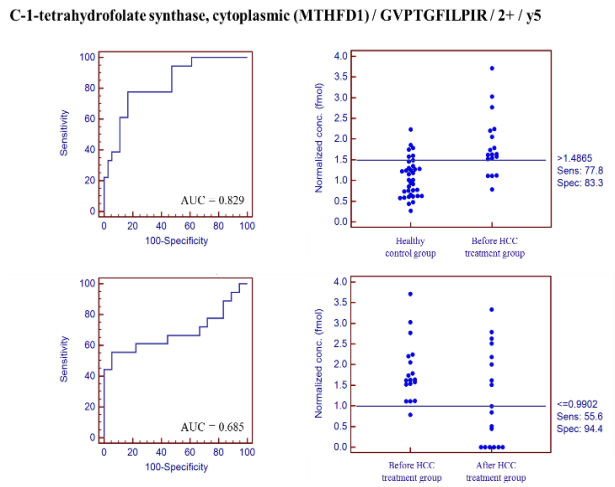

Figure 2-10D

(E)

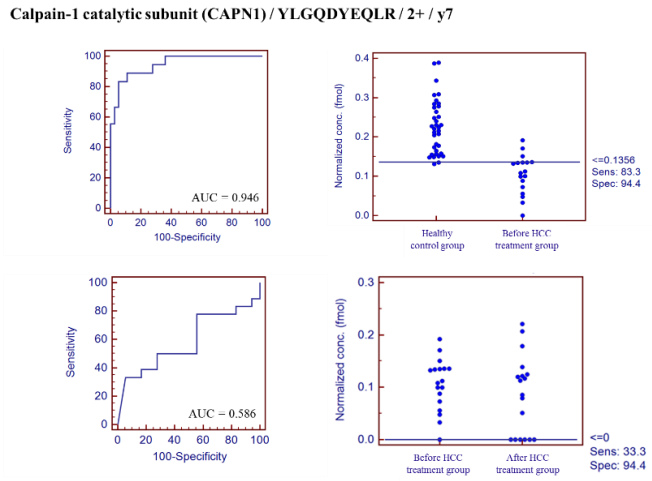

Figure 2-10E

(F)

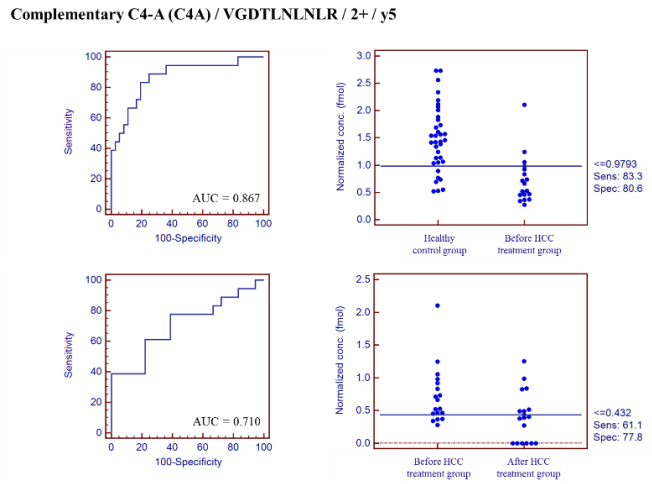

Figure 2-10F

(G)

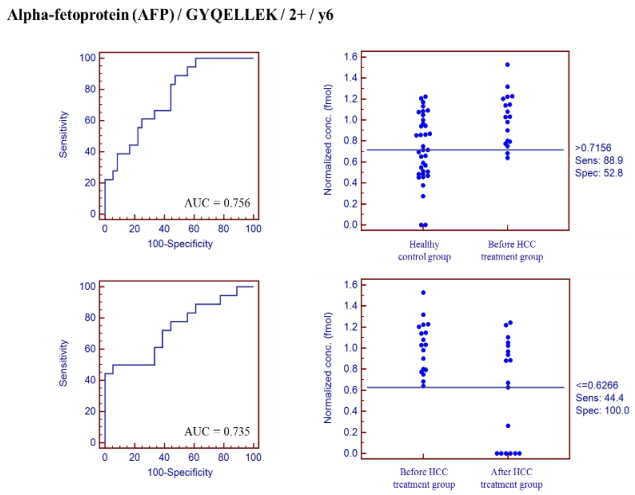

Figure 2-10G

(H)

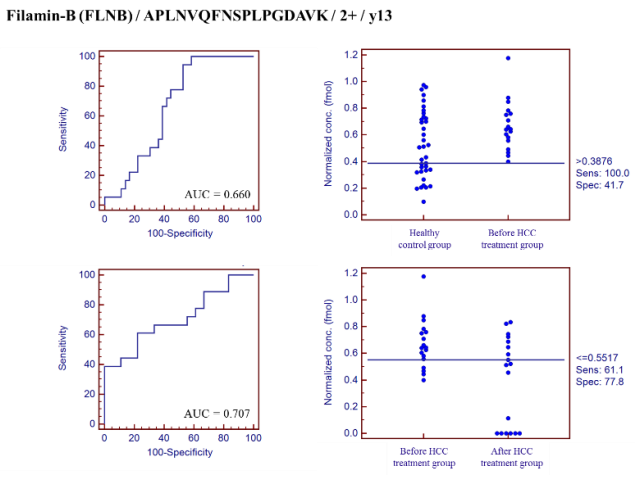

Figure 2-10H

(I)

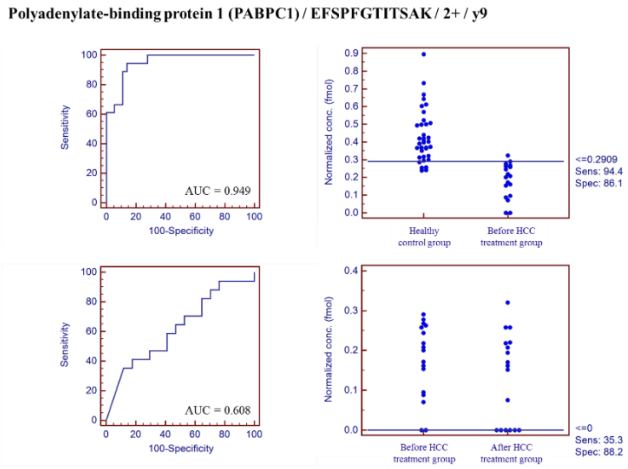

Figure 2-10I

Figure 2-10. The ROCs and interactive plots for nine verified candidate biomarkers.

The normalized peak areas of transitions were compared between the healthy control group and before HCC treatment group and between the before HCC treatment group and after HCC treatment group. The interactive plots and ROC curves are represented by the transition peak areas of the 9 proteins. Interactive plots of each target peptide were extrapolated versus the standard peptide with regard to relative concentration, sensitivity, and specificity. See also Table 2-5.

Table 2-5. List of proteins showing significant differences between different groups (*P*-values < 0.05) and their respective AUC values.

Serial No.	Gene symbol	Protein Name	Peptide Sequence	Area Under ROC Curve	
				Healthy control group vs. Before HCC treatment group	Before HCC treatment group vs. After HCC treatment group
1	ACADVL	Very long-chain specific acyl-CoA dehydrogenase, mitochondrial	ASNTAEVFFDGVR	0.701	0.691
2	AFP	Alpha-fetoprotein	GYQELLEK	0.756	0.735
3	ANLN	Actin-binding protein anillin	TQSLPVTEK	0.920	0.744
4	BASP1	Brain acid soluble protein 1	AEGAATEEEGTPK	0.951	0.719
5	C4A	Complement C4-A	VGDTLNLNLR	0.867	0.710
6	CAPN1	Calpain-1 catalytic subunit	YLGQDYEQLR	0.946	0.586
7	FLNB	Filamin-B	APLNVQFNSPLPGDAVK	0.660	0.707
8	MTHFD1	C-1-tetrahydrofolate synthase, cytoplasmic	GVPTGFILPIR	0.829	0.685
9	PABPC1	Polyadenylate-binding protein 1	EFSPFGTITSAK	0.949	0.608

Table 2-5

11. Correlation of MRM analysis with Western blot

To validate the MRM results, 9 proteins were analyzed by western blot: ACADVL, AFP, ANLN, BASP1, C4A, CAPN1, FLNB, MTHFD1, and PABPC1.

For the Western blot, 13 of 36 healthy control serum samples from the individual MRM analysis were selected randomly, and the before/after HCC treatment group, the 13 serum samples differed from what was used in the individual MRM analysis.

To limit the variability between SDS-PAGE gels, serum from the 13 healthy control, 13 before HCC treatment, and 13 after HCC treatment cases were pooled and loaded onto the first lane of all SDS-PAGE gels (12%), and its intensity on each gel was used to normalize the intensities of individual samples. As a result, the bands that were generated by ACADVL and PABPC1 were inadequate to calculate intensities; thus, 7 of the 9 candidate proteins were verified by western blot. Subsequently, the correlation between the protein quantification by MRM and western blot was determined.

AFP, ANLN, C4A, and FLNB had the same patterns of expression by MRM analysis (Figure 3). In the nondisease group, AFP, ANLN, and FLNB expression decreased compared with disease group. AFP is an established serum biomarker for HCC and was verified to have consistent expression by MRM and Western blot. C4A declined in the healthy control versus before HCC treatment group and in the before HCC treatment versus after HCC treatment group. In the comparison between MRM- and antibody-based verification, the

relative quantities of 4 proteins (AFP, ANLN, FLNB, and C4A) were similar. In contrast, by western blot, BASP1, MTHFD1, and CAPN1 had disparate expression patterns compared with MRM analysis (data not shown).

(A)

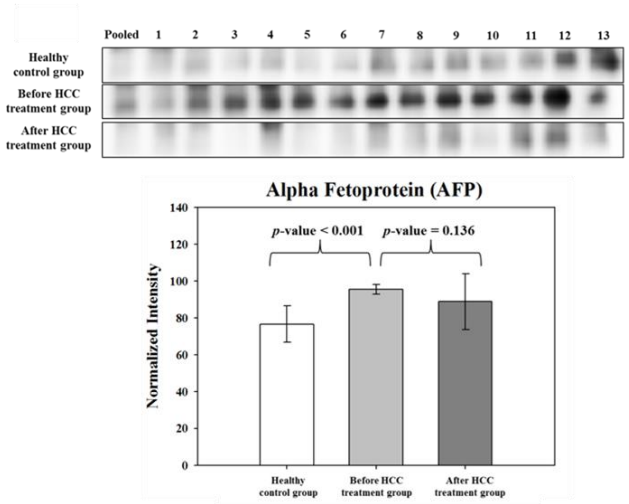

Figure 2-11A

(B)

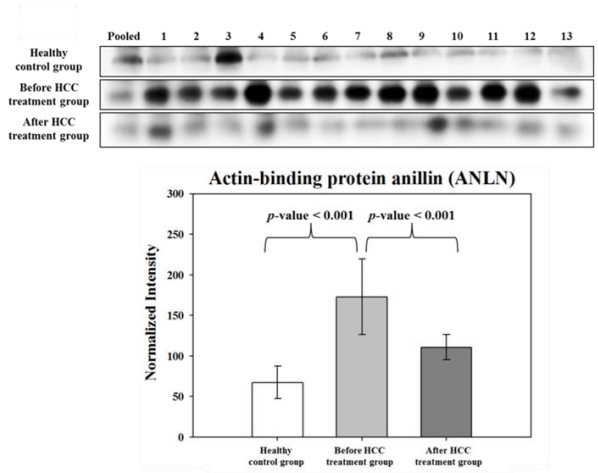

Figure 2-11B

(C)

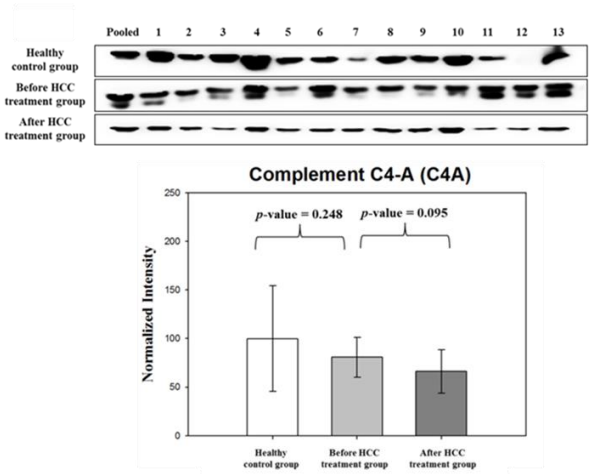

Figure 2-11C

(D)

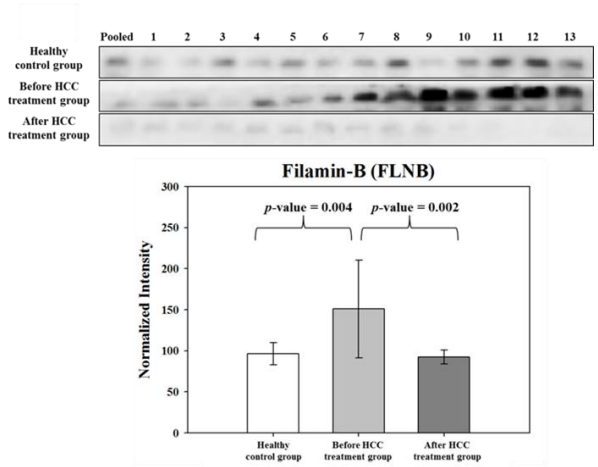

Figure 2-11D

Figure 2-11. Verification of four proteins by Western blot

Comparison and relative quantification of AFP, ANLN, C4A, and FLNB expression in serum samples from the nondisease group and disease group. Relative abundance, represented by the band intensity in Western blot, is summarized in box plot.

12. Multivariate analysis of the multimarker panel

A goal of this study was to discover potential HCC biomarkers by comprehensive global data mining and MRM and construct a multiprotein panel has improved discriminatory power over single markers. Four proteins that were validated by MRM analysis and western blot were used to generate the multimarker panel. In the first 4-marker panel that we attempted, AFP and C4A showed collinearity, with a variance inflation factor (VIF) above 10; thus, these proteins were excluded in the final multimarker model (Table 2-6). The ultimate model comprised ANLN and FLNB, for which AFP was the control model as a single marker. Three types of comparisons were made (Figure 2-12).

When AFP was used as the lone classifier, 8 of 18 before HCC treatment cases and 29 of 36 healthy control cases were classified correctly, demonstrating an AUC of 0.756 and 31% error rate. In contrast, the 2-marker panel correctly classified 17 of 18 before HCC treatment patients and all 36 healthy controls, with an AUC of 0.981 and 2% error rate, indicating that the 2-marker panel had improved discriminatory power compared with the AFP model.

The AFP-only model classified 12 of 18 before HCC treatment patients and 9 of 18 after HCC treatment patients correctly (AUC = 0.735, error rate = 42%), whereas the 2-marker panel separated 15 of 18 before HCC treatment and 11 of 18 after HCC treatment patients successfully (AUC=0.895, error rate=28%). Thus, in identifying patients in the before HCC treatment versus after HCC treatment groups, the discriminatory power of the 2-marker panel was outstanding compared with AFP alone.

The AFP-only model classified 4 of 18 in the disease group (before HCC treatment) and 50 of 54 in the nondisease group (healthy control and

after HCC treatment groups), with an AUC of 0.749 and error rate of 25%. The 2-marker panel identified 15 of 18 in the disease group and 50 of 54 in the nondisease group (AUC=0.953, error rate=10%). These results demonstrate that in all comparisons, the 2-marker panel has greater discriminatory power compared with the traditional single marker AFP.

Table 2-7 also shows the LOOCV results for AFP and the 2-protein panel. LOOCV, in which each member of the training set, using a model that was built with the other n - 1 members, one tries to predict the class of the remaining member—was also performed. The results indicate that the most accurate candidate biomarker in the respective groups was the 2-protein panel.

Table 2-6. The Multi-collinearity on the 4 protein and 2 protein are confirmed.

Tolerances and Variance inflation factors (VIFs) of collinearity analysis for 2 models.

4-protein model	Collinearity Statistics	
	Tolerance	VIF
Alpha-fetoprotein_GYQELLEK_2+_y6	.027	37.374
Actin-binding protein anillin_TQSLPVTEK_2+_y8	.035	28.918
Complement C4-A_VGDTLNLNLR_2+_y5	.177	5.665
Filamin-B_APLNVQFNSPLPGDAVK_2+_y13	.025	39.480

2-protein model	Collinearity Statistics	
	Tolerance	VIF
Actin-binding protein anillin_TQSLPVTEK_2+_y8	.152	6.591
Filamin-B_APLNVQFNSPLPGDAVK_2+_y13	.152	6.591

Table 2-6

(A)

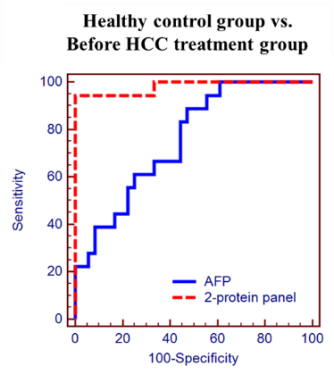

Classifier : AFP (AUC = 0.756)

	Healthy control group (36)	Before HCC treatment group (18)
Healthy control group (36)	29	7
Before HCC treatment group (18)	10	8

※ Error rate : 0.31

Classifier : 2-protein panel (AUC = 0.981)

	Healthy control group (36)	Before HCC treatment group (18)
Healthy control group (36)	36	0
Before HCC treatment group (18)	1	17

※ Error rate : 0.02

Figure 2-12A

(B)

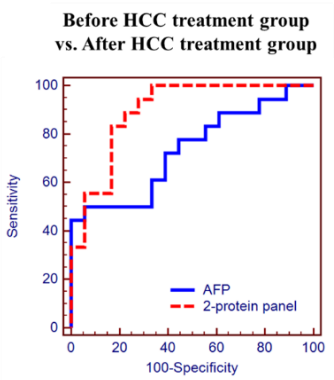

Classifier : AFP (AUC = 0.735)

	Before HCC treatment group (18)	After HCC treatment group (18)
Before HCC treatment group (18)	12	6
After HCC treatment group (18)	9	9

※ Error rate : 0.42

Classifier : 2-protein panel (AUC = 0.895)

	Before HCC treatment group (18)	After HCC treatment group (18)
Before HCC treatment group (18)	15	3
After HCC treatment group (18)	7	11

※ Error rate : 0.28

Figure 2-12B

(C)

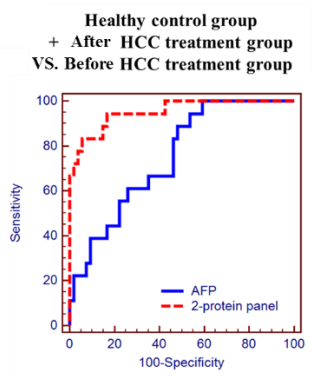

Classifier : AFP (AUC = 0.749)

	Healthy control group (36) + After HCC treatment group (18)	Before HCC treatment group (18)
Healthy control group (36) + After HCC treatment group (18)	50	4
Before HCC treatment group (18)	14	4

※ Error rate : 0.25

Classifier : 2-protein panel (AUC = 0.953)

	Healthy control group (36) + After HCC treatment group (18)	Before HCC treatment group (18)
Healthy control group (36) + After HCC treatment group (18)	50	4
Before HCC treatment group (18)	3	15

※ Error rate : 0.10

Figure 2-12C

Figure 2-12. ROC curves of AFP and 2-marker panel.

ROC curves are based on prediction models using AFP alone or the 2-marker panel. Simple ROC analysis was performed to compare AFP with the 2-marker panel. LR analysis models were prepared to determine false positive/negative rate in the classifier tables, in which error rates are also shown. Three LR analysis models were prepared: **(A)** healthy control versus before HCC treatment group, **(B)** before HCC treatment versus after HCC treatment group, and **(C)** healthy control plus after HCC treatment versus before HCC treatment group.

Table 2-7. Classification tables from logistic regression models (Cross validated, Leave-one out).

(A)

Healthy control group vs Before HCC treatment group

AFP	Predicted group		Percent correct
	Healthy control group (36)	Before HCC treatment group (18)	
Healthy control group (36)	29	7	80.56%
Before HCC treatment group (18)	11	7	38.89%
Accuracy			66.67%

* Area under an ROC curve (AUC) : 0.724

2-protein panel	Predicted group		Percent correct
	Healthy control group (36)	Before HCC treatment group (18)	
Healthy control group (36)	33	3	91.67%
Before HCC treatment group (18)	4	14	77.78%
Accuracy			87.04%

* Area under an ROC curve (AUC) : 0.887

Table 2-7A

(B)

Before HCC treatment group vs After HCC treatment group

AFP	Predicted group		Percent correct
	Before HCC treatment group (18)	After HCC treatment group (18)	
Before HCC treatment group (18)	9	9	50.00%
After HCC treatment group (18)	6	12	66.67%
Accuracy			58.33%

* Area under an ROC curve (AUC) : 0.682

2-protein panel	Predicted group		Percent correct
	Before HCC treatment group (18)	After HCC treatment group (18)	
Before HCC treatment group (18)	12	6	66.67%
After HCC treatment group (18)	5	13	72.22%
Accuracy			69.44%

* Area under an ROC curve (AUC) : 0.830

Table 2-7B

(C)

Healthy control group + After HCC treatment group vs Before HCC treatment group

AFP	Predicted group		Percent correct
	Healthy control group (36) + After HCC treatment group (18)	Before HCC treatment group (18)	
Healthy control group (36) + After HCC treatment group (18)	50	4	92.59%
Before HCC treatment group (18)	16	2	11.11%
Accuracy			72.22%

* Area under an ROC curve (AUC) : 0.720

2-protein panel	Predicted group		Percent correct
	Healthy control group (36) + After HCC treatment group (18)	Before HCC treatment group (18)	
Healthy control group (36) + After HCC treatment group (18)	48	6	88.89%
Before HCC treatment group (18)	9	9	50.00%
Accuracy			79.17%

* Area under an ROC curve (AUC) : 0.864

Table 2-7C

DISCUSSION

It is important to obtain a wide range of candidate proteins in the biomarker discovery stage, because most candidates fail to be verified in a large number of clinical samples. Global data mining can reduce the time and cost in identifying candidates for clinical verification. The 5 data mining categories enabled us to screen frequently reported candidate genes and proteins.

AFP is the most useful tumor marker for HCC and is produced by immature cells of the fetus. Newborns have AFP levels of up to 3 g/L until age 18 months, when AFP levels begin to drop below 10 µg/L, which are maintained in adulthood. AFP levels in normal adults are approximately 5-10 µg/L, which liver cancer patients usually exceed. Levels of AFP exceed 50 µg/L in 40% to 60% of HCC patients [80], and the false negative rate for HCC diagnosis solely with AFP is 20% to 30%. When AFP levels exceed 500 µg/L, it would be detectable for changes in body.

Conversely, because AFP levels in blood are high in only approximately 60% of liver cancer patients and other benign diseases (hepatitis, liver cirrhosis), there is a limitation in using AFP alone as an HCC marker in blood [81-89]. In particular, in our western blot analysis, AFP levels differed significantly between the healthy control and before HCC treatment groups but not between the before HCC treatment and after HCC treatment groups.

The reproducibility with regard to experimental and analytical variation is a major goal of MRM analysis. To minimize the variation in MRM analysis, we generated 3 pooled samples, corresponding to the 3 groups (36 healthy control, 18 untreated HCC, and 18 treated HCC samples),

and the 333 transitions that corresponded to 111 detectable peptides were monitored using MRM 5 times, in which the CV of all transition peak areas in the 3 groups was calculated. The transitions that had a CV% below 30% in all 3 groups were chosen as the final target transitions. Next, for individual MRM analysis, we selected only transitions that had a CV below 30%, as described in Figure 2-9.

We have demonstrated the value of our scheme in selecting candidate proteins by 5-cartegory global data mining and verification of the candidate proteins by clinical MRM to develop HCC markers in blood. Further, our multimarker panel has improved discriminatory power compared with single protein markers, such as AFP. Our 2-marker panel, comprising ANLN and FNAB, distinguishes healthy controls from before HCC treatment patients better than AFP. Thus, we propose that this strategy—combining global data mining to screen candidates and verification by clinical MRM—is a robust, effective pipeline for HCC marker development than can be applied to markers of other diseases.

REFERENCES

[1] Stefaniuk P, Cianciara J, Wiercinska-Drapalo A (2010) Present and future possibilities for early diagnosis of hepatocellular carcinoma. World J Gastroenterol 16: 418-424.

[2] Wang B, Chen D, Chen Y, Hu Z, Cao M, et al. (2012) Metabonomic profiles discriminate hepatocellular carcinoma from liver cirrhosis by ultraperformance liquid chromatography-mass spectrometry. J Proteome Res 11: 1217-1227.

[3] Omata M, Lesmana LA, Tateishi R, Chen PJ, Lin SM, et al. (2010) Asian Pacific Association for the Study of the Liver consensus recommendations on hepatocellular carcinoma. Hepatol Int 4: 439-474.

[4] Park JW, Korean Liver Cancer Study G, National Cancer C (2004) [Practice guideline for diagnosis and treatment of hepatocellular carcinoma]. Korean J Hepatol 10: 88-98.

[5] European Association For The Study Of The L, European Organisation For R, Treatment Of C (2012) EASL-EORTC clinical practice guidelines: management of hepatocellular carcinoma. J Hepatol 56: 908-943.

[6] Bertozzi CR, Sasisekharan R (2009) Glycomics. In: Varki A, Cummings RD, Esko JD, Freeze HH, Stanley P et al., editors. Essentials of Glycobiology. Cold Spring Harbor NY: The Consortium of Glycobiology Editors, La Jolla, California.

[7] Durand G, Seta N (2000) Protein glycosylation and diseases: blood and urinary oligosaccharides as markers for diagnosis and therapeutic monitoring. Clin Chem 46: 795-805.

[8] Spiro RG (2002) Protein glycosylation: nature, distribution, enzymatic formation, and disease implications of glycopeptide bonds. Glycobiology 12: 43R-56R.

[9] Anderson NL, Anderson NG (2002) The human plasma proteome: history, character, and diagnostic prospects. Mol Cell Proteomics 1: 845-867.

[10] Miyoshi E, Noda K, Yamaguchi Y, Inoue S, Ikeda Y, et al. (1999) The alpha1-6-fucosyltransferase gene and its biological significance. Biochim Biophys Acta 1473: 9-20.

[11] Kamoto T, Satomura S, Yoshiki T, Okada Y, Henmi F, et al. (2002) Lectin-reactive alpha-fetoprotein (AFP-L3%) curability and prediction of clinical course after treatment of non-seminomatous germ cell tumors. Jpn J Clin Oncol 32: 472-476.

[12] Li D, Mallory T, Satomura S (2001) AFP-L3: a new generation of tumor marker for hepatocellular carcinoma. Clin Chim Acta 313: 15-19.

[13] Khien VV, Mao HV, Chinh TT, Ha PT, Bang MH, et al. (2001) Clinical evaluation of lentil lectin-reactive alpha-fetoprotein-L3 in histology-proven hepatocellular carcinoma. Int J Biol Markers 16: 105-111.

[14] Chu CW, Hwang SJ, Luo JC, Lai CR, Tsay SH, et al. (2001) Clinical, virologic, and pathologic significance of elevated serum alpha-fetoprotein levels in patients with chronic hepatitis C. J Clin Gastroenterol 32: 240-244.

[15] Wang B, Chen D, Chen Y, Hu Z, Cao M, et al. (2012) Metabonomic profiles discriminate hepatocellular carcinoma from liver cirrhosis by ultraperformance liquid chromatography-mass spectrometry. J Proteome Res 11: 1217-1227.

[16] Daniele B, Bencivenga A, Megna AS, Tinessa V (2004) Alpha-fetoprotein and ultrasonography screening for hepatocellular carcinoma. Gastroenterology 127: S108-112.

[17] Colli A, Fraquelli M, Casazza G, Massironi S, Colucci A, et al. (2006) Accuracy of ultrasonography, spiral CT, magnetic resonance, and alpha-fetoprotein in diagnosing hepatocellular carcinoma: a systematic review. Am J Gastroenterol 101: 513-523.

[18] Boja E, Rivers R, Kinsinger C, Mesri M, Hiltke T, et al. (2010) Restructuring proteomics through verification. Biomark Med 4: 799-803.

[19] Bruix J, Sherman M (2011) Management of hepatocellular carcinoma: an update. Hepatology 53: 1020-1022.

[20] Kim H, Kim K, Yu SJ, Jang ES, Yu J, et al. (2013) Development of biomarkers for screening hepatocellular carcinoma using global data mining and multiple reaction monitoring. PLoS One 8: e63468.

[21] Qin LX, Zhou Q, Bogomolniy F, Villafania L, Olvera N, et al. (2014) Blocking and randomization to improve molecular biomarker discovery. Clin Cancer Res 20: 3371-3378.

[22] DeLong ER, DeLong DM, Clarke-Pearson DL (1988) Comparing the areas under two or more correlated receiver operating characteristic curves: a nonparametric approach. Biometrics 44: 837-845.

[23] Lee JY, Kim JY, Park GW, Cheon MH, Kwon KH, et al. (2011) Targeted mass spectrometric approach for biomarker discovery and validation with nonglycosylated tryptic peptides from N-linked glycoproteins in human plasma. Mol Cell Proteomics 10: M111 009290.

[24] Malaguarnera G, Giordano M, Paladina I, Berretta M, Cappellani A, et al. (2010) Serum markers of hepatocellular carcinoma. Dig Dis Sci 55:

2744-2755.

[25] Witjes CD, van Aalten SM, Steyerberg EW, Borsboom GJ, de Man RA, et al. (2013) Recently introduced biomarkers for screening of hepatocellular carcinoma: a systematic review and meta-analysis. Hepatol Int 7: 59-64.

[26] Lai Q, Melandro F, Pinheiro RS, Donfrancesco A, Fadel BA, et al. (2012) Alpha-fetoprotein and novel tumor biomarkers as predictors of hepatocellular carcinoma recurrence after surgery: a brilliant star raises again. Int J Hepatol 2012: 893103.

[27] Zhou L, Rui JA, Wang SB, Chen SG, Qu Q (2012) The significance of serum AFP cut-off values, 20 and 400 ng/mL in curatively resected patients with hepatocellular carcinoma and cirrhosis might be of difference. Hepatogastroenterology 59: 840-843.

[28] Alavi A, Axford JS (2008) Glyco-biomarkers: potential determinants of cellular physiology and pathology. Dis Markers 25: 193-205.

[29] Peracaula R, Barrabes S, Sarrats A, Rudd PM, de Llorens R (2008) Altered glycosylation in tumours focused to cancer diagnosis. Dis Markers 25: 207-218.

[30] An HJ, Kronewitter SR, de Leoz ML, Lebrilla CB (2009) Glycomics and disease markers. Curr Opin Chem Biol 13: 601-607.

[31] Drake PM, Cho W, Li B, Prakobphol A, Johansen E, et al. (2010) Sweetening the pot: adding glycosylation to the biomarker discovery equation. Clin Chem 56: 223-236.

[32] Hua S, An HJ (2012) Glycoscience aids in biomarker discovery. BMB Rep 45: 323-330.

[33] Reis CA, Osorio H, Silva L, Gomes C, David L (2010) Alterations in glycosylation as biomarkers for cancer detection. J Clin Pathol 63: 322-

329.

[34] Farinati F, Marino D, De Giorgio M, Baldan A, Cantarini M, et al. (2006) Diagnostic and prognostic role of alpha-fetoprotein in hepatocellular carcinoma: both or neither? Am J Gastroenterol 101: 524-532.

[35] Kulik LM (2007) Advancements in hepatocellular carcinoma. Curr Opin Gastroenterol 23: 268-274.

[36] Cui R, Wang B, Ding H, Shen H, Li Y, et al. (2002) Usefulness of determining a protein induced by vitamin K absence in detection of hepatocellular carcinoma. Chin Med J (Engl) 115: 42-45.

[37] Marrero JA, Su GL, Wei W, Emick D, Conjeevaram HS, et al. (2003) Des-gamma carboxyprothrombin can differentiate hepatocellular carcinoma from nonmalignant chronic liver disease in american patients. Hepatology 37: 1114-1121.

[38] Khan KN, Yatsuhashi H, Yamasaki K, Yamasaki M, Inoue O, et al. (2000) Prospective analysis of risk factors for early intrahepatic recurrence of hepatocellular carcinoma following ethanol injection. J Hepatol 32: 269-278.

[39] Nagaoka S, Yatsuhashi H, Hamada H, Yano K, Matsumoto T, et al. (2003) The des-gamma-carboxy prothrombin index is a new prognostic indicator for hepatocellular carcinoma. Cancer 98: 2671-2677.

[40] Koike Y, Shiratori Y, Sato S, Obi S, Teratani T, et al. (2001) Des-gamma-carboxy prothrombin as a useful predisposing factor for the development of portal venous invasion in patients with hepatocellular carcinoma: a prospective analysis of 227 patients. Cancer 91: 561-569.

[41] Taketa K, Endo Y, Sekiya C, Tanikawa K, Koji T, et al. (1993) A collaborative study for the evaluation of lectin-reactive alpha-

fetoproteins in early detection of hepatocellular carcinoma. Cancer Res 53: 5419-5423.

[42] Aoyagi Y, Suzuki Y, Isemura M, Nomoto M, Sekine C, et al. (1988) The fucosylation index of alpha-fetoprotein and its usefulness in the early diagnosis of hepatocellular carcinoma. Cancer 61: 769-774.

[43] Aoyagi Y, Saitoh A, Suzuki Y, Igarashi K, Oguro M, et al. (1993) Fucosylation index of alpha-fetoprotein, a possible aid in the early recognition of hepatocellular carcinoma in patients with cirrhosis. Hepatology 17: 50-52.

[44] Oda K, Ido A, Tamai T, Matsushita M, Kumagai K, et al. (2011) Highly sensitive lens culinaris agglutinin-reactive alpha-fetoprotein is useful for early detection of hepatocellular carcinoma in patients with chronic liver disease. Oncol Rep 26: 1227-1233.

[45] Yamashiki N, Seki T, Wakabayashi M, Nakagawa T, Imamura M, et al. (1999) Usefulness of Lens culinaris agglutinin A-reactive fraction of alpha-fetoprotein (AFP-L3) as a marker of distant metastasis from hepatocellular carcinoma. Oncol Rep 6: 1229-1232.

[46] Hayashi K, Kumada T, Nakano S, Takeda I, Sugiyama K, et al. (1999) Usefulness of measurement of Lens culinaris agglutinin-reactive fraction of alpha-fetoprotein as a marker of prognosis and recurrence of small hepatocellular carcinoma. Am J Gastroenterol 94: 3028-3033.

[47] Duffy MJ (2001) Clinical uses of tumor markers: a critical review. Crit Rev Clin Lab Sci 38: 225-262.

[48] Daniele B, Bencivenga A, Megna AS, Tinessa V (2004) Alpha-fetoprotein and ultrasonography screening for hepatocellular carcinoma. Gastroenterology 127: S108-112.

[49] Colli A, Fraquelli M, Casazza G, Massironi S, Colucci A, et al. (2006) Accuracy of ultrasonography, spiral CT, magnetic resonance, and alpha-fetoprotein in diagnosing hepatocellular carcinoma: a systematic review. Am J Gastroenterol 101: 513-523.

[50] Kim K, Kim SJ, Yu HG, Yu J, Park KS, et al. (2010) Verification of biomarkers for diabetic retinopathy by multiple reaction monitoring. J Proteome Res 9: 689-699.

[51] Gerber SA, Rush J, Stemman O, Kirschner MW, Gygi SP (2003) Absolute quantification of proteins and phosphoproteins from cell lysates by tandem MS. Proc Natl Acad Sci U S A 100: 6940-6945.

[52] Bruix J, Sherman M, American Association for the Study of Liver D (2011) Management of hepatocellular carcinoma: an update. Hepatology 53: 1020-1022.

[53] Stergachis AB, MacLean B, Lee K, Stamatoyannopoulos JA, MacCoss MJ (2011) Rapid empirical discovery of optimal peptides for targeted proteomics. Nat Methods 8: 1041-1043.

[54] Kirkpatrick DS, Gerber SA, Gygi SP (2005) The absolute quantification strategy: a general procedure for the quantification of proteins and post-translational modifications. Methods 35: 265-273.

[55] Kakehashi A, Ishii N, Shibata T, Wei M, Okazaki E, et al. (2011) Mitochondrial prohibitins and septin 9 are implicated in the onset of rat hepatocarcinogenesis. Toxicol Sci 119: 61-72.

[56] Ren F, Wu H, Lei Y, Zhang H, Liu R, et al. (2010) Quantitative proteomics identification of phosphoglycerate mutase 1 as a novel therapeutic target in hepatocellular carcinoma. Mol Cancer 9: 81.

[57] Lee HJ, Na K, Choi EY, Kim KS, Kim H, et al. (2010) Simple method for quantitative analysis of N-linked glycoproteins in hepatocellular carcinoma specimens. J Proteome Res 9: 308-318.

[58] Zhang J, Niu D, Sui J, Ching CB, Chen WN (2009) Protein profile in hepatitis B virus replicating rat primary hepatocytes and HepG2 cells by iTRAQ-coupled 2-D LC-MS/MS analysis: Insights on liver angiogenesis. Proteomics 9: 2836-2845.

[59] Niu D, Sui J, Zhang J, Feng H, Chen WN (2009) iTRAQ-coupled 2-D LC-MS/MS analysis of protein profile associated with HBV-modulated DNA methylation. Proteomics 9: 3856-3868.

[60] Sun Y, Mi W, Cai J, Ying W, Liu F, et al. (2008) Quantitative proteomic signature of liver cancer cells: tissue transglutaminase 2 could be a novel protein candidate of human hepatocellular carcinoma. J Proteome Res 7: 3847-3859.

[61] Chen N, Sun W, Deng X, Hao Y, Chen X, et al. (2008) Quantitative proteome analysis of HCC cell lines with different metastatic potentials by SILAC. Proteomics 8: 5108-5118.

[62] Mannova P, Fang R, Wang H, Deng B, McIntosh MW, et al. (2006) Modification of host lipid raft proteome upon hepatitis C virus replication. Mol Cell Proteomics 5: 2319-2325.

[63] Yan W, Lee H, Yi EC, Reiss D, Shannon P, et al. (2004) System-based proteomic analysis of the interferon response in human liver cells. Genome Biol 5: R54.

[64] Li C, Hong Y, Tan YX, Zhou H, Ai JH, et al. (2004) Accurate qualitative and quantitative proteomic analysis of clinical hepatocellular carcinoma using laser capture microdissection coupled

with isotope-coded affinity tag and two-dimensional liquid chromatography mass spectrometry. Mol Cell Proteomics 3: 399-409.

[65] Woo HG, Lee JH, Yoon JH, Kim CY, Lee HS, et al. (2010) Identification of a cholangiocarcinoma-like gene expression trait in hepatocellular carcinoma. Cancer Res 70: 3034-3041.

[66] Satow R, Shitashige M, Kanai Y, Takeshita F, Ojima H, et al. (2010) Combined functional genome survey of therapeutic targets for hepatocellular carcinoma. Clin Cancer Res 16: 2518-2528.

[67] Roessler S, Jia HL, Budhu A, Forgues M, Ye QH, et al. (2010) A unique metastasis gene signature enables prediction of tumor relapse in early-stage hepatocellular carcinoma patients. Cancer Res 70: 10202-10212.

[68] Hoshida Y, Nijman SM, Kobayashi M, Chan JA, Brunet JP, et al. (2009) Integrative transcriptome analysis reveals common molecular subclasses of human hepatocellular carcinoma. Cancer Res 69: 7385-7392.

[69] Acevedo LG, Bieda M, Green R, Farnham PJ (2008) Analysis of the mechanisms mediating tumor-specific changes in gene expression in human liver tumors. Cancer Res 68: 2641-2651.

[70] Segal E, Sirlin CB, Ooi C, Adler AS, Gollub J, et al. (2007) Decoding global gene expression programs in liver cancer by noninvasive imaging. Nat Biotechnol 25: 675-680.

[71] Lee JS, Heo J, Libbrecht L, Chu IS, Kaposi-Novak P, et al. (2006) A novel prognostic subtype of human hepatocellular carcinoma derived from hepatic progenitor cells. Nat Med 12: 410-416.

[72] Budhu A, Forgues M, Ye QH, Jia HL, He P, et al. (2006) Prediction of venous metastases, recurrence, and prognosis in hepatocellular

carcinoma based on a unique immune response signature of the liver microenvironment. Cancer Cell 10: 99-111.

[73] Ye QH, Qin LX, Forgues M, He P, Kim JW, et al. (2003) Predicting hepatitis B virus-positive metastatic hepatocellular carcinomas using gene expression profiling and supervised machine learning. Nat Med 9: 416-423.

[74] Chen CF, Hsu EC, Lin KT, Tu PH, Chang HW, et al. (2010) Overlapping high-resolution copy number alterations in cancer genomes identified putative cancer genes in hepatocellular carcinoma. Hepatology 52: 1690-1701.

[75] Chochi Y, Kawauchi S, Nakao M, Furuya T, Hashimoto K, et al. (2009) A copy number gain of the 6p arm is linked with advanced hepatocellular carcinoma: an array-based comparative genomic hybridization study. J Pathol 217: 677-684.

[76] Hashimoto K, Mori N, Tamesa T, Okada T, Kawauchi S, et al. (2004) Analysis of DNA copy number aberrations in hepatitis C virus-associated hepatocellular carcinomas by conventional CGH and array CGH. Mod Pathol 17: 617-622.

[77] Hernandez-Vargas H, Lambert MP, Le Calvez-Kelm F, Gouysse G, McKay-Chopin S, et al. (2010) Hepatocellular carcinoma displays distinct DNA methylation signatures with potential as clinical predictors. PLoS One 5: e9749.

[78] De Zhu J (2005) The altered DNA methylation pattern and its implications in liver cancer. Cell Res 15: 272-280.

[79] Malaguarnera G, Giordano M, Paladina I, Berretta M, Cappellani A, et al. (2010) Serum markers of hepatocellular carcinoma. Dig Dis Sci 55: 2744-2755.

[80] Cottingham K (2009) Candidate biomarkers for liver cancer. J Proteome Res 8: 428.

[81] Masuzaki R, Karp SJ, Omata M (2012) New serum markers of hepatocellular carcinoma. Semin Oncol 39: 434-439.

[82] Bertino G, Ardiri A, Malaguarnera M, Malaguarnera G, Bertino N, et al. (2012) Hepatocellualar carcinoma serum markers. Semin Oncol 39: 410-433.

[83] Bertino G, Neri S, Bruno CM, Ardiri AM, Calvagno GS, et al. (2011) Diagnostic and prognostic value of alpha-fetoprotein, des-gamma-carboxy prothrombin and squamous cell carcinoma antigen immunoglobulin M complexes in hepatocellular carcinoma. Minerva Med 102: 363-371.

[84] Alkofer B, Lepennec V, Chiche L (2011) Hepatocellular cancer in the non-cirrhotic liver. J Visc Surg 148: 3-11.

[85] Nguyen VT, Law MG, Dore GJ (2009) Hepatitis B-related hepatocellular carcinoma: epidemiological characteristics and disease burden. J Viral Hepat 16: 453-463.

[86] Nakagawa K, Koike S, Matsumura H, Yokoi K, Kitamura H (2012) [alpha-fetoprotein producing rectal cancer]. Gan To Kagaku Ryoho 39: 671-674.

[87] Donati M, Brancato G, Donati A (2010) Clinical biomarkers in hepatocellular carcinoma (HCC). Front Biosci (Schol Ed) 2: 571-577.

[88] Bei R, Mizejewski GJ (2011) Alpha fetoprotein is more than a hepatocellular cancer biomarker: from spontaneous immune response in cancer patients to the development of an AFP-based cancer vaccine. Curr Mol Med 11: 564-581.

[89] Robinson P (2008) Hepatocellular carcinoma: development and early detection. Cancer Imaging 8 Spec No A: S128-131.

ABSTRACT IN KOREAN

서론: 간암은 가장 낮은 생존율을 보이는 암 중의 하나이다. 혈청 알파-태아단백질은 오랫동안 간암 진단을 위한 마커로 사용됐지만, 논쟁의 여지가 있다. 알파-태아단백질의 수치는 비록 임상적으로 널리 이용되지만, 간암 진단 시 거짓 양성과 거짓 음성의 비율이 높으므로 문제가 있다.

방법: 1 장에서 간암 진단 마커로서 알파-태아단백질의 효능을 향상하기 위해, 질량분석기 다중반응검지법으로 전체 알파-태아단백질과 당질화된 알파-태아단백질을 측정하는 방법을 개발했다. 2 장에서, 유용한 간암 바이오마커 발굴을 위해, 단백체만을 중점에 두지 않고, 이전에 보고된 유전체와 단백체 데이터베이스의 포괄적인 데이터마이닝을 통해서 유용한 바이오마커 후보군을 선별했다.

결과: 1 장에서, 정상 대조군 집단 60 명, 간 경화 집단 35 명, 간암 환자 집단 60 명에서 알파-태아단백질의 전체 양 (비당질화 펩타이드 수치) 과 당질화된 알파-태아단백질의 양 (탈당질화 펩타이드 수치)을 검증했다. 질량분석기 다중반응검지법 분석으로, 정상 대조군 집단과 간암 환자 집단을 비교한 결과, 비당질화 펩타이드는 56.7% 민감도, 68.3% 특이도, 그리고 0.687 의 AUC 값을 갖지만, 탈당질화

펩타이드는 93.3% 민감도, 68.3% 특이도, 그리고 0.850 의 AUC 값을 가진다. 초기 간암 소집단과 간 경화 집단을 비교한 결과, 비당질화 펩타이드는 66.7% 민감도, 80.0% 특이도, 그리고 0.712 의 AUC 값을 갖지만, 탈당질화 펩타이드는 96.7% 민감도, 80.0% 특이도, 그리고 0.918 의 AUC 값을 가진다.

2 장에서, 바이오마커 후보군 단백질을 선별하기 위해 5 가지 형태 (상보적 DNA 마이크로 어레이, 유전자 복제 수 변이, 체세포 돌연변이, 후성 유전학, 정량적 단백체)의 간암 자료를 이용해서 포괄적인 데이터마이닝을 수행했다. 다음으로, 간암 바이오마커 후보군을 검증하기 위해 세 집단 (정상 대조군 집단, 간암 치료 전 집단과 간암 치료 후 집단)의 개별 혈청 시료를 다중반응검지법으로 분석했다. 다중반응검지법을 통해 후보군 단백질의 상대적인 양을 확인해서 세 집단 간 발현 수치를 비교한 결과, 네 개의 잠재적인 바이오마커를 확인했다 (ANLN, FLNB, C4A, 그리고 AFP).

결론: 1 장에서는, 정상 대조군 집단과 간암 환자 집단 간 비교 시, 알파-태아단백질의 탈당질화 펩타이드가 비당질화 펩타이드에 비해 높은 판별력을 보여준다. 이를 통해 탈당질화 펩타이드가 비당질화 펩타이드보다 정상 대조군 집단과 간암 환자 집단 간 암 상태를 더 잘 구별할 수 있다고 결론 내렸다. 2 장에서는, 알파-태아단백질에 비해 두 마커 (ANLN, FLNB)의 조합이 간암 치료 전 집단과 정상 대조군 집단 간 향상된 판별력을 가진다. 포괄적인 데이터마이닝과 다중반응검지법 검증의 조합으로 잠재적인 간암 바이오마커 선별을

향상할 수 있고, 이러한 효과적인 통합 전략은 암과 다른 질병의 마커 개발에 적용할 수 있다고 결론 내렸다.

Keywords: 다중반응검지법; 바이오마커; 간세포암종; 알파-태아단백질; 당질화된 알파-태아단백질; 포괄적인 데이터마이닝; 다중-마커 패널

Student number: 2009-21882